THE BIOCHEMISTRY OF CONNECTIVE TISSUE

LAURENT MICHEL MARIE VUILLARD

THESIS SUBMITTED FOR THE DEGREE OF Ph D

UNIVERSITY OF EDINBURGH

1989

PREFACE

I am grateful to Prof. Andrew Miller for the opportunity to carry out this work in the Biochemistry Department of Edinburgh University Medical School, and for his constant help and advice as supervisor throughout this work . I would like also to particularly thank Dr David Hulmes for having introduced me to many biochemical techniques , Mr Ian Purdom who has always been of great help as laboratory technician and Dr P.Sizer for useful discussions.

Outside the department I'm particularly indebted to Dr Jim Torbet at I.L.L. in Grenoble for his help with neutron scattering work , to Prof. Bernard Roux for the electric birefringence experiments as well as useful discussions on hydrodynamics and Prof. J.M. Rocard , Dr M. Rocard and Dr L.Dudule for their useful comments and advice . I would also like to thank Dr Boulton from the Scottish National Blood Transfusion Service for a generous supply of human plasma and Prof. Sir P. Forrest as well as his resident doctors for a supply of metastatic patient blood specimens . I ' m also very grateful to Dr McNeil from Malvern Instruments for his help with light scattering problems.

Lastly I ' m also largely indebted to my wife Dominique for her help and her patience .

Extracts from chapter V have been publised in F.E.B.S. Letters. 238 p 5 to 8 , 1988.

The work presented in this thesis was carried out between the 1st January 1986 and the 31st December 1988 , under the supervision of Professor Andrew Miller at the Department of Biochemistry , University of Edinburgh . All material presented in this thesis unless otherwise stated is the sole work of the author as is the composition.

INDEX TO FIGURES.

CHAPTER I

CHAPTER II

CHAPTER III

CHAPTER IV

INDEX TO TABLES.

CHAPTER I

CHAPTER II

CHAPTER III

CHAPTER VI.

ABSTRACT

Fibronectin is a multidomain , multifunctional, adhesion glycoprotein composed of subunits of molecular weight around 250 kD. It exists as a two subunits , soluble , form in tissue-culture media and plasma but can also exists as a multiple subunits , fibrillar , insoluble , form in tissues or in cell cultures.

Fibronectin now seems to function principally as part of the system which anchors cells in tissues. To understand this function, models of fibronectin shape and changes in its conformation are widely used and referred to .

However, despite the fact that the physicochemical study of fibronectin was started as early as 1955 , there is still little experimental data on this topic compared with other aspects of fibronectin . Furthermore many of the proposed models do not match with the observations in the literature .

Chapter I presents a review of the current knowledge of fibronectin .

Chapter II describes the various physicochemical techniques applied to fibronectin in this work.

In chapter III , the purification of the fibronectin molecule and of some of its constituent domains are developed. This includes various improvements from the classical purification method .

Chapter IV shows the construction of a model of the fibronectin molecule in solution through the combination of original data and published work.

The rotational relaxation times , as measured by electric birefringence , are 0.8µsec. in 150 mM ionic strength and 0.2 and 1.2 µsec. in 50 mM ionic strength. The radius of gyration determined by neutron small angle scattering experiments is 7.3 nm.The limited enzymatic disgestion performed in physiological conditions is found not to differ from the usual patterns and helps to establish the existence of fibronectin in solution as a compact succession of domains . The diffusion coefficient of the 145-155 kD central

domain, measured by photon correlation spectroscopy , is 3.1 10^{-7} cm^2 $sec.^{-1}$. Neutron small angle scattering experiments on the 44 kD collagen binding domain suggest that its shape is approximately spherical .

The proposed model for the conformation of the fibronectin molecule is a flat structure with anti-parallel chain position roughly equivalent to an oblate elllipsoid with a main axis of 10 nm and an extension of about 10 .

In chapter V plasma fibronectin prepared from metastatic cancer patients studied by light scattering techniques shows an abnormal aggregation property in vitro . Unsuccesful attempts to relate this with various biochemical properties are also described .

Chapter VI shows that the interaction between heparin and fibronectin do not result in any large change in conformation as shown by light and neutron scattering experiments . The published differences in physicochemical properties could rather be explained by aggregation .

An appendix describes possible evidence that vitronectin , another plasma cell-adhesion protein , could exist in two forms differing in their heparin binding properties . This finding could lead to a new purification method for vitronectin .

CHAPTER I :
STRUCTURAL AND BIOLOGICAL PROPERTIES OF FIBRONECTINS

I 1 INTRODUCTION.

Fibronectin was first identified as "Cold insoluble globulin " in 1948 by Morisson , Edsall and Miller who described this protein as the major contaminant of fibrinogen prepared by Cohn's cold ethanol fractionation technique .

Nearly thirty years later it was also found in material synthesized by cells in culture and tissues and referred to as "Surface fibroblast antigen ", "Large external transformation sensitive glycoprotein" and "Cell surface protein".

It is now defined as an extracellular , multidomain , adhesive glycoprotein . Its main function seems to be as part of the system that anchors or moves cells in the tissues.

At the moment , despite a large number of studies , there is no clear position about what fibronectin really does in this system . On the other hand the structural properties are often well documented. The review presented below will reflect those facts.

I 2 PRIMARY STRUCTURE

I 2 1 Determination of the primary structure :

The determination of the primary structure of fibronectin was not an easy task considering the size of this protein which is of the order of half a million Daltons. The sequencing was carried out by two different methods : either by the classical protein sequencing by enzymatic and chemical degradation or by molecular biology techniques.

The first step in our knowledge of the primary structure was the determination of the aminoacid composition of plasma fibronectin by Mosseson et al. in 1975 . It is now not really useful since the primary structure has been determined allowing a much more precise knowledge of the composition .

The next problem was to determine the number of subunits in the plasma fibronectin. This important point was clarified by Engvall et al. (1978) . They showed that the plasma fibronectin molecule is a disulphide bonded dimer. In a more recent work Skortengaard et al. (1986) suggested that the link between the two chains maintains them in an anti-parallel configuration . This will be of some importance in the construction of a model in chapter IV below .

Bovine plasma fibronectin was sequenced by Petersen's team in Denmark and human plasma fibronectin by Garcia Pardo's in U.S.A. (See :Petersen et al. 1983, Skortengaard et al. 1982,1983 ,1986 and in Garcia-Pardo et al. 1983,1985). Both teams

used the fact that the fibronectin molecule is composed of a succession of protease resistant functional domains. For this reason smaller fragments of the molecule can be generated . Their size is more suited to protein sequencing than the very large integral molecule .

Petersen et al. (1982) , on a partial determination of the sequence , discovered a striking feature of the primary structure of fibronectin. Three types of internal homologies called type I , II and III were found within the molecule. Further work on the sequence showed that the fibronectin molecules are made of the concatenation of those three basic structures. Their positions are shown in Fig I 1 .

Both type I and type II homologies are made on the same frame of disulphide bonded cysteine residues linked in a 1-3 , 2-4 pattern ; this pattern defines loops that have also been called "Fingers" . Their positions along the primary structure are shown below in Table I 1.

One of the most striking features of fibronectin when compared to many other proteins , is the linear arrangement in the primary structure of the sequences involved in its properties . Not only can the sequence be cut into independent active domains but , (as described below in Table I 1 and paragraphs I 3 2 & 3) , the segment of the molecule responsible for a property can , in the cases of the collagen and cell binding properties , even be restricted to a linear sequence of the size of a small peptide .

Partial amino-acid sequences deduced from cDNA clones for chicken , calf , rat and human have been described (Fagan et al. 1979,Kohrnblitt et al. 1983,1984 and Schwartzbauer et al. 1983) . Eventually Kohrnblitt et al. (1985) reported the complete primary structure of human plasma fibronectin from cDNA. (See Table I 1) . This work was followed by the total determination of the sequence from bovine plasma fibronectin by classical protein sequencing techniques thus showing the position of post transcriptional modifications such as phosphorylation or glycosylation (Skorskengaard et al. 1986) .

I 2 2 Alternative splicing of fibronectin mRNA.

Multiple fibronectin mRNA's can exist (Schwartzbauer et al. 1983 , Kohrnblitt et al. 1984) and are a consequence of alternative splicing of the gene . This explains how the primary structure can vary with the origin of the fibronectin. Presence or absence of some domains defines the various forms of fibronectins . They are Plasma , Cellular or "Oncofoetal " (i.e. from embryonic tissues or tumours) , as shown in Fig. I 2 below .

Fig I 1 .

β Subunit of plasma fibronectin.

From Skorskengaard et al. 1986

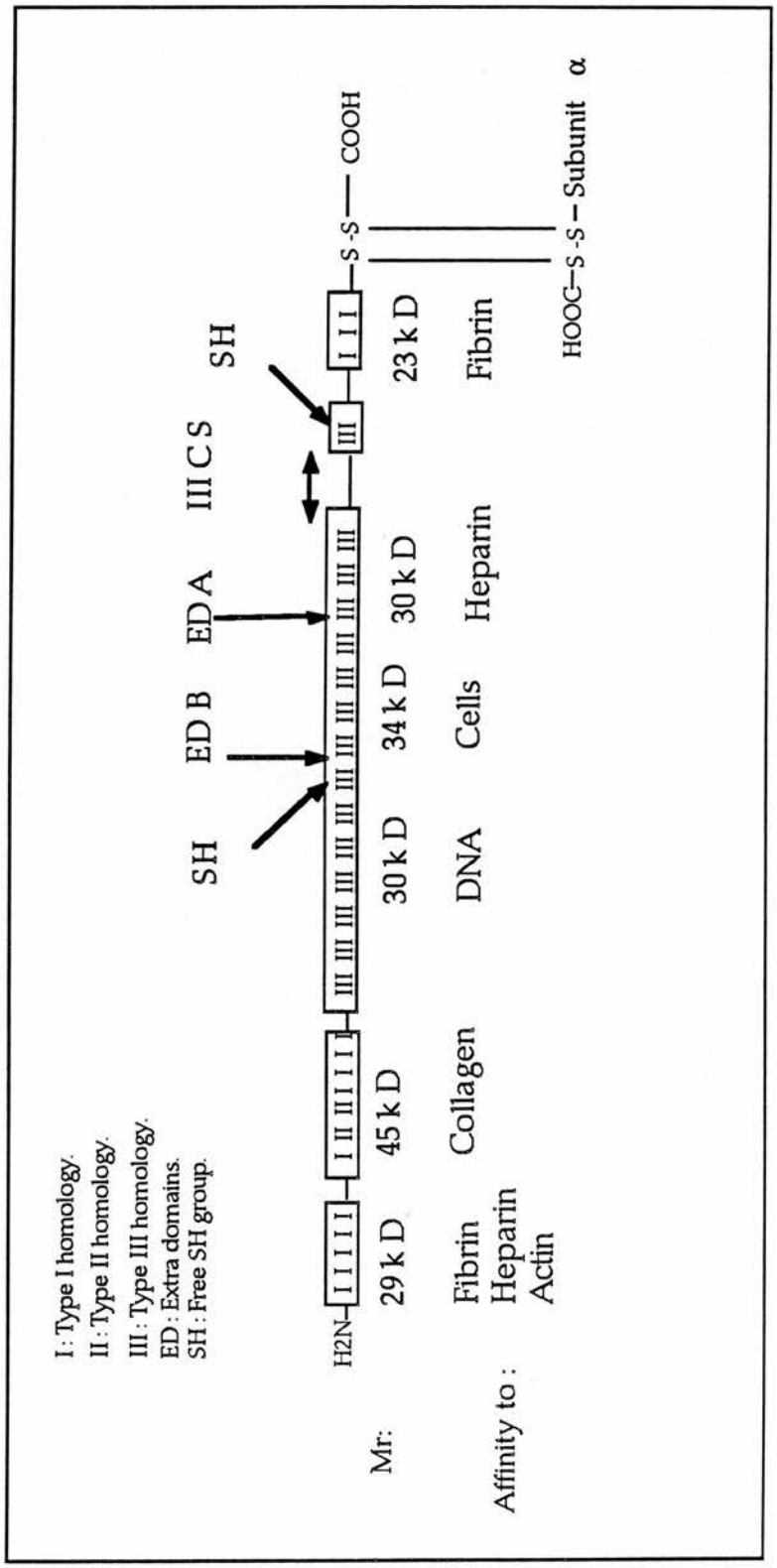

Fig I 2

Some alternative splicing patterns of fibronectin and t'ıeir expression .

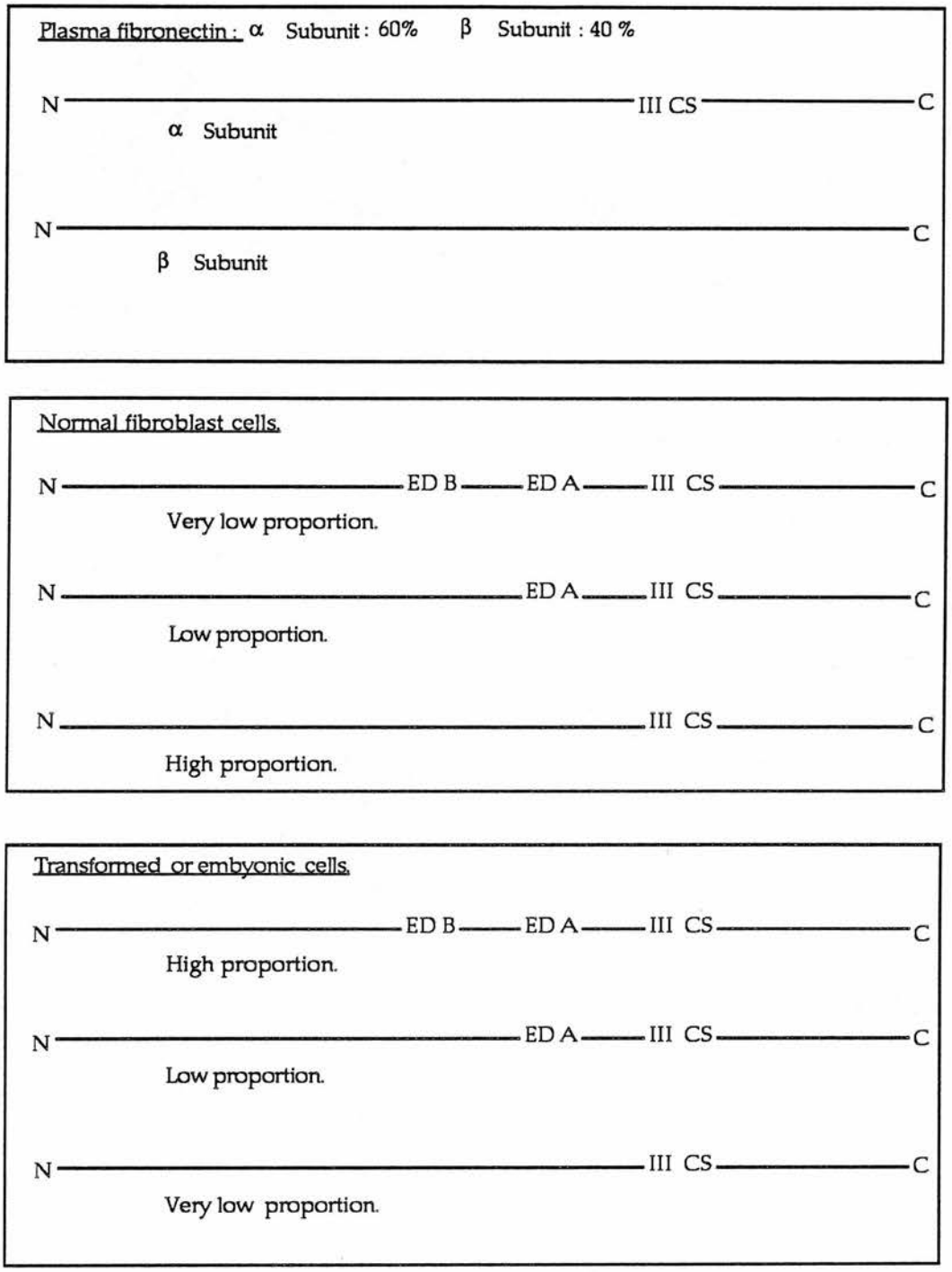

Monoclonal antibodies conjugated with affinity chromatography of limited thermolysin digest have been the investigators' favourite tool for the investigation of the expression of domains : All the alternatively spliced domains described as yet are type III homologies .

From N to C ends :

A) **ED-A** is the name of the first alternatively spliced domain . Its insertion point is residue 1599 in the bovine plasma form . It is detected by monoclonal antibodies IST 9 and FN 3 . There is no ED in human plasma fibronectin ; it is only present in a small fraction of the cellular form produced by normal cells and a high fraction of cellular form produced by transformed cells . (Paul et al. 1986,Borsi et al. 1987) .

B) The second one , is called **ED-B** and is expressed at high levels in fibronectin from transformed cells but is absent in the plasma form (Zardi et al. 1987).

C) The third one called **IIIcs** (residues 1871 to 1990 in the bovine plasma form), is also a type III homology (Seikiguchi et al 1985,Matsuara et al 1985) . Its presence defines the difference between the two chains of plasma fibronectin (Matsuara et al. 1985) .The subunit α has the IIIcs domain while the subunit β does not have it. The quantitation of the subunit expression in fibronectin from various sources (Castellani et al. 1986) shows that IIIcs is only expressed on one chain in the plasma form and that its presence is increased in normal cells fibronectin and is maximal in transformed cells fibronectin where all molecules are α, α type .

I 2 3 Structural analogies with other proteins.

The three types of internal homologies of fibronectin have been reported as being homologous to other protein sequences.

A) The **type I** homology has few known homologous proteins : Human alpha factor XIIa and tissue type plasminogen activator (Skorkengaard et al. 1986) and also Thrombospondin (Lawler et al. 1986) .

B)The **type II** homology of fibronectin , present in the fibronectin molecule only in the collagen binding domain (residues 314 to 370 and 374 to 430 in the bovine plasma molecule), is homologous to the " Kringle " structure , an autonomous structural and folding domains . Kringle type structures are also present in prothrombin , plasminogen , urokinase , tissue type plasminogen activator , alpha chain of haptoglobin , bovine seminal BSP-A3 and PDC 109 protein. Each type II homology is coded by one exon and it is believed that those modules , all devoted to protein

binding , might have evolved from a common ancestor . (Patthy 1983& 1985 , Baker et al. 1985 , Seidah et al. 1987 , Owens et al. 1986) .

C) A particular type III segment of fibronectin including the peptide RGDS (See cell binding in I 8 3) is also found in thrombospondin (Lawler et al. 1986) and vitronectin which are two other adhesion proteins of the extracellular matrix and also in Von Willebrand Factor (Tikani et al. 1986) and C3 complement factor (Wright et al. 1987)

Table I 1

Primary structure of the alpha chain of human plasma fibronectin ,(From Kohrnblitt et al 1985) . The positions of the carbohydrate side-chains are indicated by arrows.

29 k D Heparin binding N terminal domain.

QAQQMVQPQS PVAVSQSK

PGCYDNGKHYQI NQQWERTYLG NVLVCTCYGGSRGFNCESKPEAE (I 1).

ETCFDKYTGNTYRVGDTYERPKDSMIWDCTCIGAGRGRISCTIA (I 2).

NRCHEGGQSYKIGDTWRRPHETGGYMLECVCLGNGKGEWTCKPIA (I 3).

EKCFDHAAGTSYVVGETWEKPYQGWMMVDCTCLGEGSGRITCTSR (I 4).

NRCNDQDTRTSYRIGDTWSKKDNRGNLLQCICTGNGRGEWKC (I 5).

45 k D Collagen binding domain, collagen binding site is underlined.

ERHTSVQTTSSGSGPFTDVRAAVYQPQPHPQPPPY

GHCVTDSGVVYSVGMQWLKTQGNKQMLCTCLGNGVSCQE (I 6)

TAVTQTYGGNLNGEPCVLPFTYNGRTFYSCTTEGRQDGHLWCSTTSNYEQDQKYSFC TDH (II 1).

TVLVQTQGGNSNGALCHFPFLYNNHNYTDCTSEGRRDNMKWCGTTQNYDADQKF GFCPMAAHE(II 2).

EICTTNEGVMYRIGDQWDKQHDMGHMMRCTCVGNGRGEWTCIAYSQLR (I 7).

DQCIVDDITYNVNDTFHKRHEEGHMLNCTCFGQGRGRWKCDPV (I 8).

DQCQDSETGTFYQIGDSWEKYVHGVRYQCYCYGRGIGEWHCQPLQTYPSS (I 9).

Central DNA-Cell Heparin binding domain, the cell attachment site is underlined.

SGPVEVFITETPSQPNSHPIQSAPQPSHISKYILRWRPKNSVGRWKEATIPGHLNSYTI
KGLKPGVVYEGQLISIQQYGHQEVTRFDFTTT (III 1)

S TSTPVTSNTV TGETTPFSPL VATSESVTEI TASSFVVSWV SASDTVSGFR
VEYELSEEGD EPQYLDLPST ATSVNIPDLL PGRKYIVNVY QISEDGEQSL ILSTSQTT
(III 2).

APDAPPDPTVDQVDDTSIVVRWSRPQAPITGYRIVYSPSVEGSSTELNLPETANSVTL
SDLQPGVQYNITIYAVEENQESTPVVIQQETT (III 3).

GTPRSDTVPSPRDLQFVEVTDVKVTIMWTPPESAVTGYRVDVIPVNLPGEHGQRLPIS
RNTFAEVTGLSPGVTYYFKVFAVSHGRESKPLTAQQTT (III 4).

KLDAPTNLQFVNETDSTVLVRWTPPRAQITGYRLTVGLTRRGQPRQYNVGPSVSKYP
LRNLQPASEYTVSLVAIKGNQESPKATGVFTT (III 5).

LQPGSSIPPYNTEVTETTIVITWTPAPRIGFKLGVRPSQGGEAPREVTSDSGSIVVSGLTP
GVEYVYTIQVLRDGQERDAPIVNKVVT (III 6).

PLSPPTNLHLEANPDTGVLTVSWERSTTPDITGYRITTTPTNGQQGNSLEEVVHADQS
SCTFDNLSPGLEYNVSVYTVKDDKESVPISDTIIP (III 7).

AVPPPTDLRFTNIGPDTMRVTWAPPPSIDLTNFLVRYSPVKNEEDVAELSISPSDNAV
VLTNLLPGTEYVVSVSSVYEQHESTPLRGRQKT (III 8).

GLDSPTGIDFSDITANSFTVHWIAPRATITGYRIRHHPEHFSGRPREDRVPHSRNSITL
TNLTPGTEYVVSIVALNGREESPLLIGQQST (III 9).

VSDVPRDLEVVAATPTSLLISWDAPAVTVRYYRITYGETGGNSPVQEFTVPGSKSTTV
DYTITVYAVTGRGDSPASSKPISINYRTE (III 10).

IDKPSQMQVTDVQDNSISVKWLPSSSPVTGYRVTTTPKNGPGPTKTKTAGPDQTEMT
IEGLQPTVEYVVSVYAQNPSGESQPLVQTAVT (III 11).

Insertion position for the E. D. domain , (absent in plasma fibronectin).

TAIPAPTDLKFTQVTPTSLSAQWTPPNVQLTGYRVRVTPKEKTGPMKEINLAPDSSSV
VVSGLMVATKYEVSVYALKDTLTSRPAQGVVTTLE (III 12).

NVSPPRRARVTDATETTITISWRTKTETITGFQVDAVPANGQTPIQRTIKPDVRSYTIT
GLQPGTDYKIYLYTLNDNARSSPVVIDAST (III 13).

AIDAPSNLRFLATTPNSLLVSWQPPRARITGYIIKYEKPGSPPREVVPRPRPGVTEATIT
GLEPGTEYTIYVIALKNNQKSEPLIGRKKT(III 14).

DELPQLVTLPHPNLHGPEILDVPSTVQKTPFVTHPGYDTGNGIQLPGTSGQQPSVGQQ
MI FEEHGFRRTTPPTTATPIRHRPRPYPPNV (IIICS).

GQEALSQTTISWAPFQDTSEYIISCHPVGTDEEPLQFRVPGTSTSATLTGLTRGATYNII
VEALKDQQRHK (III 15).

23 k D Fibrin binding domain.

VREEVVTVGNSVNEGLNQPTDDSCFDPYTVSHYAVGDEWERMSESGFKLLCQCLGF
GSGHFRCDSS (I 10).

RWCHDNGVNYKIGEKWDRQGENGQMMSCTCLGNGKGEFKCDPHE (I 11).

ATCYDDGKTYHVGEQWQKEYLGAICSCTCFGGQRGWRCDNCR(I 12).

6 k D C-Terminal domain with the phosphorylation site (Underlined).

RPGGEPSPEGTTGQSYNQYSQRYHQRTNGTNVNCPIECFPMPLDVQADREK
DSRE

I 3 GLYCOSYLATION.

I 3 1 Introduction.

As usual with glycoproteins and very unfortunately, the nature of the glycosylation is one of the lesser known aspects of fibronectin. While the structural and biological consequences of the variability in aminoacid sequences are well documented, the structure and variations in glycosylation, (as well as their consequences), are relatively neglected .

Fibronectin is mostly a N glycan glycoprotein (Taksaski et al. 1979) thus glycosylation can be inhibited by tunicamycin (Duskin et al. 1976) and export from the cells is unaffected by 1 Deoxynojirimycin (Parent et al. 1986).

I 3 2 Carbohydrates of plasma fibronectin.

This problem has not been solved in a satisfactory way since partial determinations only exist and sometimes show variations among each other.

A) The composition in carbohydrates of human plasma fibronectin , from Mosseson et al. (1975) , in percentage of the total mass, is : sialic acid 1.2 % ,hexose 1.8 % ,hexosamine 2.1% . A possible pattern for human plasma fibronectin glycosylation has been proposed (Wrann et al. 1978) .The structure of the sugar side chains of bovine plasma is known (Taksaki et al 1979).

B) An attempt to determine the position of the carbohydrate side-chains in human plasma fibronectin was made by Hayashi et al. (1983). They found ten glycosidic chains by plasma molecule ; three chains per collagen binding domain and two chains per cell binding domain . But this does not match with the determination in the bovine plasma form , where sugar sidechains number and positions are shown below (Skorskergaard et al. 1986) :

α) Collagen binding domain : asparagine residues position 399, 497, 511.

β) Between collagen and DNA binding domains position 846.

γ) Position 976 in the DNA binding domain.

δ) Between DNA end cell binding domains on residue 1213.

ε) In the IIIcs domain on residues 1943-1944.

The carbohydrate sidechains are similar to those of other plasma glycoproteins . The sequence Galβ1- 3 GlcNac , present in the bovine plasma molecule was also found in milk oligosaccharides and in bovine prothrombin. (Taksaki et al 1979). Analysis of the porcine fibronectin carbohydrates shows that the sugar sidechains are the same as in

porcine plasma gelatin binding protein and are similar to those in human plasma-Fibronectin except for fucose distribution. (Isemura et al. 1984).

I 3 3 Carbohydrates of cellular or oncofetal fibronectins.

Oncofetal or cellular fibronectins have a different glycosylation pattern from that of plasma fibronectins (Wagner et al. 1981 ,Fukuda et al. 1982 ,Zhu et al. 1984).

A) The structure of carbohydrates from human amniotic fluid fibronectin has been determined . It shows an increase of lactosamin sidechains during gestation ; this increase in lactosamin content seems correlated with lower collagen affinity (Yamaguchi at al. 1986, Zhu et al. 1987). Near term nearly 10 % of the molecule mass is represented by carbohydrates .

B) Fibronectin produced by normal and transformed cells has , at least for a proportion of the total synthesis , a modified glycosylation .

C) They show specific Lentil lectin reactive sites in fibronectins produced by transformed cell lines .

D) They present specific binary sialosyl chain NeuAc α 2-- 3 / or 6Gal β 1-- 4 GlcNac , within the collagen binding domain for fibronectin produced by normal cells , at the N terminal region of the central domain for fibronectin produced by transformed cells. (Nichols et al. 1986.)

I 3 4 Functions of glycosylation.

The functions of carbohydrate side-chains in fibronectins are still not very well understood . Glycosylation effects on fibronectin properties were investigated in a comparative study of cellular fibronectin produced in cell culture in presence or absence of tunicamycine. (Jones et al. 1986) . Cellular fibronectin produced in the presence of tunicamycin ,free from post transcriptional modifications and therefore with no carbohydrate side-chains shows :

A) A better cell attachment efficiency as shown by a cell attachment assay ;this is in contradiction with the findings of Obara et al. 1987 who noticed that expression of the cell binding domain in E.Coli , (therefore non glycosylated) , produced a 80 kD cell attachment domain as efficient as the whole fibronectin molecule .

B) A better collagen binding efficiency. (Urea concentration greater to 3 M is required to elute nonglycosylated fibronectin from a collagen column as normal fibronectin is eluted at lower urea concentrations). In a similar way increased glycosylation as in placental fibronectin decreases the affinity between fibronectin and collagen.

(Yamaguchi et al. 1986). We must notice that this does not prove that the binding itself is affected . It might well be that only the urea denaturation is made easier .

C) Some unaffected heparin binding properties .

It has been confirmed that the glycosylation has a protease degradation protective effect particularly on the collagen binding domain . (Olden et al. 1979) .

I 4 PHOSPHORYLATION AND SULPHATION

Fibronectins from various sources are phosphorylated . The phosphorylation site of bovine plasma fibronectins is on the serine residue in position 2263 , three residues before the C End of the molecule , (Skorskengaard et al. 1986) . This position seems to be the same in fibronectin from human adult normal fibroblasts in culture metabolically labelled by ^{32}P (Ledger et al. 1981) .

The culture of various transformed cell lines produced variable results , some authors claiming that fibronectin produced by the transformed cell lines bear more phosphate , (Ali et al. 1981) , other thinking they bear less phosphate , (Teng et al. 1979).

There is one sulfatation site in fibronectin from normal cells culture, detected by metabolic labelling with ^{35}S sulphate, within type I homologies at the C terminus 17 kD domain . (Liu et al. 1987) .

I 5 FREE SULPHYDRYL GROUPS.

The existence of free sulphydryl groups on fibronectin is very important because they might be involved in its polymerisation . (See I 11 below). There are two free sulphydryl groups per fibronectin subunit (residues 1201 and 2215) in the bovine plasma molecule .

The free sulphydryl groups are not accessible to reagents in normal buffer conditions needing a guanidinium chloride concentration of 3 M to be fully exposed . (Williams et al. 1983) . Surprisingly , despite this fact , $CuSO_4$ induced polymerisation (Vartio 1986) , which, according to this author, uses those free sulphydryl groups , occurs in physiological buffers with addition of milimolar amounts of $CuSO_4$ but no chaotropic agent .It must be noticed that the characterization of polymerisation involved in this study is probably not perfect. This was shown by the fact that Vartio claims that $ZnCl_2$ cannot induce the polymerisation of fibronectin, but with a $ZnCl_2$ concentration of 10 mM fibronectin prepared for this work could be rapidly polymerised

and formed visible precipitates.

I 6 SECONDARY STRUCTURE

The secondary structure composition of plasma fibronectin , and of some of its constituent domains , is known from circular dichroism studies (Alexander 1978 , Kotelianski et al. 1981 , Odermatt et al. 1982 , Venyaminov et al. 1983, Welsh et al. 1983) . The major conclusions are shown in Table I 2 below.

Table I 2 : Secondary structure patterns of fibronectin and trypsin generated fibronectin domains.(Venyaminov et al. 1983)

	β Sheet	Non organised	α Helix
Fibronectin	35 %	50 %	0 %
70 kD Gelatin binding domain .	28 %	68 %	0 %
65-60 kD Heparin binding domain .	33 %	69 %	0 %
60 kD Central domain.	37 %	63 %	0 %

Results from various teams are similar . The most important conclusion is that the molecule is made of structurally independent domains retaining their individual conformation when they are isolated from the complete molecule. This is based on the following facts :

A) The sum of the individual domains spectra yields the spectrum of the intact molecule.

B) Although large transition in conformation is observed between pH 5 and 10.8 the C.D. spectrum remains nearly unchanged, but clearly a large irreversible denaturation occurs at pH superior to 10.8 (Odermatt et al. 1982).

I 7 THREE-DIMENSIONAL STRUCTURE

I 7 1 Results from electron microscopy.

The results from electron microscopy studies show little agreement amongst themselves. This problem will be discussed further in paragraph IV 10 1 .

One proposed structure (Engel et al. 1981,Odermatt et al. 1982) ,is a V shaped model with two equal-length arms of about 60 nm , the diameter being around 3 nm relatively constant all over the molecule. Bends in the arms are preferentially located at 20 and 40 nm from the intersection of the two arms . The angle between them being

from 40 to 110 degrees with an average of 70 degrees . A M_W shaped image has been observed , total length being 120 to 160 nm (Erickson et al. 1981).

Other teams (Koteliansky et al. 1981 , Tooney et al. 1983) report a "Patch" type structure with average dimensions of 15.5 by 8.8 and 16 by 24 nm respectively.

Some of those structures are presented in Fig I 3 below.

I 7 2 Results from analytic centrifugation.

Numerous results are available and are summarised in Table I 3 below.
(From : Alexander et al. 1978 , Kotelianski et al. 1981 , Tooney et al. 1983 , , Lai et al. 1984).

Table I 3 : Results from analytical centrifugation studies

Sample .	Buffer composition (mM).	pH	S Values (Svedberg)
Complete Fibronectin.	KCl 100 , NaP 50	7	13
" "	Same	9	11.8
" "	Same	11	8
" "	TES 20 , NaCl 150	7.4	13.5
" "	" NaCl 750	7.4	6.7
" "	1% AceticAcid	2.8	4.8
" "	AceticAcid 20 , NaCl 150	3	10.3
" "	NaCl 150 , TES 20	7.4	13
" "	" TRIS 20	9.2	12.7
" "	" CAPS	10.8	8.4
" "	NaCl 50 , TES 100	7.4	13
50 kD coll-binding domain.	Same buffer		3.3
72kD N-Terminal domain.	Same buffer		4.1
120 kD C-Terminal domain.	Same buffer		5.4
170 kD C-Terminal domain.	Same buffer		4.4
170 kD C-Terminal domain.	Same buffer		10.5
!90 kD C-Terminal domain.	Same buffer		13

I 7 3 Results from disulphide bond investigation.

The fibronectin molecule in its plasma form possesses 29 intra chain and two inter-chains disulphide bonds per 250 KD subunit.

It is important to notice that the susceptibility to reducing agents of the inter and intra chains bonds is relatively similar as shown in points A to C below . All these data suggest that the links between the two chains are not very accessible to the solvent.

A) When 90 % of the inter-chains bonds are reduced, nearly 30 % of the intra-chain bonds have also been reduced. (Engel et al. 1985).

B) Furthermore as reduction causes an unfolding of the molecule , which can be monitored by dynamic light scattering , the gelatin binding property is lost before any macromolecular conformational change is observed (Williams et al. 1983). Appearance of a macromolecular change in conformation after reduction is also relatively slow.

C) An immunological study (Vuento et al. 1980) has shown that the reactivity of human plasma fibronectin and its fragments to rabbit anti fibronectin antibodies is perturbed by alkylation or reduction resulting in high loss of antigenicity . A large fragment of 180 to 200 kD lacking only the C-Terminal region (which includes the inter-chain disulphide bonds) has the same immunological reactivity as the intact fibronectin molecule .

I 7 4 Results from denaturation.

Those results are very important because they confirmed the existence of the multidomain structure of fibronectin as suspected from circular dichroism studies. Thermal denaturation profiles show the denaturation of six to eight independent domains and also that the thermotropic properties are unaltered between pH 7 to 10 (Koteliansky et al. 1981 , Franceschi et al. 1985). Thermal influence on intrinsic or label fluorescence of fragments or complete fibronectin has been investigated (Ingham et al. 1984). The collagen binding domain (Chymotryptic digest 42 K D) retains its functional activity even after heating at 85 C where its fluorescence parameters did not show any transition. The N terminus 25 K D heparin binding domain also seems resistant to temperatures up to 85 C . The central 140 kD domain ,lacking the type I or type II homologies, is the least stable and shows a denaturation profile close to that of complete fibronectin.

I 7 5 Models of fibronectin conformation in solution.

As pointed out before there seems to be little interest in the study of the three-dimensional structure of fibronectin. Not considering the very low resolution sedimentation studies , five major works were devoted to this topic:

A) Williams et al. (1982) from fluorescence , intrinsic viscosity and dynamic light scattering measurements has proposed a flexible elongated structure susceptible of increase in flexibility and decrease on dimensions after binding of a cyanogen bromide fragment of collagen (α 1 (I) CB 7) .Their calculated axial ratio varies from 8/1 to 22/1 . The translational diffusion coefficient (Dt) value is 2.26 10^{-7} c.g.s. in phosphate buffer at neutral pH ,2.15 10^{-7} and 1.55 10^{-7} at pH 9 and 11 respectively . Dt is insensitive to temperature in a 10 to 37 C range but decreases from 2.2 10^{-7} to 2.4 10^{-7} c.g.s. with addition of collagen fragments.

B) Rocco et al. (1983, 1987) , from solution light scattering measurements (at pH = 8) , including a not-quite-satisfactory measurement of radius of gyration by light scattering proposed a model based on the succession of rigid beads , each bead representing an internal homology . Their values for the radii of gyration are 17.5 nm in 1M NaCl buffer and 10.7 nm at physiological salt concentrations.

C) Homandberg (1986) based his model on a new and original approach studying the interactions between purified domains , and between purified domains and complete fibronectin . His main conclusion is that there are two main interactions : C-Terminal part of the molecule with itself and with the N-Terminal end. In an other paper (1987) he showed the inaccessibility of N terminal region to solvents .

D) Hormann et al. (1986) used the same approach and analysed the distribution of charged residues along the protein.

E) Sjoberg et al. (1987) measured the radius of gyration by small angle x-Ray and neutron scattering and analysed the intensity as a function of Q . The conclusions from those authors are that fibronectin is a oblate ellipsoid particle of semi axis 1.44 and 13.8 nm with a volume of 1150 nm^3. They suggested to chose the the model of Hormann with inter-chain interactions.

Some of the models derived from those studies are presented in Fig I 3 below.

Fig I 3 .

Models of fibronectin three-dimmensional structure

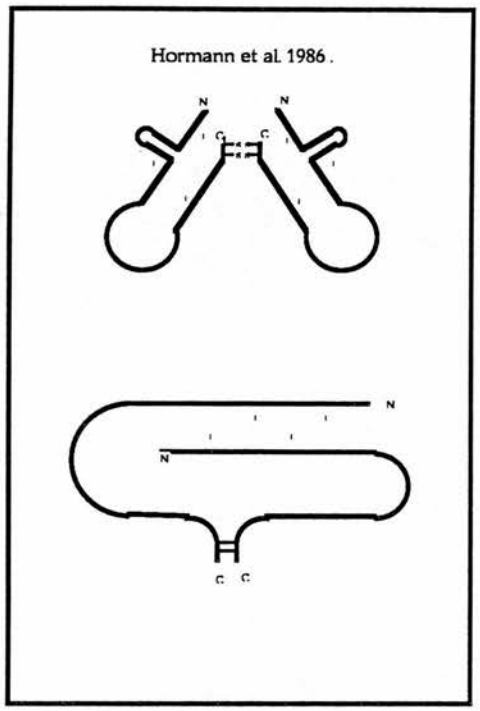

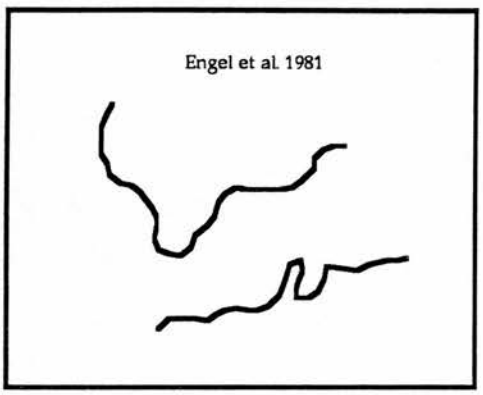

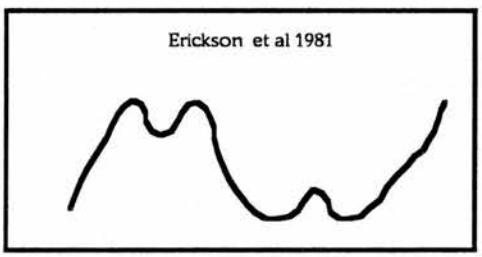

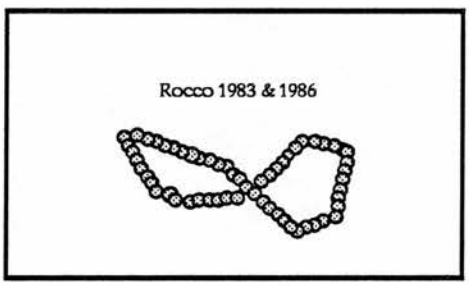

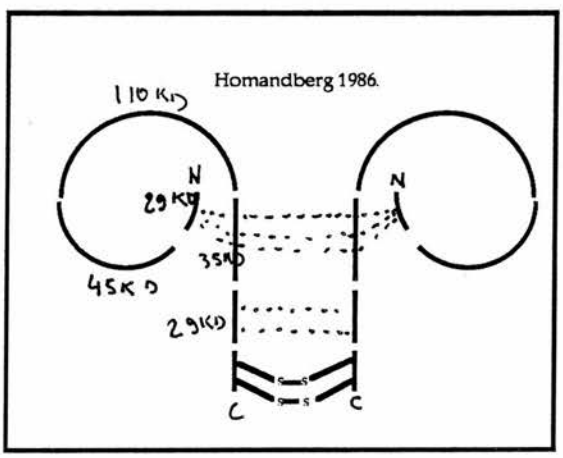

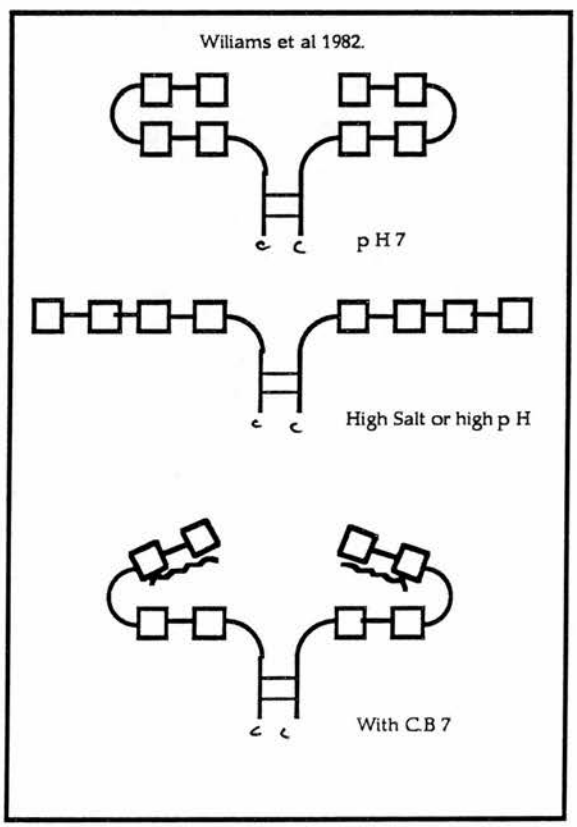

I 7 6 Transitions in conformation.

Three different ligands are reported to alter the conformation of fibronectin.

A) **Heparan sulphate** : Osterlund et al. (1985) studied the circular dichroism spectra of fibronectin in presence of cellular heparan sulphate and showed a change in the spectra he attributed to a conformational change in the fibronectin molecule .

B) **Heparin** : Welsh et al. (1983) also detected changes in conformation of fibronectin upon heparin addition by measurement of C.D. properties. The conclusion from those results was similar to those from A , unfortunately although the two ligand are very similar, the effects on the spectra appears to be rather different. This will be discussed in Section VI 6 . An electron spin resonance study by Ankel et al. (1986) also reported a conformational change due to heparin binding but at least some of those conclusions are probably incorrect as discussed Chapter VI, section 6 .

D) Williams et al (1982) showed that the diffusion coefficient of plasma fibronectin varies with addition of cyanogen bromide fragment & of **type I collagen** from its initial value of 2.4 10^{-7} to 1.19 10^{-7} and 2.08 10^{-7} upon addition of respectively 2 and 4 moles of collagen peptide per mole fibronectin.

I 8 FUNCTIONAL PROPERTIES.

I 8 1 Heparin binding

Heparin interactions with fibronectin have been widely studied .Heparin has been shown to form cryoprecipitates with fibronectin (Stathakis et al. 1977 , Jilek et al. 1979) . All those studies refer to heparin which is generally used as a model for cell surface heparan sulphate , the carbohydrates type encountered by Fn in vivo, (Hedman et al. 1982).

All fibronectin domains generated by thermolysin digest except the 40 kD gelatin binding domain , the C terminal 30 kD fibrin binding domain and the 3 kD interchain linking region bind to heparin . The fragments binding to heparin are shown in bold type in diagram below which presents the position and molecular weight of thermolysin generated domains :

α subunit : H_2N------ **28** - 40 -**14- 110** -**38** -30 -3--------- COOH

β subunit : H_2N------ **28** - 40 -**14- 110** - **29**-30 -3--------- COOH

The strong binding site (underlined), is insensitive to pH variations and calcium ions and it is possible that some sites might be hidden in the native intact molecule (Siri et al. 1986) .The weak binding sites which are inefficient at physiological salt concentrations , might only be due to non specific ion-exchange type interactions .

The best investigation of the binding is a study by Bentley et al. (1985) , of both heparin binding and heparin-induced cryoprecipitation in solution by fluorescence polarization. They found ,in physiological buffers ,two sites (per subunit) with dissociation constants values of 10^{-6} and $3.5\ 10^{-8}$ M. They showed that despite the fact that a significant amount of binding still occurs at 0.5 M ionic strength, cryoprecipitation, for which optimum ionic strength is from 0.05 M to 0.1 M , is fully abolished at ionic strength superior to 0.3 M .They also reported that binding was quicker and required lower fibronectin concentrations to occur than cryoprecipitation . Cryoprecipitation also seems to reduce the flexibility of the molecule.

According to a study on immobilised heparin , the binding with intact fibronectin seems inhibited by physiological concentrations of calcium (Siri et al. 1986). This is surprising considering the position of fibronectin in the extracellular matrix . But Richter et al. (1985), reported that precipitation by heparin is inhibited by calcium ions .

Welsh et al. (1983), Osterlund et al. (1985) Ankel et al. (1986) reported a conformational change due to heparin or heparan binding , this has been described above in I 7 8 .

Precipitation of radio-labeled fibronectin occurs slightly even at 37 degrees and electron microscopy study of the precipitate reveals fibrils leading to the hypothesis that heparin binding could uncover the polymerisation sites of fibronectin . Cryoprecipitation is a heparin concentration dependent phenomenon and is saturable . (Richter et al. 1985) .

Ogamo et al. (1985) described the interaction of fibronectin with various classes of heparin .

Heparin binding has also been shown to enhance the binding of fibronectin to collagens of various types (See I 8 2 below).

I 8 2 Gelatin-Collagen binding .

The binding between fibronectin and collagen-type proteins or their denaturation products was reported by Engvall et al. (1978) . It has provided a very easy purification method of fibronectin based on affinity chromatography on immobilised gelatin .

The binding site of collagen on the fibronectin molecule has been characterized first as a domain (Balian et al. 1978) then sequenced on the bovine plasma molecule (Skorstengaard et al. 1983) and finally by expression in E. coli (Owens et al. 1986) revealed as a linear 14 residues sequence after the second type II homology , (Starting residue 434). This sequence is:

434

Ala-Ala-His-Glu-Glu-Ile-Cys-Thr-Thr-Asn-Glu-Gly-Val-Met.

The nature of the binding with collagen is unclear . It clearly is resistant to as high salt concentrations as 2 M Na Cl ,(Forastieri et al. 1985 and personal data presented in the section of this thesis on preparation of the fibronectin molecule).

Chemical modification of arginine residues , (Vuento et al. 1983) , destroys this interaction but this is now thought to be be due to a loss of structure involving modification of all the molecule rather than an arginine residue being really involved in the interaction since no Arg is present in the binding sequence. On the other hand fibronectin can be eluted from gelatin columns by elution in the presence of 1 M Arg.

Fluorescence polarization experiments , (Forastieri et al. 1983 and 1985) , were carried out on two different systems :

A) Complete fibronectin- [gelatin-fragments] system

B) [42 kD gelatin binding domain of fibronectin]- gelatin system.

The results show that there is positive cooperativity in the case of system A with two dissociation constants of approximately 10^{-8} and 10^{-9} M : The second set of experiments (B) gave values for dissociation constants in solution ranging from $3\ 10^{-8}$ M in 10 mM phosphate pH 7.3 to $61\ 10^{-8}$ M in tris 100 mM NaCl 150 mM .

Various parameters can modulate this binding.

A)The interaction is stronger in the presence of Heparin (Jilek et al. 1979) .

B) The presence of carbohydrates on the molecule seems to weaken the interaction ; the effect of glycosylation on fibronectin properties has been studied by Jones et al. (1986) in a comparative study of cellular fibronectin produced in cell culture in presence or absence of tunicamycine. Cellular fibronectin produced in the presence of tunicamycin and therefore with no carbohydrate side-chains shows an increase in cell attachment as shown by a cell attachment assay and collagen binding efficiency. (Urea concentration superior to 3 M is required to elute nonglycosylated fibronectin from a collagen column while normal fibronectin is eluted at lower urea

concentrations). In a similar way increased glycosylation as in placental fibronectin decreases the affinity between fibronectin and collagen. (Yamaguchi et al. 1986).

C) The binding depends on the size of the fibronectin fragment : It is stronger with a small 40 kD chymotryptic collagen binding domain than with a slightly bigger 60 kD collagen binding domain. (Griffin et al. 1986). We must note that those two latter findings do not prove that the binding itself is affected and it might well be that only the urea denaturation is made easier .

The binding of fibronectin on collagen varies with various collagen types:

A) The binding is possible with many types of collagen at least types I , II , III , IV . They show the same affinity in a denatured form but native type III is more active than native type I or II . (Engvall et al. 1978) .

B) With type I collagen , it occurs on CB 7 fragment , precisely on residues 757 to 791 (Kleinmann et al. 1978 ,Dessau et al. 1977). Gross unfolding of the molecule is not required (Ingham et al. 1985) but a study with immobilised collagen binding domain shows that the binding with native type I occurs at 37 C but not at 4 C. (Engvall et al. 1981) suggesting the necessity of a slight unfolding of the collagen molecule .

C) On type IV collagen of the basement membrane the binding occurs as shown by immuno-electron microscopy at the free end of the long arm(Aumalley et al. 1986).

D) Binding with fibronectin seems to delay the rates of self assembly of collagen type III and accelerate the rate of type I .

E) The collagen-like tail of Acetylcholine esterase and of complement factor C1q can also bind fibronectin (Grassi et al. 1983) .

I 8 3 The main cell binding site on the fibronectin molecule.

The major cell attachment site on the fibronectin molecule has been characterised as a single tetrapeptide Arg-Gly-Asp-Ser "RGDS" (Ruoslahiti at al. 1984).The sequence RGDS and its reverse sequence SDGR bind to cells in suspension and inhibit BHK cell adhesion (Akiyama Et al. 1985a). This sequence is also the one recognized by the vitronectin and thrombospondin receptor .

A 80 k D cell binding domain synthesized by expression in E.Coli of its cDNA has been shown to be as active , for cell attachment , as complete fibronectin . Then post translation modifications like glycosylation or phosphorylation are not required for full cell adhesion property . But a 30 kD fragment was 50 times less active than the whole molecule showing the necessity of the environment of the peptide for full function. (Obara et al. 1987) . Furthermore a 75 kD tryptic fragment containing this sequence is able

to promote both cell spreading and motility but when restricted to a 11k fragment still containing RGDS the motility promotion is lost . (McCarthy et al. 1985).

The dissociation constant for the fibronectin-receptor interaction ,with cells in suspension , has been determined by two teams as 1.7 10^{-8} with 280,000 receptors per cell and 3.6 10^{-8} with 128,000 receptors per cell (respectively Johansson 1985 and McKeownlongo et al. 1983) .It seems (Chernoussof et al. 1985 & Pesciotta et al. 1987) that cell layers in culture, have saturated fibronectin binding sites as shown by the very small incorporation of exogenous labelled fibronectin or fibronectin fragments.

Cell binding can be modulated by collagen (Nagata et al. 1985) but type I collagen cellular receptor recognizes the RGDS peptide therefore the real influence of fibronectin and collagen in this modulation might be difficult to define . (Dedhar at al. 1987).

Recent studies suggest that the mechanism chosen by certain infectious agents also rely on an RGDS - Cell interaction ; infection by trypanosome uses a peptide modelled on RGDS (Ouaissi et al. 1984 & 1985).

It is important to notice that many of the studies involving cell binding function use a cell attachment assay where fibronectin or its fragments are adsorbed on the surface of a culture dish . The question is whether fibronectin distribution is even on them. A recent study with scanning electron microscopy determination of the adsorbed material ,shows that, in the conditions used by those authors, fibronectin distribution is even in certain places and forms a network in other parts . Therefore some results might be affected by this problem. (Murthy 1987). Furthermore the general images of fibronectin adsorbed on electron microscope grid are very different from the structure suggested by studies of fibronectin in solution raising further doubts on the retention of conformation after adsorption on cell culture dishes.

The cellular receptor to fibronectin will be described below in section I 14 2.

I 8 4 Alternative cell binding sites on the fibronectin molecule.

A possible other binding site has been identified at the mid-third of the molecule (Donaldson et al. 1985) ;possibly as 70 kD N terminal fragment promoting a cell-binding insensitive to RGDS , collagen or heparin (McKeownlongoet al 1985). This could be confirmed since the assembly in matrix requires both the 30K N-terminus end and the 110 K cell binding domain (McDonald et al. 1987) . And also the effects of cell binding domain and heparin binding domain are cooperative and resemble those of the whole molecule. (Beyth et al. 1984).

An alternative spliced site moduling cell type specificity has been reported , apparently by one team only , (Humphfries et al. 1986) .

I 9 VARIOUS OTHER BINDINGS.

I 9 1 DNA binding properties of fibronectin .

DNA binding of fibronectin and its fragments was studied by Siri et al. (1986) . It is sensitive to calcium ions and pH variations , it may occur with all thermolysin generated fragments except the 40 kD collagen binding and the 20 and 3 kD last C terminal domains . Despite the fact that Zardi et al. (1979) found some reactivity to anti-fibronectin antibodies in intranuclear material, the DNA binding of fibronectin seems to rely on simple ion exchange mechanism with the polyanion created by DNA molecule at near neutral pH and has little chance of having any physiological significance anyway since fibronectins are extracellular proteins.

I 9 2 Fibrin binding of fibronectin .

Binding between fibronectin and fibrin was shown by Stathakis in 1978 . The complexes between fibrinogen and fibronectin are cryo-insoluble . There are two binding sites : one is the N-Terminal 28 kD domain, the other the C-Terminal 31 KD domain ; the 31 kD domain requires 2mM Ca2+ and 0.15 M NaCl for binding but raising the temperature to 25 C seems to disrupt this interaction (Garcia-Pardo 1985).

I 9 3 Various other bindings.

In addition to the major binding properties reviewed above and presented in Fig. I 1 , fibronectin can also bind to various other biological material ,like :

A) Thrombospondin (Homandberg 1987b),

B) Bacterium and viruses including a transforming virus : RD114 ,p30 (Salonen et al. 1984)

C) Plasminogen activator (Salonen et al. 1985 , this might be important in cancer related degradation processes , see below in I 18)

D) C reactive protein (Salonen et al.1984) .

D) Gangliosides , through fibronectin 31 k D N-terminus end with a Kd of $1.4\ 10^{-8}\ M^{-1}$.

I 10 POLYMERISATION.

I 10 1 Polymerisation in vitro.

Two ways to induce fibronectin polymerisation in vitro are known , they both rely on disulphide bonding .

A) Williams et al. (1983) used guanidinium chloride ; exposure to at least 1 M guanidinium chloride ,(Optimum at 3 M) , resulted in exposure of 1.5 to 1.9 cryptic free SH groups and polymerisation. Blocking the free SH groups by N-Ethylmaleimide inhibits this polymerisation. Heparin,fibrin,hyaluronic acid deoxycholate , methylamine , EDTA or calcium ions have no effects on the polymerisation , (The authors omitted that in those conditions ,with a guanidinium-chloride concentration higher than 1 M, binding to collagen or heparin was impossible).

B) Vartio (1986) used various metal salts at a milimolar range from pH 7 to 9 and noticed two different types of polymerisation ,both accelarated by an increase of temperature .

α) $CuSO_4$ induced polymerisation , according to this author, is dependent on the free SH groups and occurs only within a 140 kD C terminal fragment where the free SH are. It is inhibited by blocking the free SH by N-Ethylmaleimide .

β) $FeCl_3$ induced polymerisation is possible by disulphide exchange in the type I or type II homologies as shown by the possible polymerisation of 30 kD N-terminal domain 40 kD collagen binding domain and the 120-140kD C terminal domain. Furthermore this $FeCl_3$ induced polymerisation is possible even after exposure of fibronectin to N-Ethylmaleimide .

I 10 2 Polymerisation by cellular systems.

Experiments of binding of labelled fibronectin to cells in culture , (McKeownlongo et al. 1983 & Fellin et al. 1988) , shows two different steps in fibronectin incorporation into matrix : First binding to cells in a deoxycholate sensitive mode (this corresponds to the binding of fibronectin to the cellular receptor), and then formation of deoxycholate insoluble fibrils by polymerisation of fibronectin.

Exchange in the N terminal region seems to explain this because iodoacetamide treated (free SH blocked) fibronectin is still incorporated normally in the matrix and

cathepsin G generated N-terminal 28 K D domains can be aggregated as large multimers in cell culture. (McKeownlongo Et al. 1985). This is confirmed in a recent study where the site responsible for polymerisation by cells is located in the 28 kD N-terminal domain (Mc Donald et al. 1987).

I 11 CROSSLINKING OF FIBRONECTIN.

Fibronectin can be cross linked with collagen by factor VIIIa (Mosher et al. 1979). Two sites have been shown to accept the factor VIIIa induced crosslink : the residue number 3 (Mosher et al. 1979 &McDonagh et al. 1981) and a site in the heparin binding domain (Fetsus et al. 1985). The crosslink with collagen has been proved on collagens type I (precisely on fragments CB7 and CB 8 of α1(I) collagen), Type II , Type III and Type V . Crosslink with collagen type IV has not been proven in the same study (Mosher 1984).

Crosslink to adsorbed fibronectin on glass plates is also possible with a 47 Kd intracellular protein (Aplin et al. 1981).

I 12 VARIOUS OTHER PROPERTIES.

As an enormous amount of work is devoted to fibronectin (over 400 published papers a year), various odd functions and properties have been described . Amongst the most significant were:

A) A possible proteolytic activity as S protease , coupled with self inhibition ,of fibronectin has been shown by Veil-Douhala et al. (1986) by study of fibronectin self degradation and demonstration of homology between the sequence of a type III homology of fibronectin and the sequence of SH protease inhibitors.

B)Fibronectin fragments can increase the DNA synthesis by cells in culture (Humpfries et al. 1983).

I 13 FUNCTIONAL ANALOGUES.

Other , often multidomain-multifunctionnal, proteins involved in cell anchoring are known such as :

A)Laminin present in basement membranes .

B) CAM: Cell adhesion molecules (Review by Edelman 1983) .

C) Thrombospondin from platelets and tissues or cells in culture .

D) Vitronectin also called spreading factor (Review by Ruoslahiti et al. 1987) present

in plasma,cell culture or tissues.

Some extracellular collagen-gelatin binding proteins have also been described with molecular weight of 56,62 and 47 kD ;the latter one is called Colligin and is the only one to bind to native type IV collagen (Kurkinen et al. 1984).More recently a 21kD protein was discovered (Keski-Oja et al. 1986).

I 14 FIBRONECTINS IN CELL ANCHORING PROCESS.

I 14 1 Cellular receptors to fibronectin.

Many fibronectin receptors in various cell lines have been described:

A) A 48 K receptor stabilized by Calcium but not Magnesium (Oppenheimer-Marks et al. 1984 a).

B) Two receptors 140 Kd and 45 Kd immunologically different (Urushihara et al. 1985).

C) Adhesion of cells mediated by a 145 kD or 140 kD plasma membrane receptor (Giancotti et al. 1985 , Akiyama et al. 1986 b).

D) The fibronectin receptor on platelets was described as: IIb .IIIa platelet membrane receptor complex common to fibronectin ,Von Willebrand factor and vitronectin (Pytela et al. 1985 a) .

E) Virtanen et al. (1987 a) report three receptors 45, 140, 170 kD the 140 kD being lost after transformation. But Pytela et al. (1985 b) observed the 140 kD receptor in osteosarcoma cells in culture .

F) Receptors in rat hepatocytes and fibroblasts have been prepared by affinity chromatography on immobilised fibronectin (receptor remaining bound under 1 M NaCl but released by 1.5 mM RGDS.) they appeared as 155 and 105 kD under non reducing changing to 145 k +20 k and 130 k respectively after reduction .

I 14 2 Description of the "140 Kd " cellular receptor of fibronectin.

Better biochemical characterization and cDNA cloning of the α subunit of the " 140 kD " receptor (Pytela et al. 1985 a & b 1986 , Argraves et al. 1986), define the receptor as noncovalent complexes of α and β subunits.

The α subunit being composed of two disulphide bonded chains of Mr 20 to 30 kD and 140 to 120 kD, the β subunit being composed of one chain of 90 to 140 kD . This receptor shows important primary structure similarities with the vitronectin receptor .

The light α chain should be the anchoring point of the receptor in the membrane

because it contains at its C end approximately twenty hydrophobic aminoacid residues. Reaction with antibodies raised against the beta subunit of rat fibroblast receptor suggests that the cell line specificity is in the alpha subunit .

Inhibition by monoclonal antibodies against this receptor shows that only a small fraction of the existing 140 k D receptors is required for adhesion (Brown et al 1987). A possible consequence is that receptors might exist both on the surface and internally to form a pool of spare receptors, as suggested by Molnar et al. (1987).

The fibronectin receptor is a real membrane protein : Horwitz et al. (1986) described a continuity between fibronectin , its receptor and an intracellular protein , talin .This has been suspected since a long time as Ali et al. in 1977, showed that fibronectin could be released from cell surfaces after cytochalasin treatment. The shape of transformed cells can be normalized by addition of exogenous fibronectin or RGDS peptide(Chen et al. 1986) . Continuity between the receptor and the cytoskeleton is also shown by colocalisation of fibronectin-140kD receptor and microfilaments bundles (Duband et al. 1985).

The 140 k receptor distribution on the cell is changed by transformation (not only infection by transforming virus as shown by temperature sensitive mutants) , Transformation of chick embryo fibroblasts by SV 40 virus is also associated with phosphorylation of the receptor . After transformation despite the fact that the receptors are still expressed ; the continuity:

[extracellular -fibronectin]-[receptor]-[microfilaments]

is lost , the receptors do not bind fibronectin anymore , and show only little adherence to vitronectin (Chen et al. 1986). Actin is then localised more at the periphery of the cells and this is coupled with a loss of cell-attached fibronectin (DiRenzo et al. 1985).

Investigation of the number of receptors during development in rats shows a strong decrease just before birth and keeping to a low level after. (Kawasaki et al. 1986). In a possibly similar way artificially induced lung injury is followed by an increase of the number of receptors at the surface of macrophages (Kradin et al. 1986).

I 15 LOCALIZATION OF FIBRONECTINS.

Historically the fibronectin molecule was discovered as a cold insoluble globulin from plasma by Morisson et al. (1948). In fact those authors purified the complex between fibrinogen and fibronectin which is cold-insoluble. Fibronectin alone is perfectly soluble at near zero temperatures.

Fibronectins are present as the plasma type at a mean concentration of 300 mg/l , with apparently wide differences between individuals. Cellular type fibronectins are

one of the major components of the extracellular matrix of cells in culture with the heparan sulphate proteoglycan and type I collagen (Hayman et al. 1982 , Woods et al 1984). Fibronectins seems to be present in all tissues (Steneman et al. 1978). More detailed studies have shown various type of associations such as: association with type IV collagen and heparan sulphate proteoglycan in the basement membranes (Laurie et al. 1982 & 1983), with type II collagen in cartilage (Glant et al. 1985).

I 16 POSITION OF FIBRONECTINS IN THE CELL-MATRIX INTERACTION.

Fibronectin and its receptor are one of the links between the extracellular matrix , (particularly collagen and heparan sulphate proteoglycans) and the intracellular cytoskeleton. Those links have been described with the cellular receptor to fibronectin in I 14 .

I 17 FIBRONECTINS INVOLVEMENT IN BIOLOGICAL PROCESSES.

I 17 1 Development.

Fibronectin has been shown to be associated with moving cells in embryos (Sternberg et al 1986). Antibodies against fibronectin receptor have also been shown to strongly perturbate normal embryo development (Bonner-Fraser et al. 1986). From those two examples , (amongst many other similar studies) , it is clear that fibronectin plays an important role in cell motion and development processes but its exact function is at present still undetermined. It is also interesting to note that the amount of cell surface fibronectin is reduced during the mitotic events , (Steneman et al. 1977), possibly correlated to the need of looser cell support connection to allow cell division.

I 17 2 Wound healing.

Fibronectin is involved in cell motion and therefore plays a role in wound healing. This topic has been investigated particularly in the field of ophatalmologic lesions . The work of T. Nishida in Japan and M.Berman in the U.S.A. seems the most important contribution but will not be reviewed here.

I 18 FIBRONECTIN INVOLVEMENT IN CANCER PROCESSES.

I 18 1 Modifications at the molecular level.

The differences between fibronectins produced by normal and transformed cells have been described in paragraphs I 2 , I 3 & I 4 . Briefly fibronectin from transformed cells have different primary structures , glycosylation ,phosphorylation .

I 18 2 Modification of synthesis and localisation.

Although the plasma levels of fibronectin are unchanged in patients with cancer diseases (Kawamura et al. 1983) , the synthesis of fibronectin by cell in culture is modified by transformation.

The first work relating fibronectin to transformation problems showed that addition of anti-fibronectin antibodies to the media of normal fibroblastic cells in culture , resulted in the loss of the normal morphology and appearance of transformed like rounded cells (Yamada et al. 1978). Reduction of synthesis in the matrix was reported by Smith et al. (1978) . Addition of transforming growth factor β to cell in culture results in an increase in fibronectin mRNA synthesis (Ignotz et al. 1986). Transformation of chick embryo fibroblasts by Rous sarcoma virus results in an increase of fibronectin synthesis but a decrease of incorporation in the matrix (Wen-Tien et al. 1984); this is coupled with a lack of extracellular heparan sulphate (Hayman et al. 1982). Di Renzo et al (1985) showed that non metastatic lines of transformed cells retained fibronectin better than the metastatic ones.

Although fibronectin involvement in the modification of the matrix and of cell shape ,(possibly due to action of the matrix on cytoskeleton through transmembranne links like the fibronectin-receptor), induced by transformation is clear, studies trying to correlate tumoregenicity and fibronectin incorporation in cell matrix have failed. This is no surprise considering the number of possible factors involved:

A) Changes in the fibronectin rates of synthesis and degradation .

B) Changes in fibronectin receptor number and affinity.

C) Changes in the system responsible for fibronectin incorporation into the matrix.

D) Changes in the extracellular matrix molecules that can bind to fibronectin.

E) Changes involving other adhesion molecules such as Laminin and thrombospondin.

A better understanding of all those factors will be required to explain the role of fibronectin , at cellular and tissue level, in cancer processes .

I 18 3 Degradation.

If there is no agreement on the modifications of synthesis of fibronectin after transformation, there is aggreement on the fact that fibronectin (as well as the other molecules from the extracellular matrix , see review by Tryggvason et al 1987) , undergoes substantial degradation by tumour cells:

A) Release of small (Mw less than 30 kD) peptides fragments from fibronectin covalently bound to collagen layers is increased 3 fold in transformed cells (Wen-Tien et al. 1984); this degradation process is sensitive to 1-10 phenantrolene.

B) The work of Vartio (1980) shown how a matrix of fibronectin could be degraded by a metal activated proteinase.

C) A guanidinobenzoatase has been described as associated with tumours in vivo and used for histological determination of tumours by Steven et al. (1985)

I 18 4 Transforming enhancement properties.

The collagen binding domain from fibronectin purified from metastatic cancer patients or produced by tumour cells in vitro was shown to possess transforming enhancement properties on cultured normal fibroblasts. (DePetro et al. 1983)

I 19 CONCLUSION OF CHAPTER I.

From this review it can be seen that despite the fact that fibronectin has been very much under study , its physicochemistry is still poorly understood . In subsequent chapters various physicochemical techniques , such as light scattering , neutron scattering and electric birefringence will be introduced and applied to study fibronectin's solution structure.

CHAPTER II:
BIO-PHYSICAL TECHNIQUES.

II 1 PHOTON CORRELATION SPECTROSCOPY.

II 1 1 Introduction.

This technique, first described by Pecora (1964), allows direct determination of the translational diffusion coefficient D_t. It has several advantages :

a) The error is limited to a few percent. In some conditions used in this work it even seemed to be less than 1 %, see IV 3 below.

b) 15 minutes only are required to do a measurement.

c) It is an absolute technique requiring no calibration.

d) A ligand can be added or the buffer conditions can be altered in the same sample.

e) The temperature can be adjusted over a wide range.

f) 500 µl of sample only are required. Just before this work was completed a way was found allowing measurements with a sample volume of less than 100 µl .(see II 1 11 below).

g) To some extent an estimation of D_t is possible even with polydisperse samples.

II 1 2 Principle of photon correlation spectroscopy : Relation between the correlation function and the translational diffusion coefficient D_t.

This technique has been reviewed by Berne and Pecora (1974). The light scattered by a very small volume of the sample is detected by a photomultiplier . The intensity of scattered light is proportional to the concentration of the scattering particles . In a very small volume because of the Brownian motion of the particles the concentration fluctuates . Those fluctuations are linked to the ability of the particles to diffuse in the solvent and therefore to the diffusion coefficient. Pecora (1964) showed that the first order normalized correlation function was linked to D_t :

$$g_1(\tau) = \exp(i\omega_0\tau)\ \exp(-\Gamma\tau) \qquad (II\ 1\ 1)$$

Where: $g_1(\tau)$ is the value of the normalized first order autocorrelation function for delay time τ .

ω_0 is the frequency of the incident light.

Γ is a constant equal to $D_t K^2$ with $K = 4 \Pi (n / \lambda) \sin (\theta / 2)$ (θ is the angle of scattering, n the refractive index of the sample).

As described below, in photon correlation spectroscopy an actual measure of the second order correlation function ($g_2(\tau)$), is obtained. Since $g_2(\tau)$ is related to first order correlation function ($g_1(\tau)$), $g_2(\tau)$ may readily be used to yield a value for D_t.

II 1 3 Description of the spectrometer and raw signal acquisition.

All light scattering work in this thesis has been carried out with a 4700C system built by Malvern instruments (Malvern U. K.).The spectrometer can be seen on Fig. II 1 and Fig. II 2. It comprises the following :

1) A cell holder allowing the cell containing the sample to be in a thermostated, index matching waterbath .Temperature was adjusted to a selected value above room temperature by a heating resistor controlled by a thermostat . Generally a temperature of 25 °C was used , slightly over the ambient temperature of 23 to 24°C.When lower temperatures were required , ice cold water was circulated in a heat exchange coil until the appropriate temperature was reached . Temperature was then constant , to less than +- 1 ° C ,in the small time period required to perform a measurement .The water of the index matching bath could be filtered by recirculation with a peristaltic pump through a 0.22 µm filter (Millipore France) to remove any dust which would create a high background.The pump was systematically run for 15 minutes prior to any measurement session.
2) A stepper motor driven turntable : This device allowed a photomultiplier angular positioning with a precision better than 0.1 degree. The angular position (θ) of the photomultiplier was directly controlled through the user computer.
3) A photomultiplier equipped with a special optical device ,(see fig II 3) :
   a) A focusing lens .
   b) One vertical slit and a rotatable turret presenting micron range aperture pinholes to restrict the measuring field.
   c) An interference filter to limit the detection to the proper scattering wavelength.

Fig II 1 :
Side view of the Malvern 4700 c spectrometer.

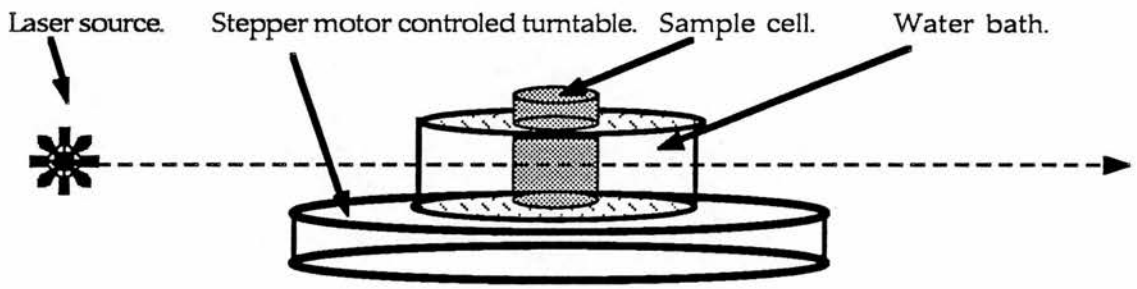

Fig II 2 :
Top view of the Malvern 4700 c spectrometer.

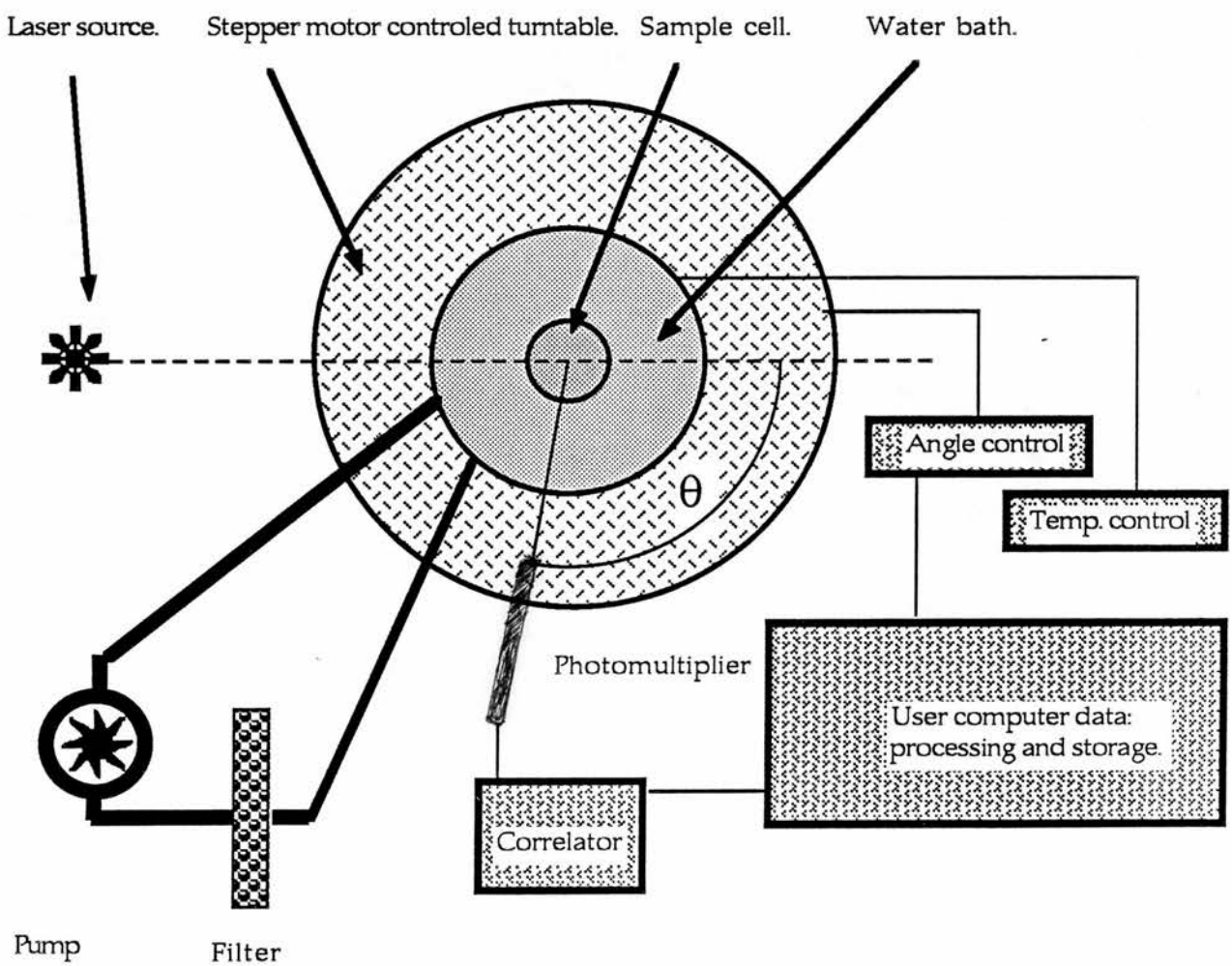

These elements allow restriction of the measurement of the scattered light to a very small volume . It is important to notice that what is in fact really measured in the 4700c Malvern system is not the light fluctuations , directly due to the particle concentration fluctuation but the light fluctuations due to interference created by the scattering of coherent light by particles in motion .This is referred to as fluctuation spectroscopy as opposed to concentration spectroscopy.The main advantage of fluctuation spectroscopy over concentration spectroscopy is that it can be done with much larger measuring volumes , thus the optical requirements are much more easy to achieve . For those practical reasons fluctuation spectroscopy is widely used.

An analogue to digital converter is included in the photomultiplier so its output is pulsed. The pulse frequency is directly proportional to the intensity of scattered light in the measured volume.

Fig II 3 below shows the disposition of those elements as well as the viewfinder which helps during the optical alignment procedure of the system.

Fig II 3 Photomultiplier optical equipment.

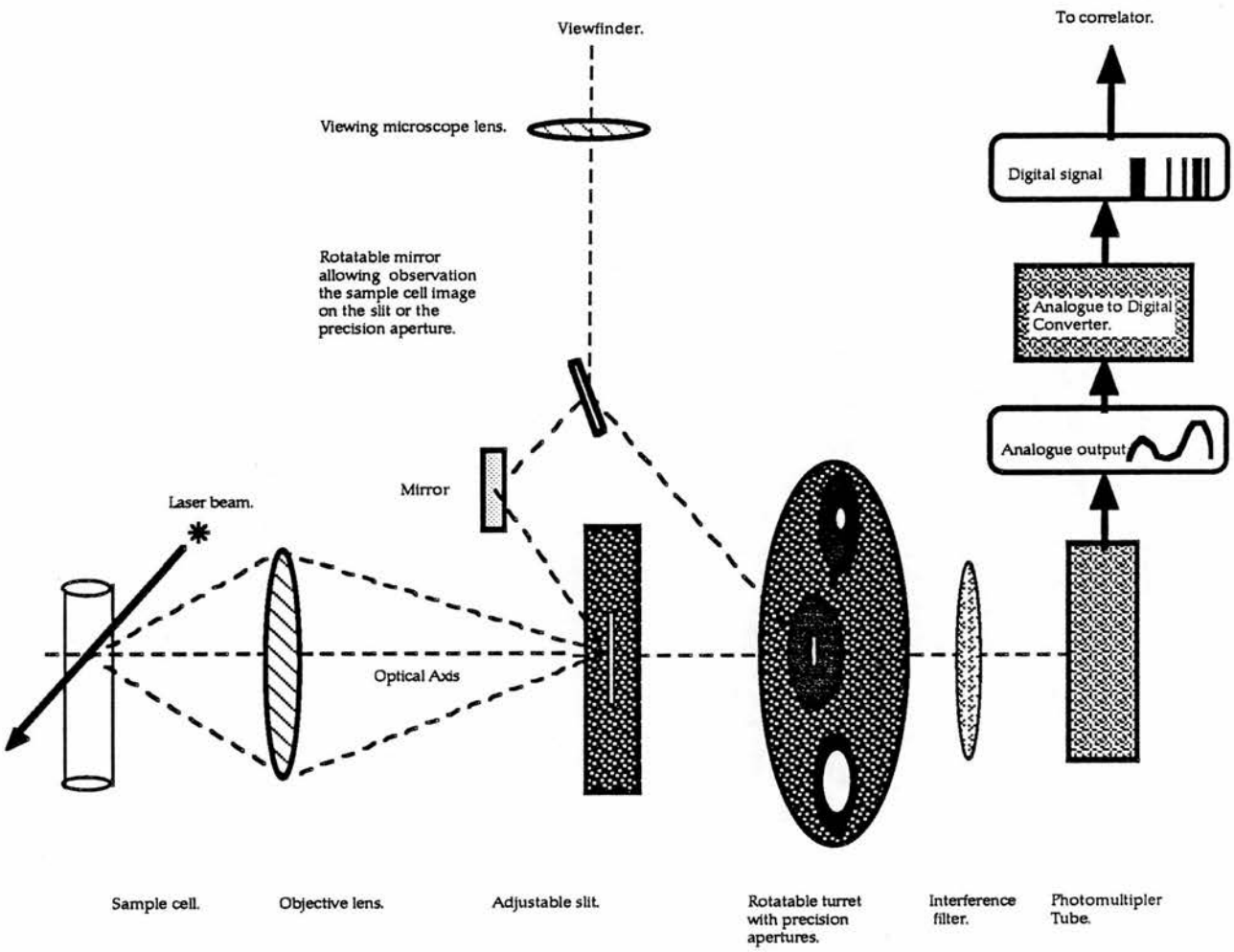

II 1 4 The observed second order correlation function.

In this paragraph it will be shown how the signal from the spectrometer can be processed to yield a correlation function.

The correlation function of the time dependent signal and a delayed version of itself also called autocorrelation is defined as :

$$C(\tau) = \lim_{t \to \infty} 1/T \quad V(t)\,V(t+\tau)\,dt \quad (II\,1\,2)$$

Where :

T is the period of the function.

V represents the signal .

τ is the time offset of the signal.

This relation is valid for an analogue function . The construction of a digital correlator requires for technical reasons the treatment of a digital signal .

The definition of the first order digital field autocorrelation is :

$$G_1(t, t+\tau) = \langle E(t).\ E(t+\tau) \rangle \quad (II\,1\,3)$$

But in fact what is measured is the second order correlation (intensity) function :

$$G_2(t, t+\tau) = \langle I(t).\ I(t+\tau) \rangle \quad (II\,1\,4)$$

We must notice that over long periods of time the value of the second order correlation function is the square of the mean intensity :

$$G_2(t, t+\tau) = \langle I \rangle^2 \qquad (II\ 1\ 5)$$

This property is used for the estimation of the "in range index" (See II 1 5). Both G_1 and G_2 can be normalized by division respectively by $\langle I \rangle$ and $\langle I \rangle^2$ creating g1 and g2 .

Fig. II 4 describes the "architecture" of the correlator. The processing of the photomultiplier (P.M.) , data , leading to the second order correlation function construction is outlined below through the steps A to G.

Fig II 4:

Malvern K 7032 Correlator, auto-correlation set-up.

(From Malvern Instruments manual, with permission)

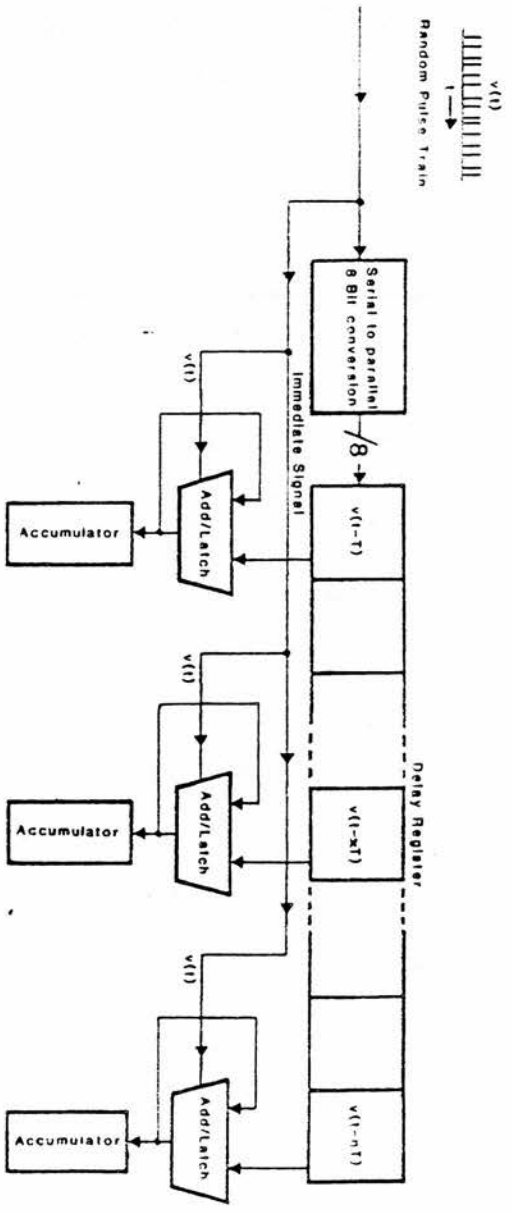

A) The raw signal from the photomultiplier is a random pulse train which arrives from the P.M as described in II 1 3 . Pulses are synchronized to 10 MHz clock . The total pulses are integrated over the experiment duration by the total sample counts monitor.

B)Counts are accumulated in the " clipper accumulator " over a period of time (T): the sample time. A sample time clock controls this duration . T depends on the particle ability to diffuse and therefore is linked to its Stokes radius. T is chosen either by the experimenter or automatically by the software, to avoid situations where :

α) T is too short . A loss of information occurs resulting from analysis of only a part of the correlation function.

β) T is too long . There is a loss of the correlation when $V(t) = V(t + x T)$.

C) The number of counts accumulated over T is transformed to 8 bit code information (Value from 0 to 255) .If the number of pulses (n) on a sample time is superior to 255 , the prescale system divides this value to avoid clipping if $n > 255$ .The prescaled number of counts is integrated all over the experiment at this level by a prescale monitor.

D) After one period T the contents of the " clipper accumulator " are moved to the first position of the delay register. As "old " samples advance in the register as every new one arrives one can say that each delay register represents a delayed version of the signal.

E) For each correlation channel every time a pulse arrives at the correlator input the content of each delay register is added to the sum of its corresponding accumulator. So the sum of over k samples in each register represents the correlation coefficient corresponding to its position , that is to its shift delay.

F) A user controllable experiment duration clock defines the total duration of the experiment .

G) Serial and parallel processing : (See Fig II 5 & 6) . This is a special feature of the Malvern correlator . It allows creation of the correlation function on a linear or a log time scale by the use of serial , or parallel processing.

If the correlator is used in a "Serial " mode all the information stored in correlator channels is linearly spaced in time : V (t - n T) with n from 1 to 64 .

But if the correlator is used in " parallel " mode , channels are divided into four subcorrelator blocks . Instead of being composed of decay registers linearly scaled in time , the decay registers are divided into four groups each having its own correlation time, the relation between the four correlation times being exponential . This mode allows a much longer time decay range to be analysed thus giving a much larger sample size range . It is called the variable time expansion .

II 1 5 Determination of the diffusion coefficient from the observed second order correlation function.

As shown in II 1 4 above, the value of registers represents the correlation coefficients for various multiples of the sample time delay: this is a measure of the second order correlation function $g_2(\tau)$. The relation between first order $g_1(\tau)$, and second order $g_2(\tau)$,normalized correlation functions has been shown by Cummins (1973) to be :

$$g_2(t, t+\tau) = 1 + [\, g_1(t, t+\tau)\,]^2 \quad (II\,1\,6)$$

As seen in II 1 2 the exponential decay shown by the correlation function is linked to the translational diffusion coefficient by :

$$g_1(\tau) = \exp(i\,\omega_0\,\tau)\ \ \exp(-\Gamma\,\tau) \quad (II\,1\,1)$$

Where :

ω_0 is the frequency of the incident light.

$\Gamma = D\,K^2$ with $K = 4\,\Pi / \lambda\, n \sin(\theta / 2)$, θ is the angle of scattering , n the refractive index of the sample .

So a plot of :

$$\text{Ln}\,(g_2(\tau) - 1) \text{ versus } \tau \quad (\text{II } 1\,7)$$

will have a slope of $2\,\Gamma$. As $\Gamma = D\,K^2$ with $K = 4\,\Pi / \lambda\, n \sin(\theta / 2)$, the calculation of the observed diffusion coefficient D_{obs} is then straightforward.

The machine calculates $D_{20,w}$, extrapolation to 20 ° C in water , using the classical formula :

$$D_{20,w} = D_{obs}\ (\eta_{sol} / \eta_{20,w})\,(293 / T_{sol})\ (\text{II } 1\,8).$$

Where :

D_{obs} is the measured diffusion coefficient in the experimental conditions of viscosity and temperature.

η_{sol} is the solvent dynamic viscosity .

$\eta_{20,w}$ is the dynamic viscosity of water at 20 ° C.

T_{sol} is the absolute temperature of experiment.

So the only requested parameters for a measurement of $D_{20,w}$ by photon correlation spectroscopy are :The scattering angle θ, the measured temperature T_{sol}, the viscosity of the solvent at this temperature η_{sol} .

Fig II 5:

Malvern K 7032 Correlator : serial configuration.

(From Malvern Instruments manual , with permission)

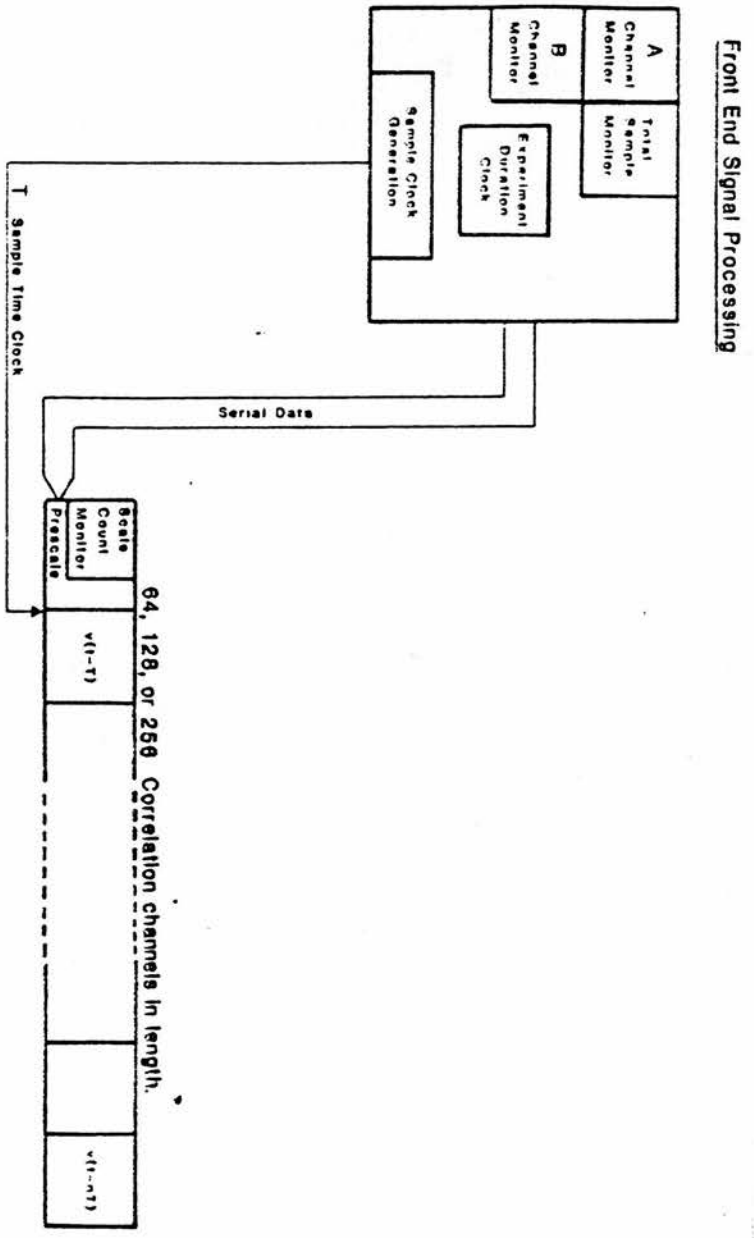

Fig II 6:

Malvern K 7032 Correlator : parallel configuration.

(From Malvern Instruments manual , with permission)

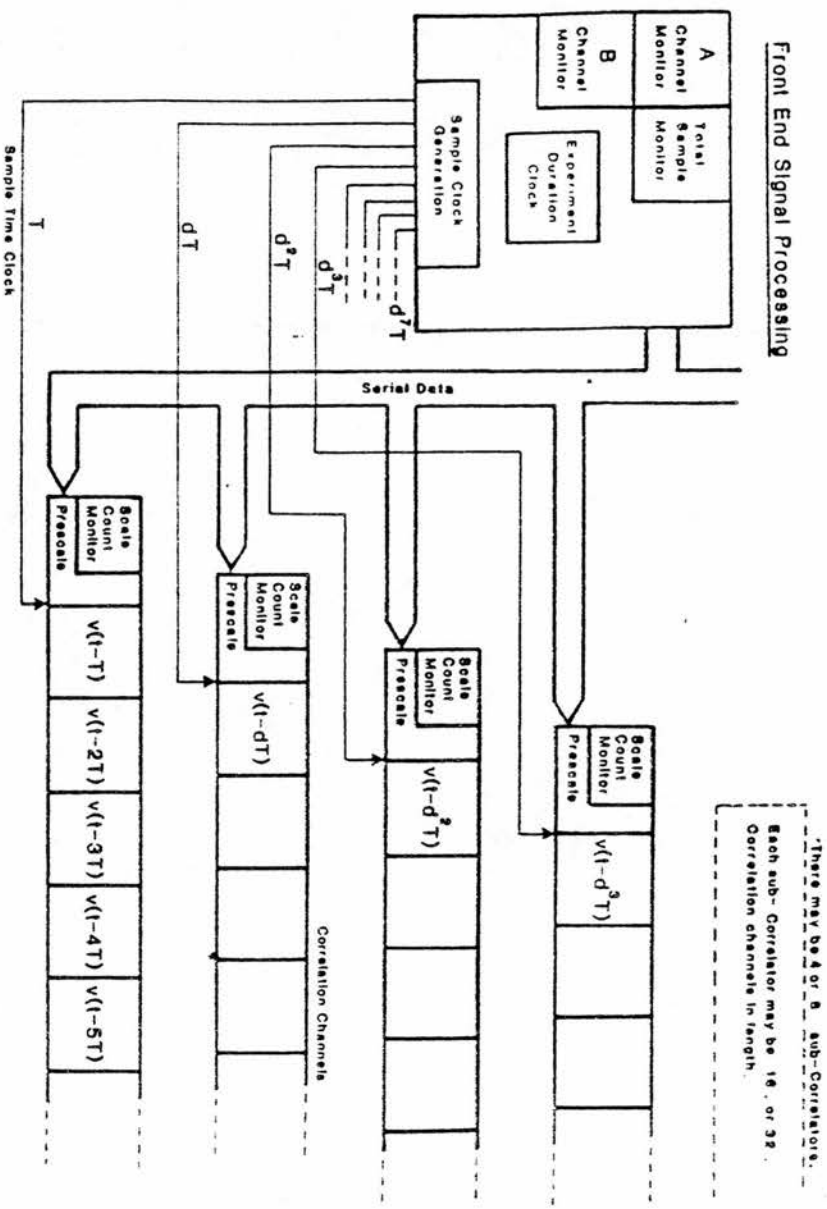

II 1 6 Problems created by large out of scale objects: "In Range index".

Any particle clearly too big for the selected sample time (T) will not be included in the diffusion coefficient distribution but will add some slower decay component background over all channels. A way of estimating this contribution is to divide the value of mean intensity $< I >$ obtained by extrapolating the experimental correlation $g_2(\tau)$ to high τ by the average of counts of the last channels. If there is no contribution of out of range particles this ratio will be 100 % but if there is any out of range contribution in the signal the average counts on the last channels will be slightly higher than the extrapolated value of $< I >$,thus the ratio will be less than 100 %.We usually had 99 % in range signal, the out-of-range contribution being probably rather due to aggregation or bubbles than dust . The presence of dust particles is easily noticed because they give rise to violent scatter bursts that can actually be seen in the solution ; this was not observed in our samples.

II 1 7 Problems created by the polydispersity of solutions : "Polydispersity index ".

We must take into account the problem created by the non monodispersity of the sample . If the sample is perfectly monodisperse we have shown above how the correlation function could be simply described by an exponential . Pusey et al (1974) have shown how this model could be transformed leading to the definition of a polydispersity index and two compound analyses.

The presence of several particle size classes will show up as a sum of exponentials and can be transformed into :

$$\mathrm{Ln}\left(\left| g_1(\tau) \right| \right) = \sum_{m=1} K_m (\Gamma)(-\tau)^m / m! \quad (\mathrm{II}\ 1\ 9)$$

Practically , m is limited to m = 2 so :

$$\mathrm{Ln}\left(\left| g_1(\tau) \right| \right) = -\Gamma_1 + \mu_2 / (\Gamma_2 / 2) \quad (\mathrm{II}\ 1\ 10).$$

This expression is fitted to the observed curve :

$$\mathrm{Ln}\left(g_2(\tau) - 1 \right) \text{ versus } \tau \quad (\mathrm{II}\ 1\ 7).$$

$2\mu_2 / \Gamma_2$ is defined as the polydispersity index and is equal to zero only if there is no polydispersity and . It is systematically calculated . Under 10% a "monodisperse" single exponential fitting is used. If this index is over 10% the software has a specific feature to estimate the distribution. The software possesses in memory the shape of correlation functions for a large number of diffusion coefficients; it then calculates a multi-exponential curve and fits it with the observed one. We must notice that no assumption on the distribution (like two compounds distribution as above) is made .

So each analysis provides the following parameters :

An average $D_{20,w}$.

A distribution of $D_{20,w}$ as a function of signal intensity .

A polydispersity index .

An "in range index" testing the presence of large objects out of scale .

II 1 8 Limitations of the technique.

In all those calculations no account is taken of a so called shape factor whose contribution is zero only if particle size is reasonably small, compared to wavelength of the light used or at zero angle for large particles .

Furthermore as the intensity of scattering is proportional to the square of the mass of the scattering particle, it is then proportional to the sixth power of their size . This means that the contribution of larger particles easily overwhelms that from smaller particles . This is a special concern in the presence of aggregates .

II 1 9 Experimental parameters.

A) The laser source : an Argon - Ion laser (Innova 4 U.S.A.) was set at 514.5 nm with a power range from 100 to 250 m W approximately. A light control mode allowing control of the laser power directly by a photoelectric cell feed back limited the source intensity fluctuations to approximately 1 or 2 %.

B) The buffer viscosity , because of its low salt and very low protein concentration , was taken as water viscosity . The software automatically corrected for temperature induced variations.

C) The refractive index was measured and found to be 1.335 for our standard buffer.

D) Experimental time for measurements on the fibronectin molecule was set between 5 and 15 sec. with very little difference in observed results.

F) The sample fundamental time was set to a time placing diffusion coefficient of the investigated particle in the middle of a hundred fold scale. In practise the approximate Stokes radius (Rs) for the investigated particles was entered in the computer. The Stokes radius was then transformed into the corresponding diffusion coefficient by direct transformation from Rs to the diffusion coefficient D by the classical Einstein relation : (where η is the solvent viscosity):

$$D = k\,T / 6\pi\,\eta\,Rs \quad (II\,1\quad 11)$$

Then D was related to the decay of the observed function and sample fundamental time was calculated.

G) Each measure was made up of several runs , (typically 20 to 50); the software calculated the mean value of the integration of counts for each run , and rejected any run with a significant difference in integration .

II 1 10 Sample handling and preparation.

To remove any possible dust or contaminant from the 1 cm diameter quartz cells (ALV Lasers F.R.G.), they , as well as their teflon caps , were stored in pure sulphuric acid . Prior to use they were washed twenty times with double distilled water to remove any acid traces and three times with filtered sample buffer to make sure the buffer composition of the sample would not be altered by some remaining water.

The buffers as well as the sample were filtered on "Nucleopore" filters (U.S.A.). They are well known for their very constant pore size as well as low sample retention because of their design as flat surfaces as opposed to ordinary filters which have mesh like surfaces .Filtration was preferred to centrifugation because it is a quicker process and also the size control was easier .

When filtering the samples care was taken to :

A) Reject the first two drops corresponding to the filter "dead volume " .

B) Transfer the drops on the side of the cell to the main body of the solution, allowing them to slide gently down , thus avoiding reformation of aggregates after filtration.

This technique also avoided the use of metal needles which leads to metal contamination triggering fibronectin polymerisation as well as creating high speed flows leading to aggregation.

II 1 11 Photon correlation spectroscopy of very small volume samples.

A way was found, unfortunately too late to be applied to this work, that allows the measurement of samples with a volume smaller than 100 µl. The sample cell was a micro-fluorescence cell of internal dimensions of 2cm high by 1 cm long by 0.2 cm wide. The laser beam goes through the 1cm path allowing the cell liquid interface to be far enough from the measured volume. As the cell does not need to be full for a measurement, samples with a volume as small as 50 µl can be used. The limitation on the sample volume is due more then to the problems created by the filtration or centrifugation of such small volumes. The setback of this technique is that measurements can only be performed at angles between 50 and 130 degrees.

II 2 MOLECULAR WEIGHT MEASUREMENTS BY LIGHT SCATTERING

II 2 1 Introduction .

There are many techniques allowing molecular weight determination in solutions; among them light scattering has several disadvantages as discussed below . However it was helpful in our work because it could be carried out conveniently in the Biochemistry department , in the same conditions , using the same samples for photon correlation spectroscopy . This provided a good complement to photon correlation spectroscopy by determining quickly if changes in the diffusion coefficient were due to changes in conformation only , or to changes in molecular weigh also . So it was used as a comparative technique more than for absolute Mr measurements .

II 2 2 Molecular weight determinations .

Rayleigh (1871) studied light scattering from a dilute gas. Developments by Schmoluchowsky (1908) ,Einstein (1910) and Debye (1947) allow treatment of scattering from large molecules in solutions . They show that vertically polarized light, scattered by a dilute solution of macromolecules is described by :

$$K_c / R_\theta = 1 / Mr [1 + (16\Pi^2 n^2 / 3 \lambda^2) Rg^2 \sin^2 (\theta/2)] + 2a^2 c + 3 a^3 c + \ldots$$

(II 2 1)

Where :

K is an optical constant : $2\ \Pi^2\ n^2\ (dn/dc)^2\ /\ \mathcal{N}\ \lambda^4$; dn /dc represents the refractive index increment with concentration , n is the refractive index of the solvent , λ the incident light wavelength and $\mathcal{N}$ is Avogadro's number .

c is the concentration of the studied molecule in g / ml .

R_θ is the Rayleigh ratio of the molecule $(I_\theta / I_0)(r^2 / 1+\cos^2 \theta)$ with r as the sample to detector distance .

Mr is the molecular weight of the studied molecule .

Rg is the radius of gyration of the studied molecule .

I_θ / I_0 the ratio of scattering intensity over incident beam intensity .

θ is the scattering angle .

a_2 ,a_3 represents Virial coefficients .

It is important to notice that :

A) At concentration c = 0 the expression becomes :

$$K_o / R_\theta = 1/Mr \; [1 + (16 \Pi^2 n^2 / 3 \lambda^2) Rg^2 \sin^2(\theta/2)] . \quad (II\ 2\ 2)$$

B) At concentration c = 0 and angle $\theta = 0$:

$$K_o / R_0 = 1/Mr . \qquad (II\ 2\ 3)$$

C) If molecules are small compared to λ (practically $Rg < \lambda / 20$) the factor ($16\Pi^2 n^2 / 3 \lambda^2$) $Rg^2 \sin^2(\theta/2)$ tends towards zero so that the angular dependence of K_o / R_θ is very small and in practise only measurements at one angle with a range of concentrations are required for a simple zero concentration extrapolation.

Zimm (1948) presented a representation now called Zimm Plot or extrapolation technique which allows the determination of both Mr and Rg in the general case of molecules with a radius of gyration non negligible compared to λ .By plotting: $K c / R_\theta$ as a function of $\sin^2(\theta/2) + Z c$ (Z is a constant arbitrarily chosen to spread the data on the graph), an array of points is created allowing the extrapolation of a line towards c=o , and a line towards angle θ=o. Those two lines have the same intercept on the y axis which is the value of K_o / R_0 at c = 0 and $\theta = 0$ that is 1/ Mr. (II 2 3) .The slope of the zero concentration extrapolation is ($16\Pi^2 n^2 / 3 \lambda^2$) $Rg^2 \sin^2(\theta/2)$ (from equation II 2 1) . From the measured slope the radius of gyration Rg is easily calculated.

Practically the Rayleigh ratio is very difficult to measure because of the requirement of the determination of absolute light intensities . This problem is solved by the use of a standard scatterer . We chose toluene . Let us define :

R_θ as the specimen Rayleigh ratio

R_θ t the toluene Rayleigh ratio

I_θ the scattering intensity of the sample at angle θ

$I_{\theta t}$ the scattering intensity of toluene at angle θ

I_0 the incident beam intensity.

$Kc/ R_\theta = [Kc / R_\theta (R_\theta t)^{-1}] (R_\theta t)^{-1}$ becomes, if we replace all the Rayleigh ratios in brackets by their values, :

$$K_c/ R_\theta = \{ K_c / [(I_\theta / I_0) (r^2 / 1+\cos^2 \theta)-1][(I_0 / I_{\theta t}) (r^2 / 1+\cos^2 \theta)] \}$$

$$(R_\theta t)^{-1} = [K_c /(I_\theta / I_{\theta t})](R_\theta t)^{-1} \quad (II\ 2\ 4\ )$$

So that only I_θ and $I_{\theta t}$ have to be measured since a reference value of $(R_\theta t)$ is given by the instrument maker and used as a standard.

Practically I_θ must represent the scattering from the solute only . The intensity scattered by a buffer cell $I_{\theta b}$ is subtracted from the measured solution scattering. Furthermore every photomultiplier generates a " dark current ", i.e. an electronic background current generated in absence of light. It is measured by putting a lid on the photomultiplier optics and it is subtracted systematically from every measured intensity.

II 2 3 Experimental set up and techniques.

The PCS 100 spectrometer was the same as for the photon correlation studies and is described in II 1 2 . To minimize possible experimental errors due to the source or detection the specific following precautions were taken for molecular weight measurements:

A) The laser was set in light regulation mode where a small portion of the beam is directed on a photoelectric cell controlling the tube current by a feed back mechanism.

B) The laser cooling system temperature might also affects the laser output; we checked that the fluctuations were limited within a 2 ° C range and that no long term drift occurred in the laser cooling water temperature.

C) When a small power laser output was required the laser current was kept fairly high

(over 20 A) but the laser aperture was closed . This allows the laser to work with a fairly high current where its output is steadier.

D) To avoid any drift in the photomultiplier sensitivity, room temperature had to remain constant during the experiments . This was checked and we verified that the temperature fluctuations were kept within the range of + - 1 ° C .

E) To avoid saturation of the photomultiplier, the maximal count rate at lower angle and higher concentration was set at about 200,000 counts per sec. giving a reference intensity of around 50,000 counts / sec and a buffer background of around 5000 counts per sec .

F) All buffers have been degassed .

G) The software has a specific feature to limit the effect of possible dust or bubble contamination . All measurements are split into a number of shorter runs, the mean value and standard deviation of intensity is calculated, allowing the rejection of any run with a significantly different value from the average.

H) Before each measurement the optical alignment of the cell was checked by observing the position of the transmitted beam on a distant wall without and with the cell in position .

II 2 4 Experimental parameters and sample handling.

These were the same as those used for correlation spectroscopy; the specific parameters for Mr determination were :

A) The use of spectroscopic analytical grade toluene (Aldrich Co U.S.A.) as a standard of refractive index 1.494 and Rayleigh ratio 18.3 10^{-6} cgs .

- In the absence of a published value of dn / dc for fibronectin at 514.5 nm a standard value of 0.19 was chosen only slightly different from the published value for fibronectin at 633 nm of 0.174 ml / g .

II 2 5 Limitations of this technique.

This technique (Mr measurements by light scattering) has several limitations :

A) It requires calibration against a known scatterer .

B) A refractive index increment with concentration increase must be measured with high accuracy, which was not possible in our work .

C) It is very sensitive to dust and aggregates . The intensity of scattering is proportional

to the square of the mass of the scatterer and therefore to the sixth power of its size .

D) Source and detector fluctuations might be difficult to control over a long period of time.

E) As sample preparation might alter the initial sample concentration , its concentration is measured on the last dilution by spectrophotometric determination of absorbance at 280 nm . Obviously any error will be amplified by a 2.5 factor when , as is generally the case, this optical density reading was carried out on the 4 /10 dilution .However the worst remaining error comes from the index increment determination, but this was not a problem in this work because it only generated a constant error and thus did not interfere with comparative Mr determinations .

II 3 SMALL ANGLE NEUTRON SCATTERING

II 3 1 Introduction.

This technique has benefited from the availability of high flux reactors coupled with better neutron detection. Neutrons are scattered by nuclei and unlike X-radiation do not show any systematic variation of scattering length with Z , allowing , despite a lower flux by cross-section , smaller sample concentration than required for X-Ray small angle scattering. The reason for this is that scattering is proportional to the fourth power of the wavelength and longer wavelength can be obtained with neutrons . Furthermore with neutrons the samples can be larger samples than for X-radiation .See reviews of the technique by Jacrot (1976), Stuhrmann and Miller (1978) , Perkins (1988). Its main advantage as opposed to X-Ray solution scattering is the absence of radiation-induced damage to the sample.

II 3 2 Theory of small angle scattering.

This has been developed by Guinier and Fournet (1955).It is valid for neutron and also for X-Ray scattering . Let us first consider the set up :Fig II 7

Fig II 7

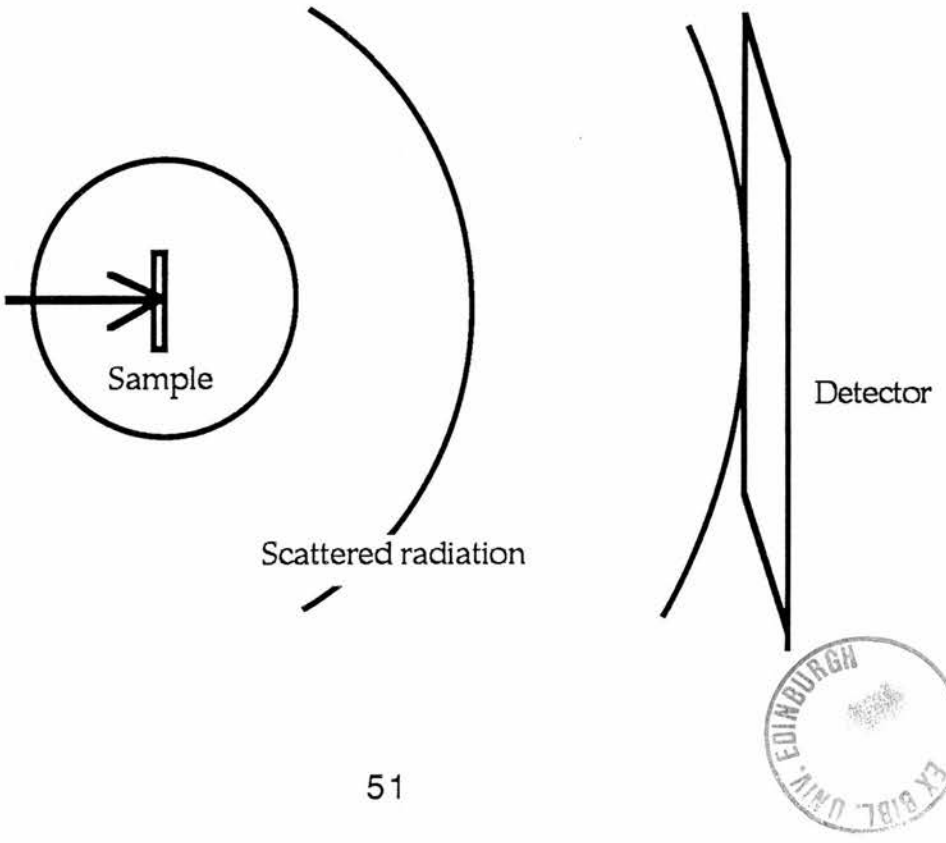

A thin sample is hit by a monochromatic radiation beam .The scattered radiation has the shape of spherical waves. If the detector intercept is a very small solid angle this spherical portion can be considered plane.Guinier showed that the relation between the scattered radiation intensity and the scattering angle is :

$$\text{Log } I = \text{Log } Nb^2 - 4\Pi^2 / 3\lambda^2 \; 0.4343 \; Rg^2 Q^2 \quad \text{(II 3 1)}$$

Where :

I is the scattered radiation intensity .

Nb is related to the number of particles scattering radiation.This factor is related to the molecular weight M_r (see II 3 5 below).

λ is the radiation wavelength.

R_g is the radius of gyration of the particle.

Q is related to the scattering angle 2θ and the wavelength λ by

$Q = 4 \Pi \sin \theta \, (\lambda)^{-1}$.

The graph of Log I versus Q gives : Log $I(Q) = B - a (Q)^2$ .B is the value of Log I when Q = o, value which is related to M_r; on the other hand, the radius of gyration R_g of the particle can be evaluated from the slope of the line Log $I = B - a(Q)^2$: (See II 3 1)

$$Rg = 0.416 \lambda \, (a)^{1/2} \quad \text{(II 3 2)}.$$

II 3 3 Experimental set up.

All neutron scattering experiments in this work have been carried out at the Institut Laue Langevin in Grenoble (France).The instrument called "D 11" has been described by Ibel (1976). It is described in Fig. II 8 below . Very small alterations have been made since then : samples are now in a free environment at atmospheric pressure (Fig II 9 below), the position of the detector ,the beam stopper and the sample cell are now remote-controlled through the machine computer by stepper motors.

Fig II 8
D11 Small angle neutron scattering camera

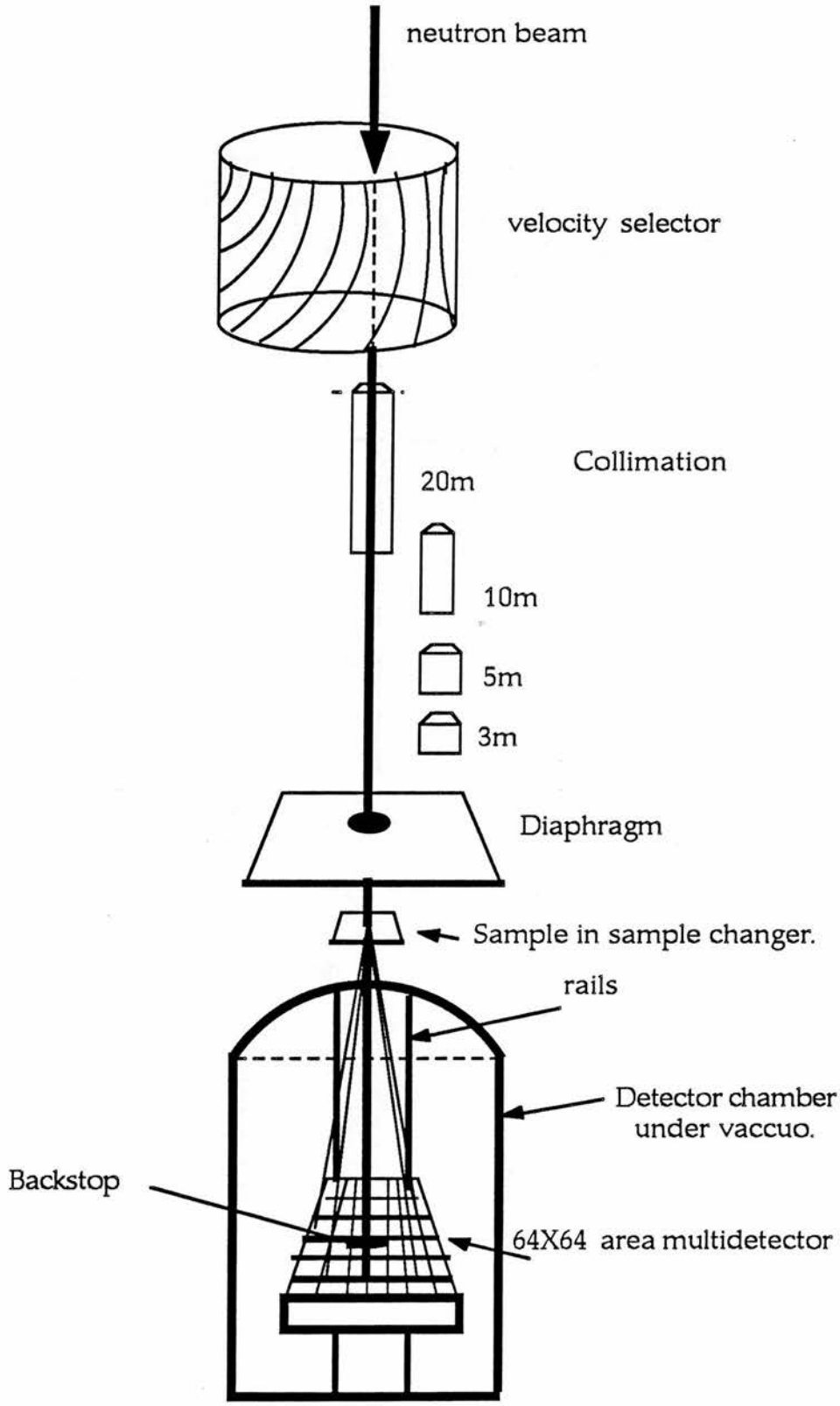

Fig II 9 :

View of the sample holder of the
D 11 neutron small angle scattering camera.

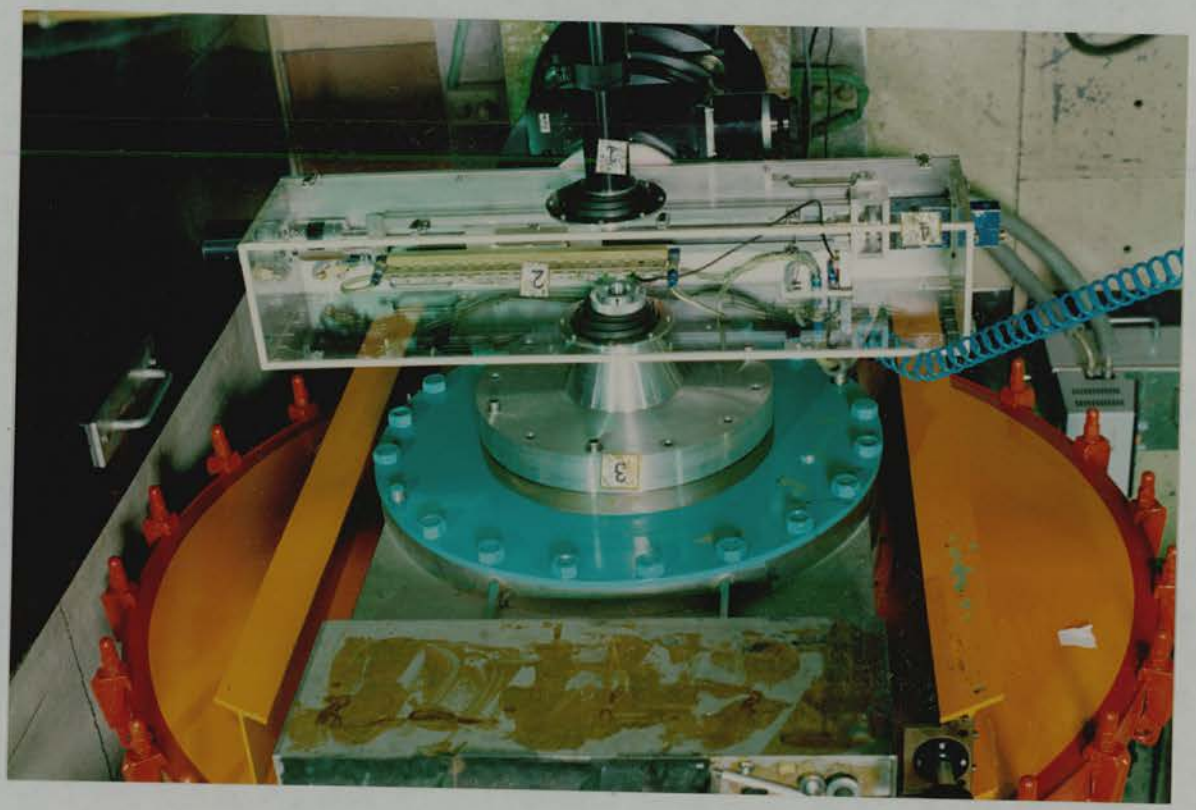

1) Neutron guide.
2) Sample cells.
3) D 11 camera.
4) Sample changer system.

Briefly a beam of cold neutrons with wavelength from 0.4 to 1.8 nm leaves the reactor via a cold neutron guide . A velocity selector , composed of helical slots is positioned 40 m from the reactor core. This selector allows only neutrons within a 10 % range of a defined velocity to be transmitted. This allows the selection of neutrons within a 10 % range of the desired wavelength. After collimation , neutrons hit the sample over an area of approximately 1 cm^2 .

The samples are enclosed in quartz cells (Hellma FRG) with a thickness of 0.1 cm and 0.2 cm respectively for H_2O and D_2O solutions. This way of handling the sample is very convenient because optical density readings are easily done on the sample itself allowing a precise concentration determination . Furthermore the sample has little risks of aggregation or polymerisation induced by handling as it goes directly out of the filtration filter into the measurement cell with very little disturbance.(see IV 3 below).

The detector is made from 4064 1 cm^2 BF_3 filled cells arranged in a square array of 64 x 64 cells. The detector and its associated Cd beam-stopper are positionable under vacuum by remote control.

Run duration is determined by setting a value of neutron counts for the integration of a small fraction of the incident beam. This ensures that two runs with the same time integration effectively have the same number of incident neutrons . Because of small source fluctuations a time based integration would not be as precise. For each run the counts on each cell are integrated.Those counts constitute the raw data which come out of the detector.

II 3 4 Application to our measurements: data processing and determination of the radius of gyration Rg .

The raw data (i.e. integrated counts for each cell for a certain number of incident neutrons) are processed as follows.

A) First all equivalent runs are added : all water runs, all sample x runs and so on .This creates a set of raw data output from the 4096 cells of the detector.

B) This raw data is then reduced by circularly averaging and transformation into a one dimension data $I(Q)=f(Q)$. All those transformations are carried out by a computer programme at I.L.L. called " RNIL ".

C) Afterwards another programme called " SPOLLY " performs subtraction of

intensities for each Q value, creating two spectra :

1) **Water final spectrum** =

{ [(water-filled cell spectra) minus (detector response spectra)] minus

A_1 [(empty cell spectra) minus (detector response spectra)]}.

A_1 represents the water transmission factor which is used to attenuate the empty cell scattering to the level it really has in the water spectrum.

2)**Sample final spectrum** =

{ [(Sample-filled cell spectra) minus (detector response spectra)] minus

A_2 x [(Buffer-filled cell spectra) minus (detector response spectra)] } .

A_2 is a correction factor equal to the ratio of sample to buffer transmissions and is very close to 1 because the solutions are very dilute (0.05 to 0.15 %).

For each value of Q the intensity of the water final spectrum is subtracted from sample final spectra , creating for each sample a file of

$$I(Q) / I_{inc}(Q) = f(Q).$$

Where I (Q) is the intensity of radiation scattered by the sample and I_{inc} (Q) is the incoherent scatter from pure water.

D) The curves are smoothed and "RGUIM " programme produces the classical Guinier representation by fitting the experimental points to a line in a preset range of Q , calculating Rg and extrapolating the value of $I(0) / I_{inc}(0)$ at Q = 0 ,(origin of the curve).

II 3 5 Principle of the determination of Mr by small angle neutron scattering.

In solutions neutrons are scattered by nuclei producing both coherent and incoherent scattering. Only coherent scattering can be used to derive some structure information. At zero scattering angle the intensity of coherent scattering I(0) depends only on the size and number of nuclei present and not on their arrangement .Furthermore the incoherent scattering by the solute in 0.05 to 1% wt/vol concentration range of biological studies is negligible compared to incoherent scattering due to the solvent. This allows Mr determination by extrapolation of I (0) intensity to zero scattering angle . The technique of Mr determination from this work has been described by Jacrot

and Zaccai (1981) and will be briefly reviewed below. (The various parameters required for calculations are also from this work.)

The relation between the zero angle scattering intensity and the number of particles in solution, valid for any radiation providing the proper contrast term $(\Sigma_b - \rho_s V)^2$, is chosen, is given by :

$$I(0) = Nb \ (\Sigma_b - \rho_s V)^2 \ A \qquad (II\,3\,3)$$

Where: I(0) is the coherent scattering intensity at zero scattering angle.

C is the concentration in g/cm^3

Σ_b is the sum of coherent scattering length for the considered molecule.

ρ_s is the solvent scattering density ,(scattering length per unit volume of the solvent).

V is the dry volume of the particle.

Nb is the number of particles diffracting.

$$Nb = C \ \mathcal{N} \ t \ s \ 1/M_r \qquad (II\,3\,4)$$

With :

M_r is the molecular weight to be determined.

C is the concentration of solute g/ml.

t is the sample cell thickness.

s is the intercept of the neutron beam with the cell .

$\mathcal{N}$ is Avogadro's number.

A is a factor depending on the geometry of the system and the incident beam I_o as defined below:

$$A = T_s \ I_o \ \Omega \qquad (II\,3\,5)$$

With:

T_s is the sample transmission : the ratio of the intensity transmitted by the sample cell and the intensity of the incident beam. T_s is easily measured.

I_o is the incident beam intensity in neutrons per second. It is important not to confuse it with I (0) solution forward scattering at angle zero.

Ω is the solid angle of the scattered beam intercepted by the detector.

As the number of particles diffracting at a given concentration Nb is proportional to the invert of the molcular weight M_r and $(\Sigma_b - \rho_s V)^2$ is proportional to Mr , the expression II 3 3 can be seen as : $I(0)/ C = \text{constant} \times Mr$.

II 3 6 Estimation of the incoherent scatter from water as an absolute scale for molecular weight determination by neutron small angle scattering.

In order to determine Mr ,at first, an estimation of A , (T_s times Io Ω) ,is required:

A) T_s is the sample transmission : the ratio of the intensity transmitted by the sample cell and the intensity of the incident beam. T_s is easily measured as follows : an attenuator is inserted in the incoming neutron beam to bring down its intensity then the beam backstop is removed . The ratio of the integration of the counts measured for a given period by the cells at the centre of the detector with the sample over the integration of the counts measured by the same cells for the same period with no sample is the sample transmission Ts.

B) The product Io Ω I_o : the incident beam intensity in neutrons per second. (It is important not to confuse it with I (0) solution forward scattering at angle zero.) , and Ω : the solid angle of the beam intercepted by the detector.

An absolute measurement of I_o is difficult but this problem is avoided by measuring both scattering and transmission from a pure water filled cell. The

estimation of I_o is based on the fact that ,at the 10 Å neutron wavelength used for our experiments, incoherent scattering from water is strong and has very little angular dependence. Let us first consider the experimental set up and define the parameters (Fig II 10 below):

Fig II 10:

Water filled cell.

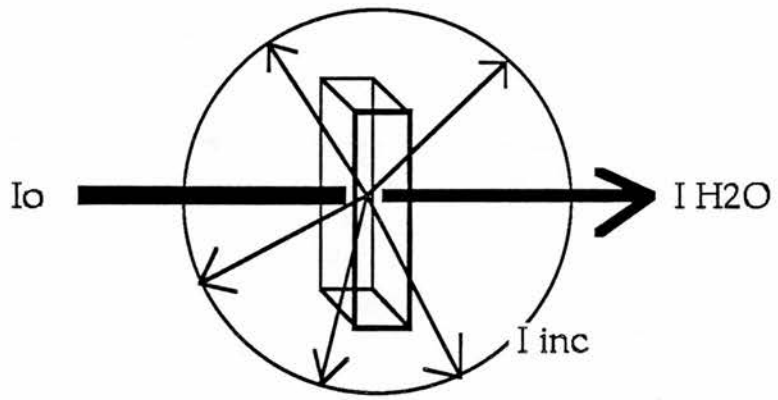

I_o is the incident beam we intend to measure.

I_{inc} corresponds to the incoherent scatter of water.

I_{H2O} is the beam transmitted by the water filled cell .

S is the cross-section of the beam.

As $I_o = I_{inc} + I_{H2O}$ and $I_{H2O} = T_{H2O} I_o$,we can define the transmission factor for water : T_{H2O}

$$T_{H2O} = I_{H2O} / I_o \quad (II\ 3\ 6).$$

The incoherent scattering from water at a solid angle of 4 Π is : $I_{inc} = (1 - T_{H2O}) I_o S$ for the solid angle Ω defined by the intercept of the scattered beam by the detector is:

$$I_{inc} = (1 - T_{H2O}) I_o (4 \pi \Omega)^{-1} \quad (II\ 3\ 7) .$$

So the measured I_{inc} incoherent scatter from water over an angle Ω is linked to the

incident beam I_o. (For neutron wavelength less than 0.1 nm a correction factor arises from the fact that the incoherent scattering of water becomes non isotropic . See Jacrot (1976) . This was not required in the measurements performed in this work where the wavelength was 1 nm)

In practise $I(0)_{inc}$ can be measured from the intensity of incoherent scattering from water at Q = 0. A water spectrum for all Q range is measured ; a spectrum of an empty cell is subtracted to suppress the contribution of quartz scattering . Because the measurements from water and specimens are all performed with the same sample and detector position , Ω is constant and can be ignored in the ratio : $I(0)_{sample}$ over $I(0)_{inc}$. So :

$$A = T_s \, I(0)_{inc} \, 4\Pi / 1 - T_{H2O} \qquad (II\ 3\ 8).$$

(TH2O is equal to I H2O / Io as defined over in equation II 3 6).

The expression II 3 3 can now be written as

$$I(0) = C\mathcal{N} t \; M_r \; T_s \; I(0)_{inc} \; 4\Pi / 1 - T_{H2O} \; [1/Mr(\Sigma_b - \rho_s V)]^2$$

Then can be rearranged in :

$$M_r = \frac{I(0)}{I(0)_{inc}} \; [C\mathcal{N} t \; T_s]^{-1} \; [4\Pi / 1 - T_{H2O}]^{-1} \; [1/Mr(\Sigma_b - \rho_s V)]^{-2}$$

(II 3 9)

The various parameters are determined as follow:

A)A value for $I(0) / I(0)_{inc}$ is calculated for each sample as described in II 3 4 C.

B) C is the solute concentration in g /ml . As the experiments are performed in quartz cells this concentration can easily be determined , providing the extinction coefficient is known , by a measure of the absorbance at 280 nm.

C) t is the sample thickness in cm

D) $4\Pi / 1 - T_{H2O}$ can be measured an equals 0.072.

E) The only remaining factor to estimate is : $[1 / Mr (\Sigma_b - \rho_s V)]^2$, the contrast term . Because its estimation requires some calculations it will be described in a special paragraph : II 3 7 below .

II 3 7 Determination of the contrast factors for fibronectin and the 44 k D gelatin binding domain of fibronectin.

The contrast factor is composed of two terms both dependent upon the D_2O content of the solvent.

The proportion of D_2O in the buffer % D_2O must be measured for each sample containing D_2O from transmission experiment in the following way:
The transmission of a 100 % water buffer and a 100 % (In practise > 99 %)D_2O buffer are measured. With those two points, drawing a line of transmission as a function of D_2O concentration , allows determination of the D_2O content of an unknown sample buffer by simply measuring its transmission. (As the samples are dilute solutions the absorbance due to the solute or the buffer salts are neglected) . This is important because the samples are equilibrated by dialysis and therefore the D_2O concentration must be measured.

A) The first term of the factor is $\Sigma_b (1 / Mr)$, the sum of scattering length of the constituents of the molecule per mass unit , values of Σ_b in H_2O and Σ_b in D_2O are tabulated . The knowledge of the D_2O percentage in the solution allows determination of the share of respective scattering lengths in H_2O and D_2O as follows:

$$\Sigma_b (1 / Mr) = \Sigma_b H2O + \% D2O (\Sigma_{D2O} - \Sigma_{H2O}) (1 / Mr) \quad (II\ 3\ 10).$$

As the amino-acid residues composition is known both for fibronectin and the domains we studied we can calculate the scattering length $\Sigma_b (1 / Mr)$ for both of them , see Tables II 1 to 4 below.

B) The second term ρ_s V (1/ Mr) is the product of the solvent scattering length per volume unit ρ_s by the dry volume of the particle V divided by Mr , both V and Mr can be calculated from the molecule composition.

For a mixture of H_2O and a certain percentage of D_2O called % D_2O as a solvent

$$\rho_s = (- 0.0056 + 0.0697 \% D_2O) 10^{-12} \text{ cm } \text{Å}^{-3}$$

Table II 1.

Calculation of Σ_b / Mr for the complete plasma fibronectin molecule.

Column 1: Amino acid residue.
2: Number.
3: $\Sigma_b H_2O$ (10^{-12} cm).
4: $\Sigma_b D_2O$ (10^{-12} cm).
5: $\Sigma_b D_2O$- $\Sigma_b H_2O$(10^{-12} cm).
6: Mass (D).
7: Mass x number (D).
8: Number . $\Sigma_b H_2O$ / Mr (10^{-12} cm / D).
9: Number . $\Sigma_b D_2O$- $\Sigma_b H_2O$/ Mr (10^{-12} cm / D)

1	2	3	4	5	6	7	8	9
Gly	358	1.728	2.769	1.041	57	20406.000	1.300e-3	7.728e-4
Ala	175	1.645	2.686	1.041	71	12425.000	5.970e-4	3.778e-4
Val	358	1.479	2.52	1.041	99	35442.000	1.100e-3	7.728e-4
Leu	226	1.396	2.437	1.041	113	25538.000	6.543e-4	4.877e-4
Ile	202	1.396	2.437	1.041	113	22826.000	5.848e-4	4.361e-4
Phe	95	4.139	5.180	1.041	147	13965.000	8.154e-4	2.051e-4
Tyr	188	4.719	6.802	2.083	163	30644.000	1.800e-3	8.119e-4
Trp	76	6.035	8.118	2.083	186	14136.000	9.512e-4	3.283e-4
Asp	213	3.845	4.886	1.041	114	24282.000	1.700e-3	4.597e-4
Glu	254	3.762	4.803	1.041	128	32512.000	2.000e-3	5.483e-4
Ser	351	2.225	4.308	2.083	87	30537.000	1.600e-3	1.516e-3
Thr	483	2.142	4.224	2.082	101	48783.000	2.100e-3	2.085e-3
Asn	189	3.456	6.58	3.124	114	21546.000	1.400e-3	1.224e-3
Gln	239	3.373	6.497	3.124	128	30592.000	1.700e-3	1.548e-3
Lys	147	1.586	5.752	4.166	129	18963.000	4.835e-4	1.270e-3
Arg	229	3.466	9.714	6.248	157	35953.000	1.600e-3	2.967e-3
His	87	4.959	6.521	1.562	136.5	11875.500	8.947e-4	2.818e-4
Met	49	1.764	2.805	1.041	131	6419.000	1.793e-4	1.058e-4
Cys	124	1.93	4.013	2.083	103.1	12784.400	4.963e-4	5.358e-4
Pro	336	2.227	2.227	0.000	97	32592.000	1.600e-3	0.000
Total	4379					482220.900	0.024	0.0167

Table II 1 2

Calculation of V/Mr for the complete plasma fibronectin molecule.

Amino.Acid.	Number of residues.	Volume ($Å^3$).	Volume x number of residues ($Å^3$)
Gly	358	66.4	23771.200
Ala	175	91.5	16012.500
Val	358	141.7	50728.600
Leu	226	167.9	37945.400
Ile	202	168.8	34097.600
Phe	95	203.4	19323.000
Tyr	188	203.6	38276.800
Trp	76	237.6	18057.600
Asp	213	113.6	24196.800
Glu	254	140.6	35712.400
Ser	351	99.1	34784.100
Thr	483	122.1	58974.300
Asn	189	135.2	25552.800
Gln	239	161.1	38502.900
Lys	147	176.2	25901.400
Arg	229	180.8	41403.200
His	87	167.3	14555.100
Met	49	170.8	8369.200
Cys	124	105.6	13094.400
Pro	336	129.3	43444.800
Total	4379		602704.10 $Å^3$, (V).

Mr (482,220 D), has been calculated in Table II 1 above , then V/Mr = 1.25 D/$Å^3$

Table II 1 3.

Calculation of Σ_b / Mr for the gelatin binding domain of the plasma fibronectin molecule.

Column 1 : Amino acid residue.
2: Number.
3: $\Sigma_b H_2O$ (10^{-12} cm).
4: $\Sigma_b D_2O$ (10^{-12} cm).
5: $\Sigma_b D_2O$- $\Sigma_b H_2O$(10^{-12} cm).
6: Mass (D).
7: Mass x number (D).
8: Number . $\Sigma_b H_2O$ / Mr (10^{-12} cm / D).
9: Number . $\Sigma_b D_2O$- $\Sigma_b H_2O$/ Mr (10^{-12} cm / D)

1	2	3	4	5	6	7	8	9
Gly	41	1.728	2.769	1.041	57	2337.000	1.608 e-3	9.686e-4
Ala	9	1.645	2.686	1.041	71	639.000	3.360e-4	2.126e-4
Val	21	1.479	2.52	1.041	99	2079.000	7.048e-4	4.961e-4
Leu	14	1.396	2.437	1.041	113	1582.000	4.435e-4	3.307e-4
Ile	10	1.396	2.437	1.041	113	1130.000	3.168e-4	2.362e-4
Phe	12	4.139	5.180	1.041	147	1764.000	1.127e-3	2.835e-4
Tyr	20	4.719	6.802	2.083	163	3260.000	2.142e-3	9.454e-4
Trp	11	6.035	8.118	2.083	186	2046.000	1.507e-3	5.200e-4
Asp	21	3.845	4.886	1.041	114	2394.000	1.832e-3	4.961e-4
Glu	18	3.762	4.803	1.041	128	2304.000	1.537e-3	4.252e-4
Ser	23	2.225	4.308	2.083	87	2001.000	1.161e-3	1.087e-3
Thr	36	2.142	4.224	2.082	101	3636.000	1.750e-3	1.701e-3
Asn	23	3.456	6.58	3.124	114	2622.000	1.804e-3	1.631e-3
Gln	31	3.373	6.497	3.124	128	3968.000	2.273e-3	2.198e-3
Lys	12	1.586	5.752	4.166	129	1548.000	4.319e-4	1.135e-3
Arg	17	3.466	9.714	6.248	157	2669.000	1.337e-3	2.410e-3
His	16	4.959	6.521	1.562	136.5	2184.000	1.801e-3	5.672e-4
Met	9	1.764	2.805	1.041	131	1179.000	3.603e-4	2.126e-4
Cys	27	1.93	4.013	2.083	103.1	2783.700	1.183e-3	1.276e-3
Pro	20	2.227	2.227	0.000	97	1940.000	1.011e-3	0.000
Total	391					44065.700	0.025	0.017

Table II 1 4.

Calculation of V/Mr for the gelatin binding domain of the plasma fibronectin molecule.

Amino.Acid.	Number of residues.	Volume ($Å^3$).	Volume x number of residues ($Å^3$)
Gly	41	66.4	2722.400
Ala	9	91.5	823.500
Val	21	141.7	2975.700
Leu	14	167.9	2350.600
Ile	10	168.8	1688.000
Phe	12	203.4	2440.800
Tyr	20	203.6	4072.000
Trp	11	237.6	2613.600
Asp	21	113.6	2385.600
Glu	18	140.6	2530.800
Ser	23	99.1	2279.300
Thr	36	122.1	4395.600
Asn	23	135.2	3109.600
Gln	31	161.1	4994.100
Lys	12	176.2	2114.400
Arg	17	180.8	3073.600
His	16	167.3	2676.800
Met	9	170.8	1537.200
Cys	27	105.6	2851.200
Pro	20	129.3	2586.000
Total	391		54220.800

Mr (44,066 D), has been calculated in Table II 3 above , then V/Mr = 1.23 $D/Å^3$

II 3 8 Formulae for the determination of the molecular weight of complete fibronectin and the 44 k D gelatin binding domain of fibronectin.

Using (II 3 4) and the proper contrast term calculated from Table II 1 to 4 over.we have :

A) For Fibronectin :

$$Mr = 0.072\ (\ I(0)\ /\ I(0)\ inc)\ (\ C\ Ts\ e\ )^{-1}\ (31\ -\ 70.4\ \%_{D2O}\ )^{-2}\ 10^{9}$$

(II 3 11)

Where :

$\%_{D2O}$ is the proportion of D_2O in the solution.

Ts is the sample transmission.

e thickness of the cell in cm.

B) For the 44 kD gelatin binding domain.

$$Mr = 0.072\ (\ I(0)\ /\ I(0)\ inc)\ (\ C\ Ts\ e\ )^{-1}\ (31.9\ -\ 70.5\ \%_{D2O}\ )^{-2}\ 10^{9}$$

(II 3 12)

II 3 9 The problem of the carbohydrate content of those proteins.

The complete fibronectin molecule and the 44 kD gelatin binding domain are both glycosylated. As the amount of carbohydrates is in the range of 5 % of the mass and considering that the precision of the measurement of Mr in solution is only of the order of 10 % , it seems reasonable not to consider this problem.

II 4 POLYACRYLAMIDE GEL ELECTROPHORESIS

II 4 1 Experimental conditions.

The technique of Laemlli (1970)was used . Gels were cast in 16 x 14 x 0.15 cm dimensions between two glass plates with the gel and buffers composition given by this author. Gradient gels were cast with the help of a two channel peristaltic pump at a flow of 200 ml/h . Solutions of acrylamide or buffers were not degassed prior to use .

For a separation range from approximately 800 kD to 50 kD Mr , 200 kD to 40 kD Mr or 100 kD to 15 kD Mr , 3.5 % - 5 % , 3.5 % - 6 % or 4.5 % - 10 or 12 % acrylamide gels were respectively chosen.

The 3.5 % acrylamide top gel created much finer bands with the high molecular weight material than the ordinary 4.5 % concentration generally used . On the other hand gels were then difficult to handle .

Various grades of acrylamide from B.D.H. (U.K). gave no apparent differences in results. The Acrylamide - Bis Acrylamide mixture was stored in the dark at 4 ° C . Bio - Rad (USA) Type AG 501 X 8 ion exchange beads were added in this stock solution to remove any acrylic acid formed by acrylamide degradation in solution.

The gels were run at a constant current of 50 to 55 mA per gel (this corresponds to a power of 30 W at most in each gel). The gel running kits were equipped with a water cooling device. To ensure proper cooling, the lower buffer solution was stirred continuously. The duration of the run was determined by the time required for the dye front to reach a position a few millimetres over the end of the gel plate. This was dependent on the amount of salts in the sample but generally in the order of 150 minutes.

Fixation and staining were carried out :

Either :

A) through normal Coomassie - R staining procedure (from Fairbanks et al. 1971):

Fixation for 1 h in 40 % Ethanol , 10 % Ethanoic Acid ,50 % water.

Overnight staining in 0.125 % Coomassie R 250 in 40 % Ethanol , 10 % Ethanoic Acid ,50 % water.

Destaining by several changes of destaining solution : 15 % Ethanol ,10 % Ethanoic acid in water.

Or :

B) by a quick staining method derived from Versterberg et al. (1977) allowing visualization of the bands in less than one hour , as well as a much better background

after destaining which increases the quality of the photography of gels.

Fixation for 30 min in 40 % Ethanol , 10 % Ethanoic Acid ,50 % water, warming at 60 °C .

Staining 45 min at 60 ° C in a stain prepared in the following way : 0.125 % Coomassie G 250 is dissolved in approximately 200 ml of water with vigorous stirring ; 8.5 ml of perchloric acid are added slowly . This allows the stain to form large micelles with colour turning from blue to brown . Water is then slowly added , up to 250 ml . Stirring is carried on for one hour and followed by filtration on Whatman 1 paper.

The bands are immediately visible and destaining is done by several changes of destaining solution : 15 % Ethanol ,10 % Ethanoic acid in water removes the slight remaining background.

Photographs of all gels were taken on Polaroid 667 film (Positive + negative) allowing permanent record with no risks of band fading . When required, gels in the wet state were scanned on a Joyce Loebl scanner with digital analysis .

II 4 2 Analysis.

The gels were analysed by the classical technique of Weber et al. (1969), by a representation of Log (Mw) as a function of Rf. Rf for a specific band is the distance from the top of the separating gel to the specific protein band divided by the distance from the top of the separating gel to the front as defined by the bromophenol dye line.

This plot when applied to the molecular weight standards yielded a straight line from which the unknown molecular weight of the samples could be deduced from their measured Rf.

II 5 ELECTRIC BIREFRINGENCE

II 5 1 Introduction.

The most frequent application of electric fields to macromolecules is electrophoresis where macromolecules are moved across a gel by an electric field. Electrophoresis is present in nearly all biochemical research as an analytical technique and is sometimes also used in a preparative way.

But an electric field can also orientate molecules (if they have a permanent or field induced electric moment). An orientation induced birefringence can be detected if the molecules possess an optical anisotropy. This effect has been described by Kerr as early as 1875,(Kerr 1875 & 1880). When applied to large biomolecules, this effect can help to investigate not only some of the hydrodynamic properties but also some of the properties of the molecules' structure such as their flexibility. As opposed to electrophoresis this technique is extremely rarely applied in biochemical studies.. Just a few teams in the world currently publish experiments carried out by this technique in the field of biochemistry .

II 5 2 Theoretical background of the electric birefringence effect.

As the electric birefringence effect has been fully described by Fredericq and Houssier (1973), a short description will be presented below.

A medium is said to be birefringent if the velocity of light propagating through it is dependent upon the plane of polarisation of the incident beam. For one direction of propagation of the light beam, the solution possesses two refractive indexes : $n_{=}$ and $n_{\perp}$. The parallel and perpendicular compounds of the polarized light therefore travel at two different speeds in the medium .When the beam comes out of the birefringent medium , the two compounds are out of phase by an angle ϕ .

The birefringence of the medium , (Δn) , is defined as the difference in refractive index (n) between two orthogonally polarized beams :

$$\Delta n = n_{=} - n_{\perp} \quad (II\ 5\ 1).$$

The birefringence ,Δn is related to the shift in phase, ϕ by the relation :

$$\Delta n = \phi \lambda / 2 \pi l \quad (II\ 5\ 2).$$

Where l is the length of the path in the birefringent media. After passing through the analyser, the intensity of the beam I is related to the initial intensity Io by the relation:

$$I = Io \sin^2 \phi \quad (II\ 5\ 3).$$

In the absence of an electric field an homogeneous solution is optically isotropic therefore as the analyser is oriented in order to stop the beam no signal is detected. In the presence of an electric field the molecules undergo orientation . As the solution becomes anisotropic $n=$, the refractive index in a direction parallel to the electric field, and $n_{\perp}$, the refractive index in a direction perpendicular to the field become different. The parallel and perpendicular compounds of the polarized light therefore travel at a different speeds in the cell , and as a birefringence occurs a signal can now be detected after the analyser.

In practice , in order to obtain the sign of Δn as well as a higher sensitivity , a quarter-wave plate is inserted before the analyser . The latter is rotated at an angle α from the crossed position. (See Fig II 11). The field-off intensity is then different from zero and defined as I_{α}. Therefore the measurement of I_t intensity at time = t will be linked to Δn. and not Δn^2. This configuration changes the relationship between I t and ϕ which becomes :

$$(I_{(t)} - I_{\alpha}) / I_{\alpha} = \sin^2 (\alpha + \phi_{(t)}/2) (\sin^2 -1)^{-1} \quad (II\ 5\ 4)$$

Which can be rearranged as :

$$\phi_{(t)} = 2 \{ \sin^{-1} [(I_{(t)} - I_{\alpha}) / I_{\alpha} + 1)^{1/2} \sin \alpha] - \alpha \} \quad (II\ 5\ 5).$$

$\phi_{(t)}$ can be related to the time-dependent birefringence $\Delta n_{(t)}$ by the relation II 5 6 below:

$$\Delta n_{(t)} = \lambda \phi_{(t)} / 360 l \quad (II\ 5\ 6).$$

Fig II 11

Electric birefringence optical set-up with quarterwave plate.

(Size reduced along optical axis,expanded along the electric field axis)

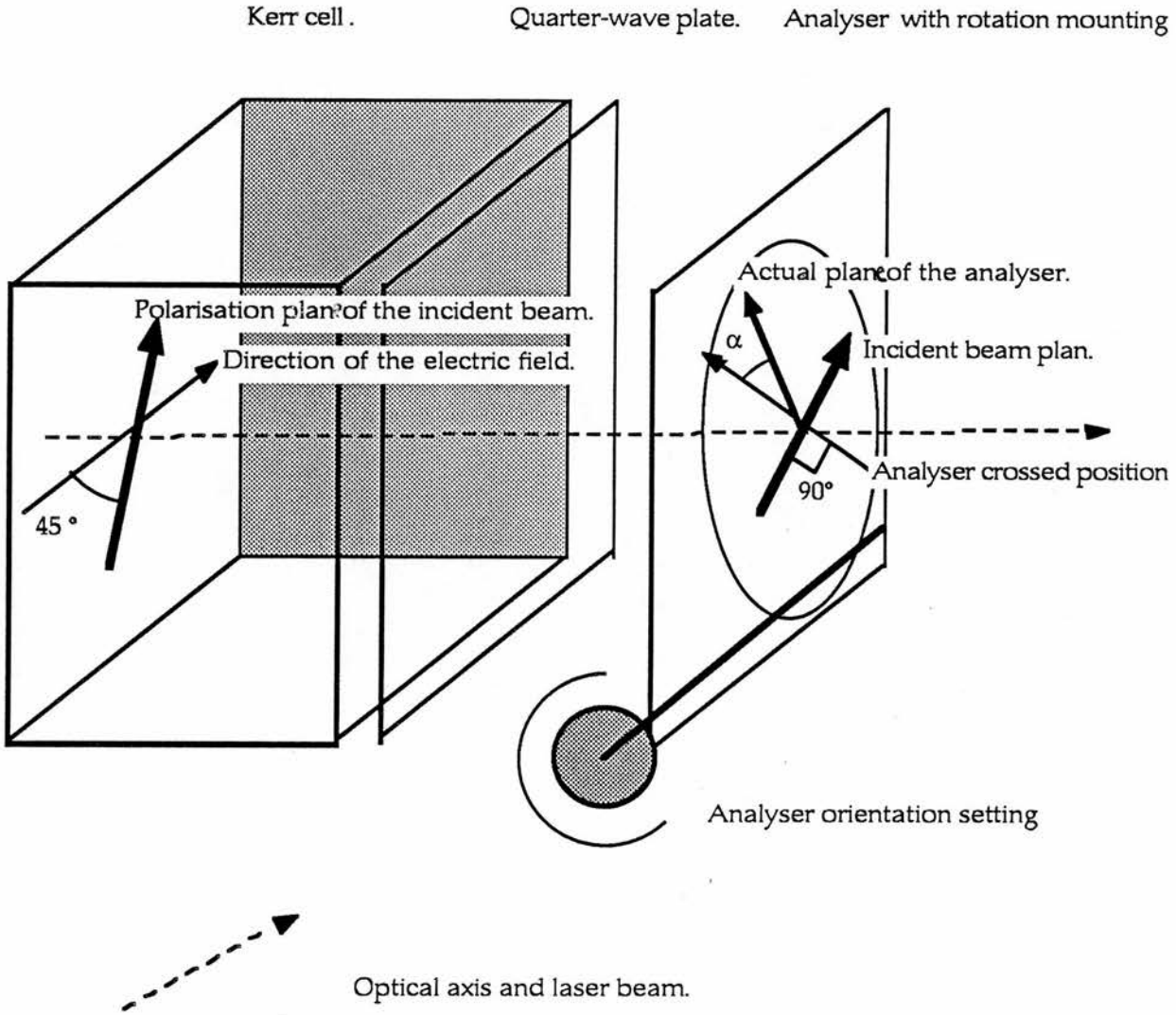

It must be noticed that the variations in the intensity of the transmitted beam: $(I_{(t)} - I_{\alpha})$ that are in fact detected are not strictly related to $\Delta n(t)$. But in the conditions where : $(I_{(max)} - I_{\alpha}) / I\alpha < 0.1$ with $I_{(max)}$ being the field on steady state birefringence it must be noticed that $n_{(t)} - n_{(max)} / n_{(max)}$ does not differ of more than 1 % from $(I_{(t)} - I_{(max)}) / I_{(max)}$. It is then possible to treat the variations of intensity as a good indication of the variations of the birefringence.

II 5 3 Experimental set up.

All the birefringence experiments from this work were performed by the author in The " Laboratoire de Biologie Physicochimique " in the Université C.Bernard in Lyon (France) with the supervision of Professor Bernard Roux . The electric birefringence equipment was "custom made" for this laboratory by Dr C.Bernengo . It is shown in Fig II 12 below.

The sample is carefully transferred into a Kerr type cell made of two parallel electrodes and two transparent windows mounted on a teflon base (see Fig II 13). A high voltage source can create fields up to 10 kV/cm through the electrodes. The operator triggers both the high voltage source and the oscilloscope sweep by a single switch. The oscilloscope is equipped with a memory device allowing a trace recording. A 10 mW laser is used as a monochromatic polarized light source . It is important to notice that the laser source is oriented in order that the plane of polarisation forms an angle of 45 degrees with the electric field. The beam travels through the Kerr cell, a quarter-wave retarder, an analyser which is oriented to stop the incident beam and finally is detected by a photomultiplier directly connected to the oscilloscope.

Fig II 12: Electric birefringence set up.

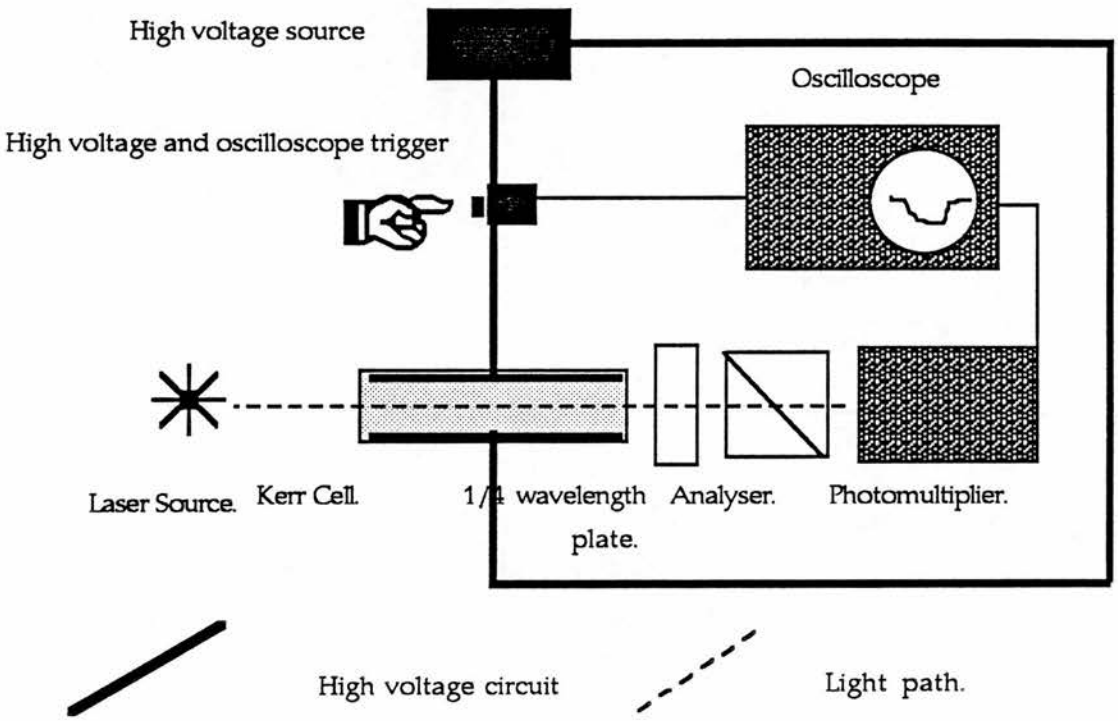

Fig II 13: Kerr Cell

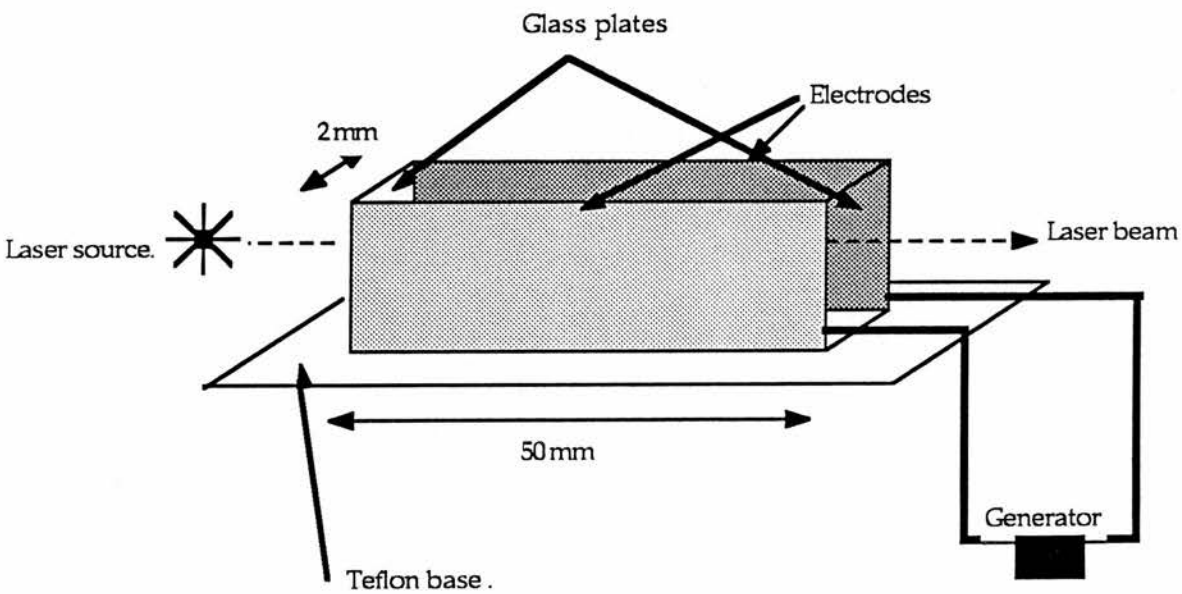

II 5 4 General interpretation of a birefringence measurements.

Fig II 14 shows the data obtained for a 11 mg/ml solution of fibronectin in 100 mM NaCl,1 mM EDTA, 50mM Tris , pH 7.4. The spikes indicated with arrows are artefacts created in the electronics when the field is created or suppressed. The curve can be divided in four parts.

Fig II 14 :

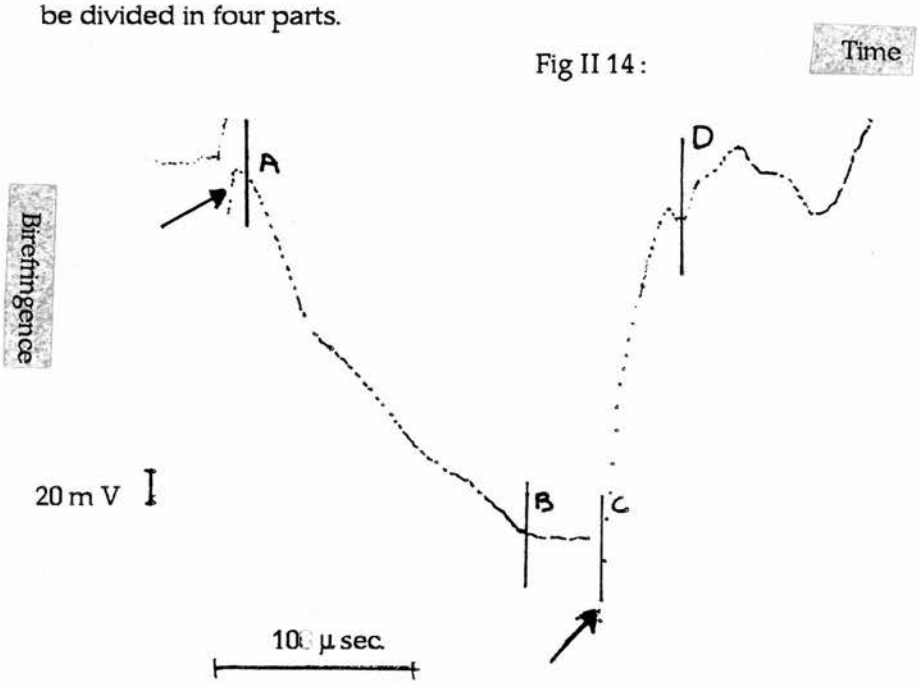

A) The rise of the birefringence: this step corresponds to the time during which the molecules orientate within the solution. The speed of the appearance of birefringence is linked to the ability of the molecule to orientate and depends both on its electrical and hydrodynamic properties.

B) The steady state birefringence is shown by the flat part of the curve. The amplitude of the steady state birefringence is linked to the optical and electrical properties of the molecules, the electric field properties and the concentration of the macromolecules.

C) The decay of birefringence. This corresponds to the time immediately following the interruption of the field. Therefore the molecules lose their orientation and the birefringence disappears. As at the start of this phase the electric field is suppressed and the decay rate is only related to the hydrodynamic properties of the molecules in solution.

D) A fourth section can exist when the measurements are performed in a buffer where the conductance is very high for this technique . This happens over 50 mM ionic strength . In this case an oscillation of the signal might be observed in the final section of the decay. It is due to perturbations created in the solution and must be ignored. Fortunately it appears when the birefringence is only a small portion of its maximal amplitude.

The points enclosed in boxes are artefactual . They are the consequence of electric interferences when the field is created or interrupted . They are in fact quite useful because they show the exact position on the curve of those two events.

II 5 5 Molecular interpretation of the measurements of the sign of the birefringence .

The birefringence can be positive or negative and this provides information about the orientation of the molecule's electric dipole. In the cylindrical model of Benoit (1951), the birefringence is positive and the electric dipole is aligned with the main axis of the molecule.

II 5 6 Hydrodynamic interpretation of the decay of the birefringence.

Because of the involvement of the optical, electrical and hydrodynamic properties of the molecule , the interpretation of the rise and the steady- state birefringence is an extremely complex problem which has not yet been solved in a satisfactory way . Since the decay of the birefringence occurs only when the field is interrupted , the decay is not linked to the electrical properties of the system but only to the optical and hydrodynamic parameters of the molecules.

Various authors have worked on this problem . The interpretation is the most simple in the case of models assuming the molecule shape as long cylindrical rods. In the cylindrical model of decay of Benoit (1951 a & b) , the birefringence decay is given by:

$$\Delta n_{(t)} / \Delta n_{eq} = e^{(-t / \tau)} \quad (II\ 5\ 7).$$

Where:

$\Delta n_{(t)}$ is the birefringence at time t after interruption of the field.

Δn_{eq} is the steady state birefringence (generally just before the field interruption).

τ is the orientation relaxation time .

In this cylindrical model τ is related to θ: rotational diffusion coeffcient by the relation :

$$\tau = 1/\ 6\,\theta\ (\text{II}\ 5\ 8).$$

this relation allows a direct calculation of θ rotational diffusion coefficient from the normalized decay rate : τ.

In a more recent work Wegener and his co-authors (1979) , have worked out the general expression of the decay. They show that in a general case the expression of the decay was a multiexponential function involving five decay rates. Considering the limits of the resolution on the measurement , such functions cannot be analysed. Fortunately , in some cases the general expression shows that only one or two decay rates are involved (this is due to symmetry relationships within the molecule) . In those cases the experimental curve should be single or bi-exponential . These authors show that this could exist when the molecules could be approximated by long rods (as in the Benoit model), but this is of little interest for the fibronectin molecule , as various other hydrodynamic measurements allow us to rule out this model (See chapter IV paragraph 3 & 4). They confirmed that (as pointed out by Tao in 1969 in a study of fluorescence depolarisation) to a good approximation , for oblate ellipsoids as defined by Perrin which are a shape more likely to fit with fibronectin , the five relaxation times (τ) are equal and were also given by the relation II 5 8 above .

II 5 7 Practical data processing for the birefringence measurements.

The raw data was transferred from the memory of the oscilloscope to an Apple IIc computer where it was processed by a locally written programme in the following way:

A) First the portion of the curve of interest was selected, in this precise case the decay of the signal was analysed. (The rise of birefringence can also be analysed which yields informations on the electrical properties of the molecules in the cylindrical model from Benoit).

B) The curve was transformed in semi-log coordinates and analysed for a single exponential decay by a classical least square fitting of the points corresponding to the longer times after field suppression.

C) If the line created above was not crossing the origin, the values obtained for this function were subtracted from each point leading to the calculation of a second exponential decay function corresponding to a shorter relaxation time.

D) In this latter case the two functions were combined and plotted on the same graph as the experimental data allowing an appreciation of the fitting of the model to the experimental points. Fig IV 1 and 2 (in chapter IV), shows that in the application to the fibronectin molecule , the two situations occurred depending on the buffer conditions.

II 5 8 Practical and theoretical limitations of the birefringence measurements.

The electric birefringence technique presents a number of specific experimental and theoretical problems.

A) The main experimental limitation is that the creation of an electric field within a solution can create a current and thus generate heat. The current is obviously linked to the conductivity of the solution (i.e. its ionic strength). Ionic strength of approximately 150 mM seems to be currently an upper limit. The type of buffers that can be chosen for those experiments is therefore limited . No information can be obtained for high ionic strength buffers.

B) In order to avoid any excessive heating of the solution the field is maintained only for a fraction of a millisecond (generally 20 µs for the experiments presented in this work). Unfortunately triggering the high voltage source for such a short period appeared to be rather temperamental with the rather old generator used in this work. This generator also had a tendency to sometimes keep the field for a much longer time than requested , resulting in the loss of the sample. A new generator is expected soon on this apparatus that should solve this problem.

D) An other problem is the synchronization between the field pulse and the oscilloscope sweep. As the times involved are of the order of the µ second this is not always satisfactory. A proper generator would be a considerable help here as well .

E) Fairly high concentrations had to be reached before any decent signal could be recorded. This does not create good conditions for the study of fibronectin.

F) Nevertheless the main concern is not experimental but is due to the difficult

interpretation of those measurements because of the complexity of the problem from the theoretical point of view. Fortunately the fibronectin specimens did not present any multi-exponential decay curves with more than two decay rates. This permitted the measure the relaxation times with a reasonable accuracy.

CHAPTER III
SPECIMEN PREPARATION

III 1 ONE STEP FIBRONECTIN PURIFICATION FROM PLASMA .

III 1 1 Introduction.

The plasma fibronectin purification technique in this work was derived from two papers : Vuento et al. (1979) and Ruoslahiti et al. (1982). They both rely on affinity chromatography as described by Cuatrecasas et al. (1968) but neither mentions any precautions against clotting of blood during preparation.

The purification method is based on the high affinity of fibronectin to collagen (or its denaturation product, gelatin) . As this property is shared by very few plasma proteins, separation based on this property immediately results in a dramatic purification from complete plasma to fibronectin in one step.

III 1 2 Plasma preparation.

The two types of starting material were :

A) Citrate treated frozen human plasma was supplied by the Scottish National Blood Transfusion Service .

125 ml of plasma were made 1mM in PMSF 5 mM in EDTA NaN_3 100mg/l

It was then spun for 2h at 25 0C at a 10,000 g field and then for 10 minutes at very low speed at 10 0C to solidify the lipidic top layer formed by centrifugation.

Human plasma is associated with three problems:

1) Possible contamination by human virus . This plasma was screened by the S.N.B.T.S. and was transfusible , nevertheless, the contamination risks are not totally suppressed.
2) Human plasma as opposed to bovine plasma may contain a noticeable amount of lipids which tend to deposit on the glassware or the columns.
3) Proteolytic degradation might occur during the plasma collection and storage times which are much longer than those for bovine plasma.

On the other hand most of the literature is devoted to the human plasma molecule

therefore it is helpful to work with it.

B) Bovine blood anticlotted by 1 to 5 vol A.C.D. spun 3000 rpm for 5 minutes to remove blood cells , was pelleted and then processed exactly as human plasma except for the centrifugation step where the absence of a significant amount of lipoproteins s allowed reduction of the centrifugation time to 15 min.

III 1 3 Flow rates in column chromatography.

During all this work the usual flow rates depended on the column diameter and are presented below:

Column diameter. (cm)	Flow: Affinity chrom.(ml/h)	Flow: Gel filtration (ml/h)
2.5	20 to 25	10 to 15
1.6	10 to 12	5
1	8 to 10	-

III 1 4 Affinity chromatography of plasma.

Plasma was applied to a $5cm^2$ by 5 cm column of commercial gelatin-sepharose . Prior to plasma application the column was equilibrated by 100 ml of pH 7.35 phosphate buffer, P.B.S. (150 mM ionic strength), containing 5 mM EDTA . During all gelatin affinity work the flow was kept at 25 ml/h . It was then rinsed by the following buffers:

A) 100ml of the equilibration buffer to elute all unbound material.

B) 75 ml of 50 mM Tris 2 M NaCl pH 7.4 PMSF 1mM, 5 mM EDTA. This step allowed elution of all the contaminants either binding to gelatin or to the sepahrose-beads' carbohydrates .

C) 100 ml of PBS buffer to lower the salt concentration if immobilized Lysin or heparin affinity chromatography was to be performed later .

D) For the elution, various buffers have been tested with success

1)Urea 4 M tris 50 mM pH 7.5

2)Urea 2M 1 M NaCl 50 mM tris pH 7.5

3)Citrate 50 mM NaCl 100 mM pH 5.2

4)Lysine1 M Tris 50 mM pH 7.4

5) Lysine2 M Tris 50 mM pH 7.4

Fig III 1 shows the absorbance profile at 280 nm of the preparation.

Before any salt or Tris addition , all urea solutions were deionized by passing them through a 8 ml column of ion-exchange beads (Bio Rad AG 501 X 8) to remove urea degradation products. The conductivity of urea solutions was then smaller than that of double distilled water.

Buffers 1-3 (urea or citrate) allow elution as a sharp peak. Buffer 1 was abandoned as its very high urea concentration could give rise to irreversible denaturation of fibronectin. Apparently the use of citrate in buffer 3 causes irreversible denaturation of the affinity media. Lysin elution (buffer 4) has the disadvantage of resulting in a very broad elution peak and also the buffer shows some absorbance at 280 nm perturbing the protein detection. On the other hand, buffer 4 represented the mildest possible elution conditions. A good alternative was developed in this work by the use of 2 M Lysine(Buffer 5). The fibronectin was eluted as a sharp peak and this avoided the use of urea . Buffer 5 is then a good solution to the problem of the elution buffer .

Dialysis from high concentration solution to Tris 50 mM ,NaCl 100 mM ,EDTA 1mM , PMSF 50 µM pH 7.4 was performed in three steps :

A) 4h dialysis which removes most of the passing material as shown by some refractive index measurements of a 4 M urea solution in our experimental conditions. See Fig III 2 below.

B) Then two longer steps(generally 24 h) .

Fig III 1:

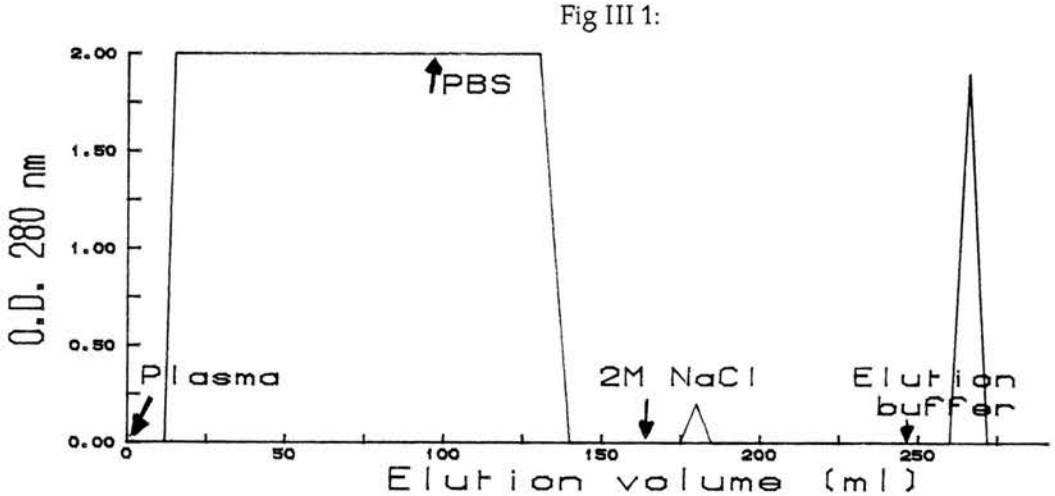

Fig III 2 :

Dialysis of urea elution buffer.

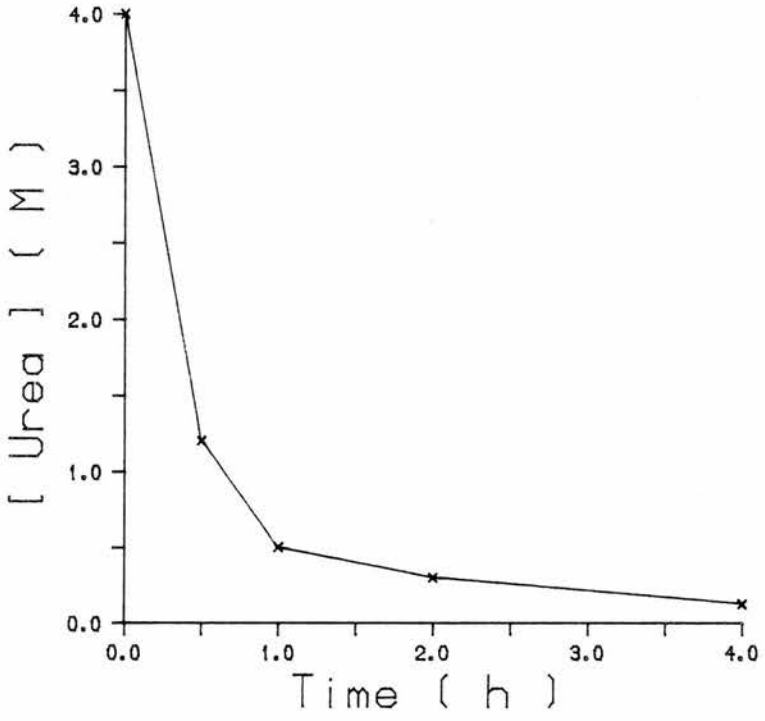

III 1 5 The problem of proteolytic degradation.

In this preparation, as often in protein purification , enzymatic proteolytic degradation occurs and is the main problem in this preparation. Two protease inhibitors were systematically added:

A) Phenyl-methyl-sulphonate-fluoride (PMSF) , described by Farney et al. (1963) was added to irreversibly inhibit serine activated-proteases present during preparation by sulfonation of the serine residue of the active site . The concentration range was from 0.5 to 0.05 mM. The main experimental problems with this inhibitor are :

α) Its poor solubility in water solutions (approximately 1mM). The use of a isopropanol stock solution is then required. This results in two problems : Isopropanol contamination of the solutions if a rather dilute stock solution is used,

or inhibitor precipitation in the case of a very concentrate stock solution which tends not to mix quickly enough with the buffers.

β) A poor stability : The half life of PMSF is , at 25 C and physiological pH , is of the order of 1 to 2h only .

γ) A slow reactivity with its substrate at low temperatures (i.e. 4 C).

B) Ethylene-diamine-tetracetate , (EDTA), was added to reduce metal ions activity, thus inhibiting metal activated proteases as well as inhibiting calcium dependent clotting in plasma . It also prevents metal ions triggering fibronectin polymerisation as shown by Vartio (1986).

No inhibitor for Thiol-activated proteases was added as fibronectin presents two free SH groups which might have important physiological applications (see chapter I). As all preparations were usually conducted at physiological pH no acid protease inhibitors ,such as pepstatin, were added.

The most immediate effect of degradation was to cut the molecule near the C-Terminus end generating two slightly different subunits :

i) one with the double disulphide inter-chain bonds and a small part of the other chain.

ii) the other one missing the C end .

It must be pointed out that in physiological conditions , those fragments remained associated by non covalent interactions. This degradation process is easily shown on a non-reducing PAGE (Fig III 3 below). It must be noticed that most of the literature present reducing gels where no estimation of the degradation can be done because after reduction the bands of native fibronectin and of the main degradation products are at the same place .

III 1 6 Results.

Yields have not been calculated for all the preparations carried out (over 50). For example on 13 preparations an average of 17 mg of fibronectin per run has been prepared. This represents a yield of 56 % with a theoretical plasma fibronectin concentration of 300 mg/l. Large variations in the yields of the preparations were observed , they seemed to reflect the normal variations of fibronectin concentrations of healthy blood donors as described in chapter I. Fig III 3 below shows a PAGE gel of the preparation .

Fig III 3:

6 % P.A.G.E.

Lane 1 Plasma , total protein loaded , aprox. 200 µg.

Lane 2 Plasma , total protein loaded , aprox. 40 µg.

Lane 3 Purified fibronectin , aprox. 30 µ g .

Lane 3 Purified fibronectin , aprox. 10 µ g .

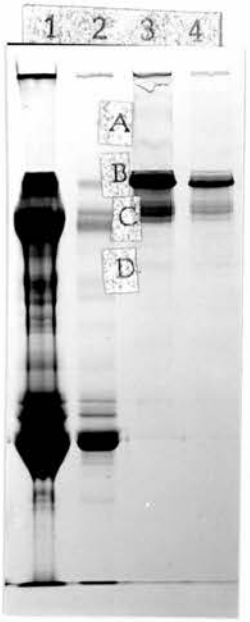

As the gel was realized in non-reducing conditions, the following bands can be seen:

A :Traces of multimers formed during boiling .
B: Native fibronectin made of two chains.
C: Isolated chains formed by degradation:
the two type of chains one missing the C terminal domain, the other with two C terminal domains are visible on lane 4.
D: Large degradation products of fibronectin.

III 2 FURTHER PURIFICATION STEPS .

III 2 1 Introduction.

Further purification has sometimes proved to be necessary , mainly because of degradation of fibronectin . This degradation probably occurred when the plasma was collected because its extent was very variable with human material although the purification procedure remained constant. With bovine plasma the degradation seemed more limited possibly because of quicker collection and processing of the plasma. The three techniques tested for the re-purification of fibronectin are described below :

III 2 2 Heparin affinity chromatography:

This method is based on the affinity of fibronectin to heparin; this was a convenient way of obtaining higher concentration fractions without requiring the use of an ultrafiltration concentrator leading to high gas solubilisation in the buffers . This is a problem in light scattering experiments. Large fibronectin fragments containing both the gelatin-binding domain and the strong heparin-binding domain were not separated from the complete molecule .

III 2 3 Lysin affinity chromatography:

This technique (from Vuento et al .1979), was proven to be good but resulted in poor yields probably due to poor binding to the column.

Fibronectin previously dialysed against 50mM NaCl, 25 mM Tris, 1 mM EDTA, pH 7.4 was loaded on a 5 cm by 2.5 cm diameter column of commercial poly-L-Lysin sepharose equilibrated with the same buffer . It was then rinsed by 100 ml of the same buffer. The elution was carried out by 1 M NaCl 50 mM Tris, 1 mM EDTA, pH 7.4 buffer .

III 2 4 Gel filtration:

Gel filtration (Technique described by Porath et al. 1959), on sephacryl S 500 was applied to the re-purification of fibronectin in this work. It had the disadvantage of diluting the fractions and was also rather slow . Nevertheless gel filtration in 1M NaCl 1 M urea 50 mM Tris pH 7.4 was the only technique that could separate intact fibronectin molecules from the non covalent associations of hydrolysed subunits as described above.

III 2 5 Problems associated with fibronectin solutions.

Fibronectin has a strong tendency to form large visible aggregates upon stirring , shaking , freezing and thawing or fast changes of ionic strength. This was particularly marked in low ionic strength solutions in presence of urea. Proteolytic decomposition of purified material did not seem to represent a problem.

III 3 PREPARATION OF SOME FIBRONECTIN DOMAINS.

III 3 1 Thermolysin limited digestion.

The thermolysin (E. C. 3.4.24.4.) digest technique is from Seikiguchi et al (1983).

Fibronectin was dialysed against 50 mM NaCl , 25 mM Tris , 0.5 mM EDTA pH 7.6 , just before enzyme addition $CaCl_2$ was added to a final concentration of 2 .5 mM . Enzyme concentration was 5 micrograms thermolysin per mg fibronectin . There was no attempt

to quantify the yields of the digestion methods. The use of EDTA and excess Calcium ions during the reaction seems strange but it is based on the fact that EDTA - Metal dissociation constant is several orders of magnitude smaller for calcium than for metals susceptible to inhibit thermolysin action . Therefore addition of EDTA chelates all disponible metal contaminants assuring a reproducible enzyme action over different batches. The reaction was stopped by the addition of EDTA at a 5 to 10 mM concentration. The various domains are recovered by affinity and gel-filtration chromatography as follows.

III 3 2 Preparation of the gelatin binding domain.

The gelatin binding domain was prepared by loading the digest on a gelatin-sepharose column equilibrated with digestion buffer, containing no calcium but 10 mM EDTA, rinsing the non-binding material with the same buffer and eluting the bound material with 4 M Urea 50 mMtris 5mM EDTA pH 7.4 .

III 3 3 Preparation of the larger heparin binding domains.

The heparin binding domains were prepared by loading the digested sample on a Heparin-sepharose column equilibrated with digestion buffer containing no calcium but 5 mM EDTA , rinsing with the same buffer and eluting by a gradient from 25 mM Tris 50mM NaCl to 25 mM Tris 0.5 or 1 M NaCl . The peak fractions were analysed on SDS PAGE and the high molecular weight high affinity material 145-155k D was purified by sephacryl S 200 gel filtration chromatography resulting in homogeneous material as shown by SDS PAGE .

CHAPTER IV
MODELS OF FIBRONECTIN IN SOLUTION

IV 1 INTRODUCTION.

Understanding the contacts between cells and the extracellular matrix requires an accurate description of the three-dimensional structure of the elements that create those connections . Thus the need for reliable models of all the molecules involved in this anchoring system is clear. The involvement of fibronectins in the cell anchoring and matrix organisation has been described in I 4 above and this seems to be the main function of those molecules. Therefore good models of fibronectin might help to understand fibronectin function and also how the cell-tissue interaction is created.

Crystallographic techniques allowing high resolution structure determination to be carried out have not been applied to fibronectin yet. Crystallisation attempts were performed by various teams and also on fibronectin prepared for this work with no success yet . The fibronectin molecule tends to polymerise easily and therefore crystal production does seem easily possible . One of the leading teams working on fibronectin (Ruoslahiti in the U.S.A.), seems even now to have given-up the idea of crystallising fibronectin and is at present trying to obtain crystals from vitronectin which also possesses the sequence responsible for cell attachment : RGDS .

This lack of high resolution data for fibronectin is a real concern because , despite a relatively large number of studies on this molecule , the tertiary structure of the fibronectin molecule is still very poorly understood. Fortunately fibronectin does not self-aggregate in solution. This is very important because studies in solution are therefore possible with fibronectin . Laminin , for instance , has such strong self-aggregation properties that it has been impossible yet , with this molecule , to perform many types of studies in solution like light scattering .

IV 2 RESULTS FROM ELECTRIC BIREFRINGENCE EXPERIMENTS.

IV 2 1 Introduction.

The electric birefringence data acquisition , processing and analysis has been described insection II 5 . The original data as recorded by the oscilloscope and the representations of the decay of the birefringence as a function of time are presented in Fig IV 1 to IV 4 below.

IV 2 2 Samples.

The fibronectin samples were prepared as described in chapter III . In order to quickly reach the high concentration required for this study reverse dialysis against high molecular weight Polyethylene glycol was performed . This allowed the concentration to be raised quickly up to 11 mg /ml in 150 mM ionic strength buffer. The reverse dialysis is preferred to the use of ultrafiltration . The contact of the protein with the ultrafiltration membrane has been shown to lead to some denaturation effects on some proteins . It has been shown , for instance, that the sign of the electric birefringence induced in an F1 ATPase solution was reversed , therefore indicating an important modification in the protein structure, when the protein solution had been concentrated in an ultrafiltration cell , (from a personal communication of B. Roux 1988). The requirement to high protein concentrations is always a concern but this permitted the electric birefringence measurements to be performed in physiological ionic strength conditions .

IV 2 3 Data.

Fig IV 1 :

Electric birefringence measurement : Raw data.

[Fn] 11 mg/ml Buffer 100mM NaCl ,50 mM Tris pH 7.4

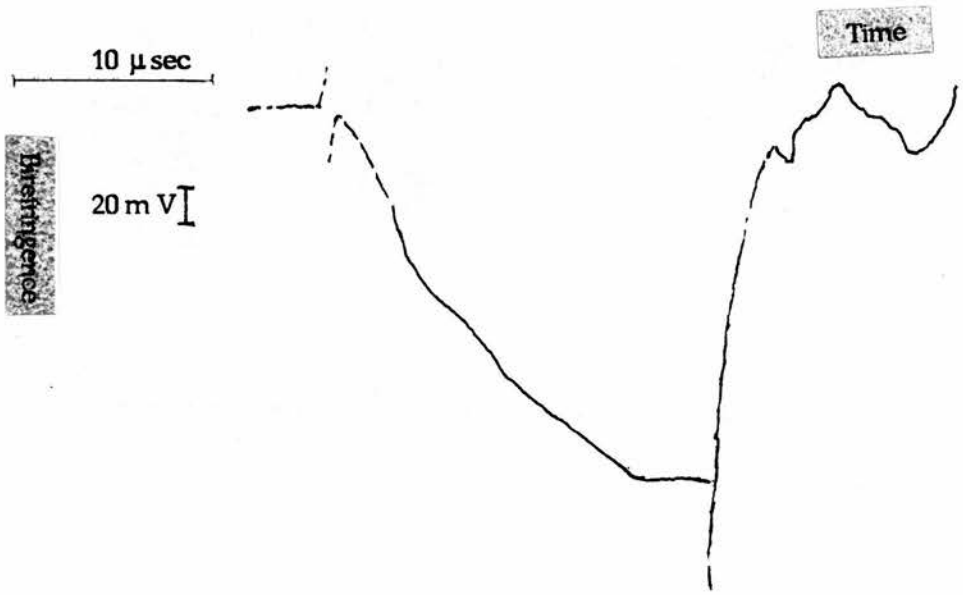

Fig IV 2 :

Electric birefringence measurement : Raw data.

[Fn] 5.5 mg/ml Buffer 50mM NaCl ,25 mM Tris pH 7.4

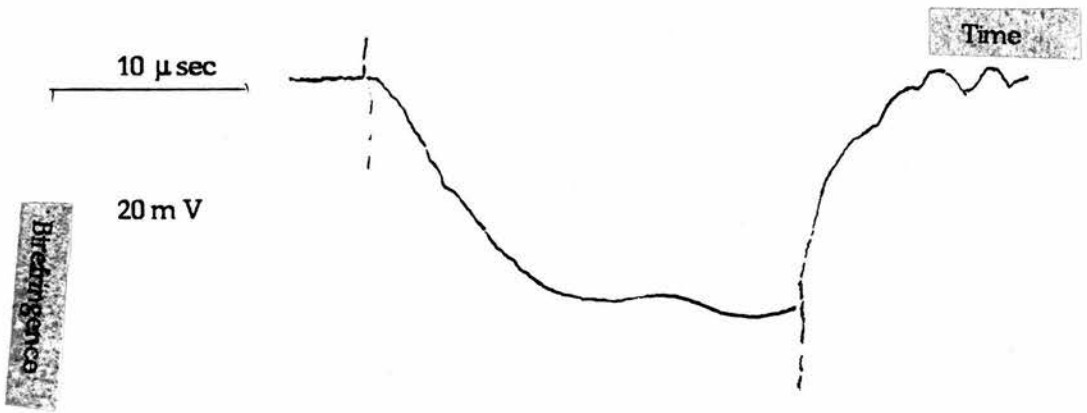

Fig IV 3:

Electric birefringence measurement : .

[Fn] 11 mg/ml Buffer 100mM NaCl ,50 mM Tris pH 7.4.

representation of Ln Dn (t)/ Dn (eq) as a function of time .

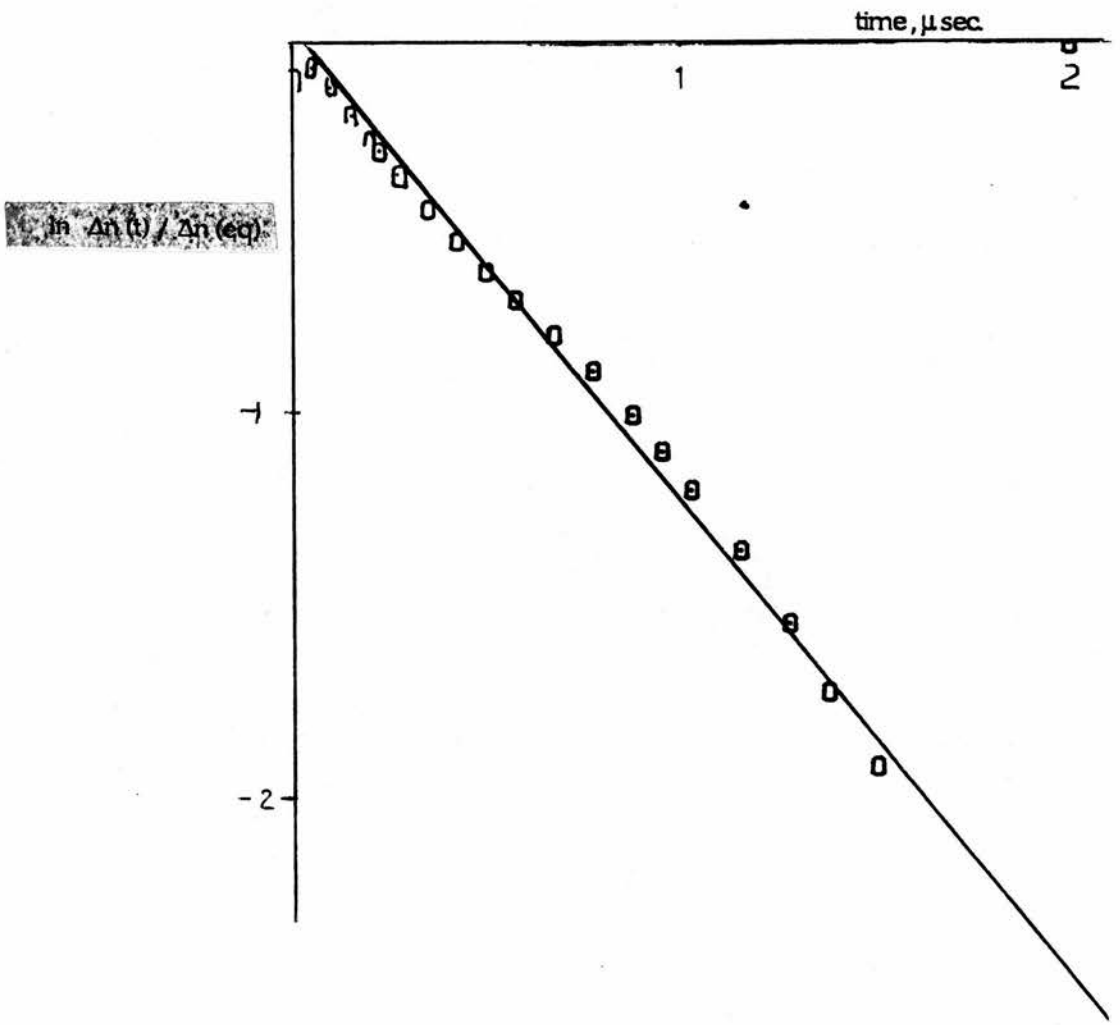

Fig IV 4:

Electric birefringence measurement :

[Fn] 5.5 mg/ml Buffer 50mM NaCl , 25 mM Tris pH 7.4

representation of Ln Dn (t)/ Dn (eq) as a function of time

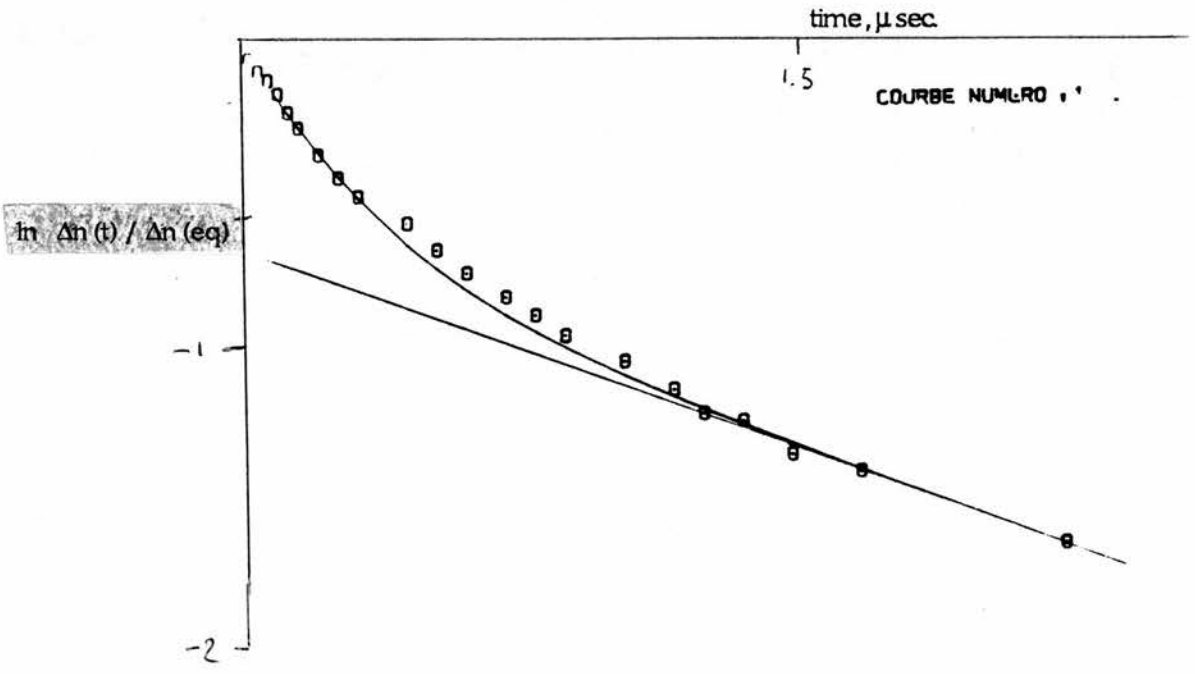

IV 2 4 Analysis of the decay of the birefringence.

Table IV 1 :Results from electric birefringence measurements: Relaxation times τ .

Buffer	[Fn] mg/ml	Field kV/cm	τ_1 µs	% of signal.	τ_2 µs	% of signal
100mM NaCl 50mM Tris pH 7.4	11	10	0.8	100	-	-
50 mM Na Cl 25mM Tris pH 7.4	5.5	10	1.2	94	0.2	6

With the restrictions mentioned in paragraph II 5 above , equation II 5 8 can be applied and allows deduction of the rotational diffusion coefficient (θ) from the measured relaxation time (τ) from the relation :

$$\theta = (6 \tau)^{-1}.$$

Table IV 2 : Correspondence between the relaxation tine τ and the rotational diffusion coefficient θ , (assuming the relation $\theta = 1/ 6 \tau$) .

τ (µ sec.)	0.2	0.8	1.2
θ (10^3 sec^{-1}.)	833	208	139

IV 2 5 Remarks on the electric birefringence data.

In order to achieve a correct signal to noise ratio , both fibronectin concentrations and the electric field had to be much higher than generally required for similar studies of proteins of the same size (Roux 1988) . This could be explained if the sum of the field induced and permanent electric momentum of fibronectin was clearly smaller than the average for proteins . This hypothesis might be backed up by the extremely asymmetrical profile of the birefringence recording showing that disorientation is much faster than orientation. This could be explained if the fibronectin molecule , which is made of two nearly similar chains , was symmetric and will be an important point in section IV 10 2 & 3 below .

IV 3 LIGHT SCATTERING EXPERIMENTS ON THE COMPLETE MOLECULE.

The determination of the translational diffusion coefficient of fibronectin by dynamic light scattering was first reported by Williams et al. in 1982.

In this work, with better equipment, those results were confirmed as a part of the controls for experiments described in chapter V and VI below. The diffusion coefficient of bovine plasma fibronectin at 40 degree angle as being 2.33 (+- 0.014) 10^{-7} c.g.s in 50 mM Tris-HCl, 100 mM NaCl 1 mM E.D.T.A. , pH 7.4 at 25 ° C. For human plasma , in the same conditions, the mean value was 2.2c.g.s. This value seemed not to depend of the angle of measurement as expected for a particle that is at least 25 times smaller than the wavelength.

IV 4 SMALL ANGLE NEUTRON SCATTERING OF WHOLE FIBRONECTIN.

IV 4 1 Introduction.

Neutron scattering measurements were performed at Station "D 11 " at the I.L.L. (Grenoble France) in June 87 for the work on the complete molecule and March 88 for the domains. Unfortunately similar experiments on the complete molecule appeared in the literature immediately after our own experiments. (Sjoberg et al. 1987). The technique has been described in section II 3 above.

It has been possible to perform some measurements allowing only a few percent error on the line fitting for the Guinier representations with a relatively low protein concentration of approximately 1.5 mg/ml. Neutron scattering studies requires lower concentrations than X-Ray scattering studies (the fibronectin concentrations were in the order of 1 to 2 mg/ml) therefore , not only the chances of multiple scattering are reduced but the sample preparation and handling techniques are better :

A) It has been possible to obtain the samples without further concentration of the samples. This allowed avoiding the use of ultrafiltration devices which migth lead to the denaturation of the protein due to the interaction of the protein and the ultrafiltration membrane.

B) Because of the low protein concentration , aggregation which is always a possible consequence of working with high concentrations were reduced.

C) An important condition to guarantee the validity of those measurements is that samples for neutron small angle scattering experiments are enclosed in quartz cells . As opposed to this , in X-Ray small angle scattering experiments the samples are generally in capillaries (i.e. Sjoberg et al. 1987) or special cells . The handling of

the sensitive fibronectin solution in quartz cells is much more gentle, and corresponds to conditions where it could be checked by light scattering that no aggregation or polymerisation occured.

Pavlov and Feodorov (1986) showed that the scattering curves for neutron scattering of protein solutions (as opposed to nucleic-acid solutions), in D_2O buffers do not significantly differ from those obtained with X-Ray scattering in H_2O buffers. Therefore the data obtained in D_2O buffers can be considered as fully valid for the construction of models of the fibronectin molecule. This is confirmed by the small differences shown between the measure of the radius of gyration in D_2O and H_2O in this work . Those minor differences can probably be explained by the better signal/noise ratio in D_2O rather by a real change in the conformation of the molecule.

IV 4 2 Samples.

The samples for neutron small angle scattering were prepared by immobilized gelatin followed by immobilized heparin affinity chromatography as described in chapter III. The samples were checked by PAGE and photon correlation .The samples were studied in light water buffer by dynamic light scattering :

The diffusion coefficient measured at 90 degrees and 25 °C was: $2.27\ 10^{-7}$ cgs .

The polydispersity index , as defined in II 1 7 above , was only 6 % .

The "in range " index , as defined in II 1 6 above , was 99.5 %.

All those figures are a good indication that those samples were monodisperse and free of aggregation in the conditions used for neutron small angle scattering experiments.

The fibronectin sample was also checked by 5 % acrylamide concentration S.D.S.P.A.G.E. A scan of this gel is shown in fig IV 5 below. The amount of contamination by degradation fragments made of only one chain was found, as determined by the ratio of their respective peaks areas in the gel,to be less than 10 % of the total sample mass.

Fig IV 5

Scan of S.D.S.P.A.G.E. : 10 µg Fibronectin sample for neutron small angle scattering.

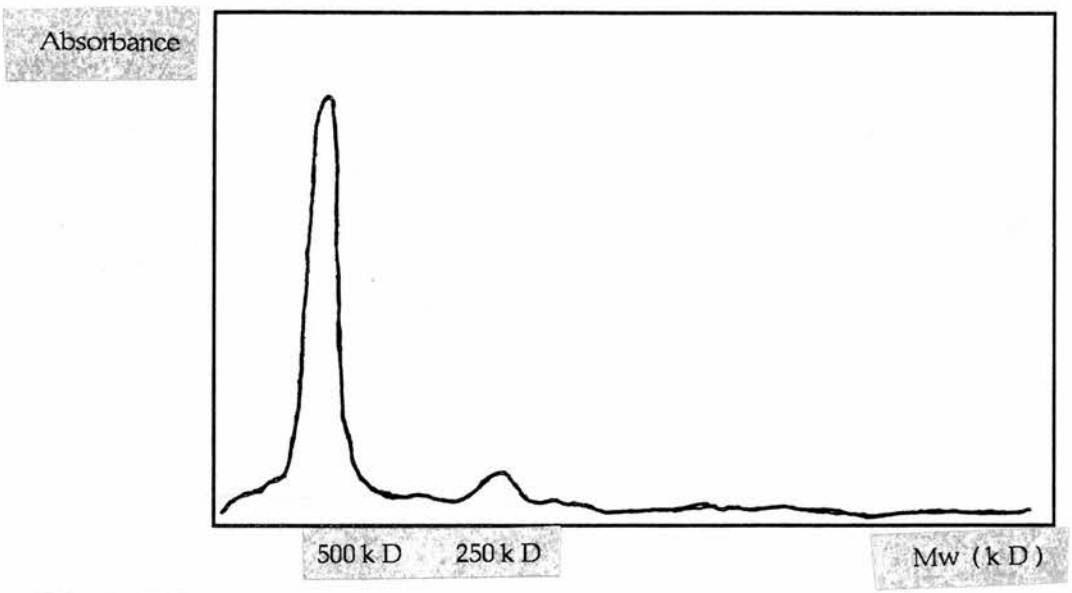

IV 4 3 Results.

Data collection and analysis has been described in section II 3 above. They are presented in Table IV 3 and Fig IV 6 to IV 8 below.All measurements were performed in at 25 °C in 50 mM Tris , 100 mM NaCl, 1 mM EDTA pH 7.4 ,PMSF 50 µM.

Table IV 3 : Determination of the radius of gyration of fibronectin from neutron small angle scattering experiments

Solvent.	Q.Rg min.	Q.Rg max	Rg (r Å)	Error %	Mw k D.
H_2O	0.5	1.95	71	2.3	505 k D
H_2O	0.53	1.71	75	3	520 k D
D_2O	0.5	1.65	73	0.9	510kD
D_2O	0.5	1.40	74	1.4	505 k D
D_2O	0.5	1.91	70	0.7	525 kD

It can be shown from those results that an average value of 73 Å is a good approximation to Rg . The experimental molecular weight determined by the techniques described above in section II 3 5 to 8 (The concentrations were determined by the measure of the optical density at 280 nm using an extinction coefficient of 12.8), is in good agreement with the theoretical value of approximately 500 k D obtained form the composition of this molecule.

Fig IV 6:

Determination of the radius of gyration of fibronectin by Guinier representation.

Buffer :H_2O

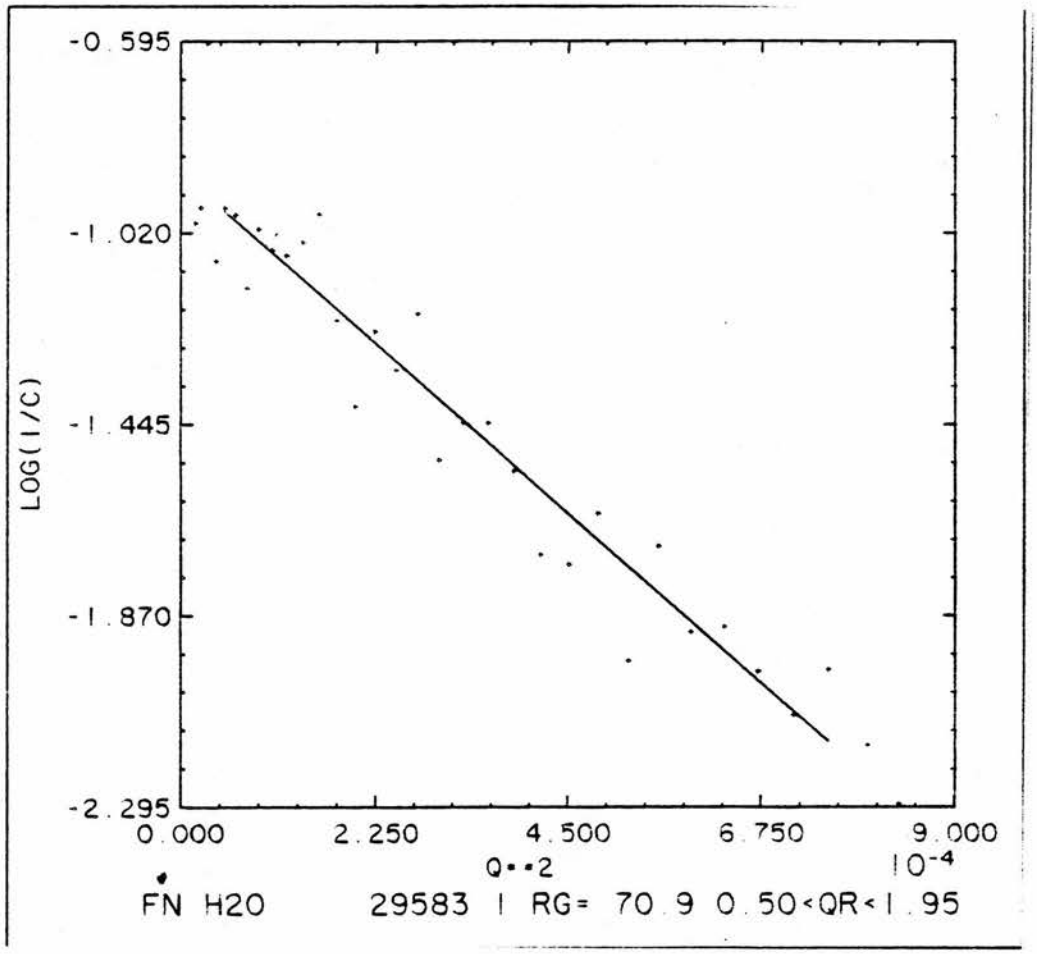

Fig IV 7:

Determination of the radius of gyration of fibronectin by Guinier representation.

Buffer : D_2O

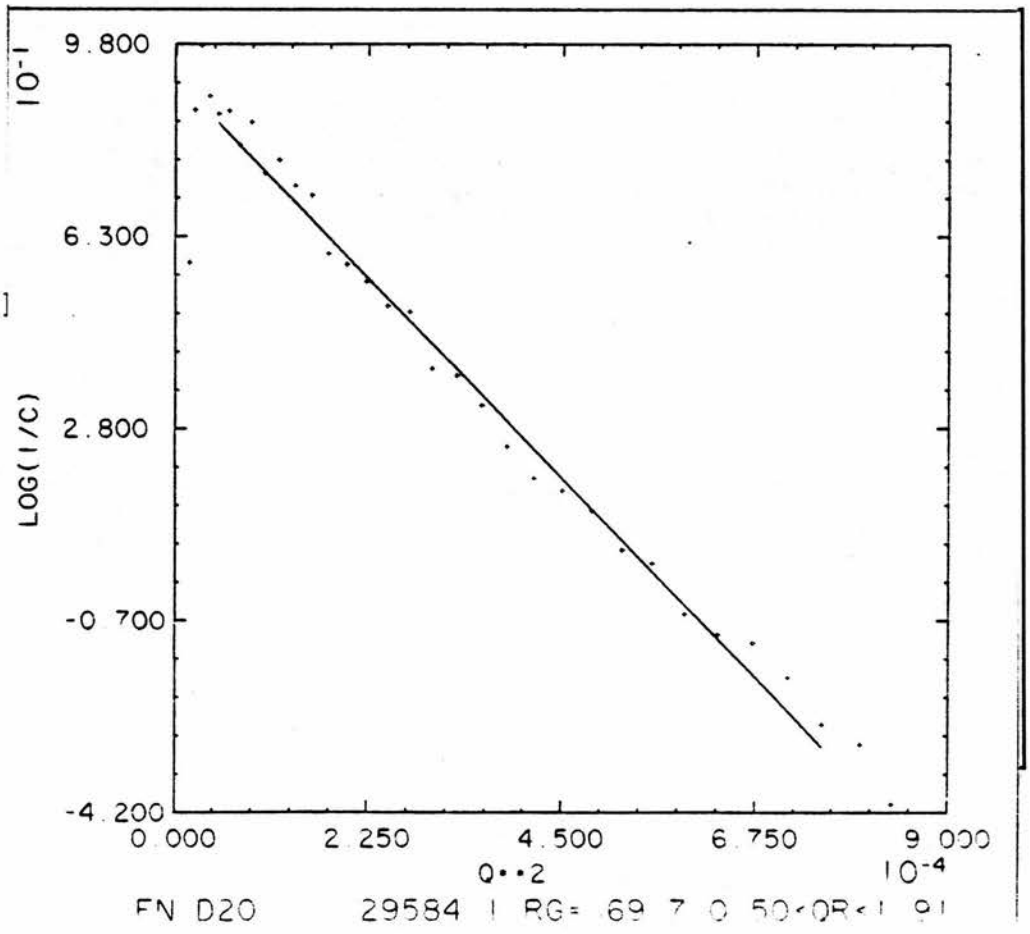

Fig IV 8 :

Scattering curve of fibronectin.

Buffer : D_2O

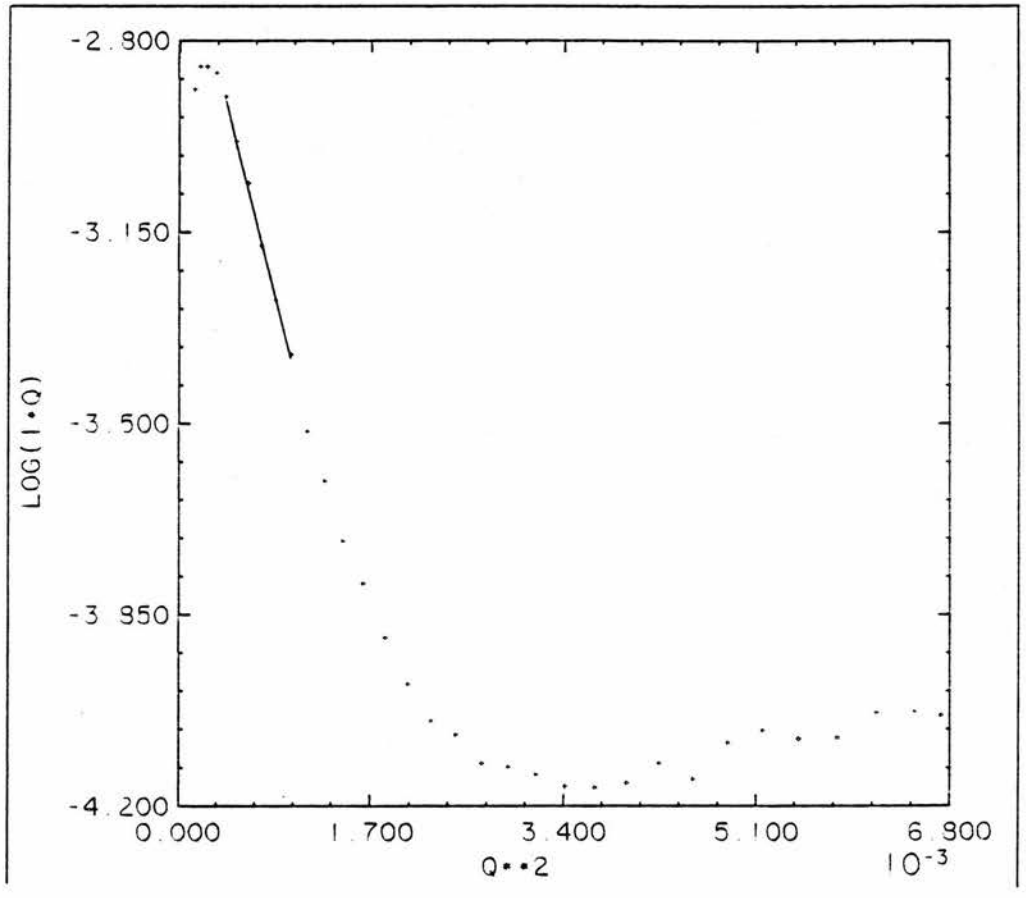

IV 5 RESULTS FROM ENZYMATIC LIMITED DIGESTION.

Limited proteolysis is a cheap and easy to perform technique that allows investigation of the tertiary structure of proteins. It has been extremely important for fibronectin as shown in chapter I .

The structure of fibronectin as a concatenation of protease resistant domains linked by protease sensitive segments is well known . The sequences that could theoretically be cut are regularly distributed in the primary structure. Therefore , the resistance to proteolysis of some large parts of the molecule as well as the high sensitivity of some fragments(which remain more or less the same whatever enzyme is used) ,are a good indication of the existence in the fibronectin molecule of a succession of compact domains connected by more extended segments.

It must be noticed that this point does not rule out the possible existence of a compact structure for the complete fibronectin : the domains might well be strongly associated together creating a compact structure with the connecting segments away from their surface as shown in diagrams below.

A)Compact , rigid structure :

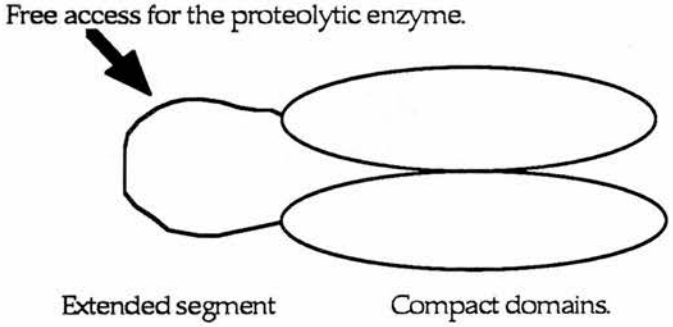

B) Extended , floppy structure:

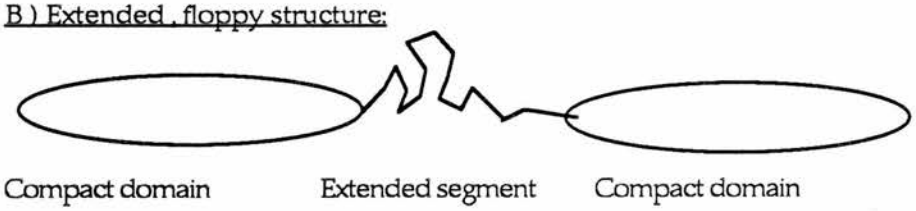

The published procedures include digestion conditions performed at non physiological ionic strength or pH. (i.e. : Thermolysin : Seikiguchi et al1986 : 50 mM Tris pH 7.6 ;). As apparently , there were no attempts to repeat a limited digest experiment in physiological conditions, it seemed important to confirm that the multi-domain model was still valid in a buffer of ionic strength of approximately 150 mM and pH 7.4.

Limited digestion with thermolysin has been performed at 25° C in 50 mM Tris,100 mM NaCl , 0.5 mM EDTA,2.5 mM $CaCl_2$. pH 7.4, stopped after 1, 10, 30 or 60 minutes by addition of E.D.T.A up to 10 mM, and analysed by a 5-15 % gradient S.D.S.P.A.G.E gel which is shown in fig IV 9 below.

Fig IV 9 :

S.D.S. P.A.G.E , Reducing conditions ,

of thermolysin digestion in physiological ionic strength:

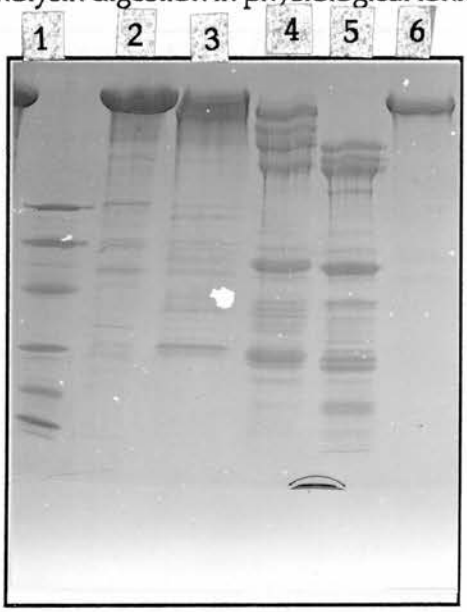

Lane 1 : Molecular weight standards 14, 19.6, 30 ,44 ,69, 96 k D.

Lane 2 : 1 minute thermolysin digest.

Lane 3 : 10 minutes thermolysin digest.

Lane 4 : 30 minutes thermolysin digest.

Lane 5 : 60 minutes thermolysin digest.

Lane 6 : control , undigested fibronectin.

After 60 minutes limited thermolysin digestion in 100 mM NaCl , 50 mM Tris ,2 mM $CaCl_2$,0.5 mM EDTA (lane 5), fibronectin fragments were at positions corresponding

to Mr of : 160 , 140 , 130 , 110 , 63 , 44 , 30, 27 k D . This is very similar to the pattern reported in the literature in in 50 mM Tris pH 7.6 (Seikiguchi et al. 1983), and our own data obtained in 50 mM Tris,25 mM NaCl pH 7.4.

IV 6 RESULTS FROM LIGHT SCATTERING ON PURIFIED 145-155 K D CENTRAL ,HEPARIN AND CELL BINDING DOMAIN.

Although the 145-155 k D thermolysin fragment represents a large portion of the molecule ,because of problems in its preparation (it is not easy to generate this fragment with high yields because it is easily cleaved) . Gel filtration on sepahacryl S 200 of a purified 145-155k D central heparin-cell binding domain showed that this domain was excluded from S200 media which has an exclusion limit of 200 kD for spherical proteins. This was the first indication of the fact that the shape of this fragment was non spherical. Unfortunately the attempts to determine the radius of gyration of the 145-155k D central heparin-cell binding domain both by small angle neutron at the I.L.L. and X-ray scattering at the Daresbury laboratories were failures because of a too weak signal/noise ratio.

The diffusion coefficient has a value of $3.1\ 10^{-7}$ (+- $0.8\ 10^{-7}$) cm^2s^{-1}. for this fragment. The in range index, as defined in II1 6 , was approximately 98 % . This showed that only a small contribution to the signal was due to particles out of the measuring range defined by the fundamental time. The fundamental time was set to scan a range of particles sizes corresponding to Stokes radius of 2 to 200 nm . The Stokes radius of this domain is can be calculated from the classic relation between the Stokes radius and the diffusion coefficient . Its value is 7.8 nm (assuming a viscosity of 0.009 c.g.s.) , as the Stokes radius of a spherical particle of Mr 150 k D should be only 4 nm approximately , we can conclude that this domain has a fairly extended structure .

IV 7 ESTIMATION OF THE SIZE AND SHAPE OF THE COLLAGEN BINDING DOMAIN.

IV 7 1 Introduction.

Gel filtration on sepahacryl S 200 of a 44k collagen binding domain preparation allowed a rough estimation of its shape. The determination of Kav (As described by Porath et al. 1959) was compatible with a globular shape when compared with a standard calibration curve from the gel manufacturer.

The determination of the diffusion coefficient of the gelatin binding domain by

light scattering techniques was impossible because of noticeable self aggregation property . Fig IV 10 shows the scattering intensity as a function of the diffusion coefficient. It clearly shows that most of the scattering intensity is due to aggregates with a very low diffusion coefficient. Because the signal corresponding to isolated 44 kD particles (i.e. with a diffusion coefficient around $4\ 10^{-7}\ cm^2s^{-1}$ is too weak , deduction of the diffusion coefficient of the 44kD gelatin binding domain from this data is impossible. Results from the work of Homandberg et al (1986) confirmed that a weak self interaction is observed for this domain .

Fig. IV 10 :

Scattering intensity as a function of the diffusion coefficient,
44 kD Gelatin binding domain.

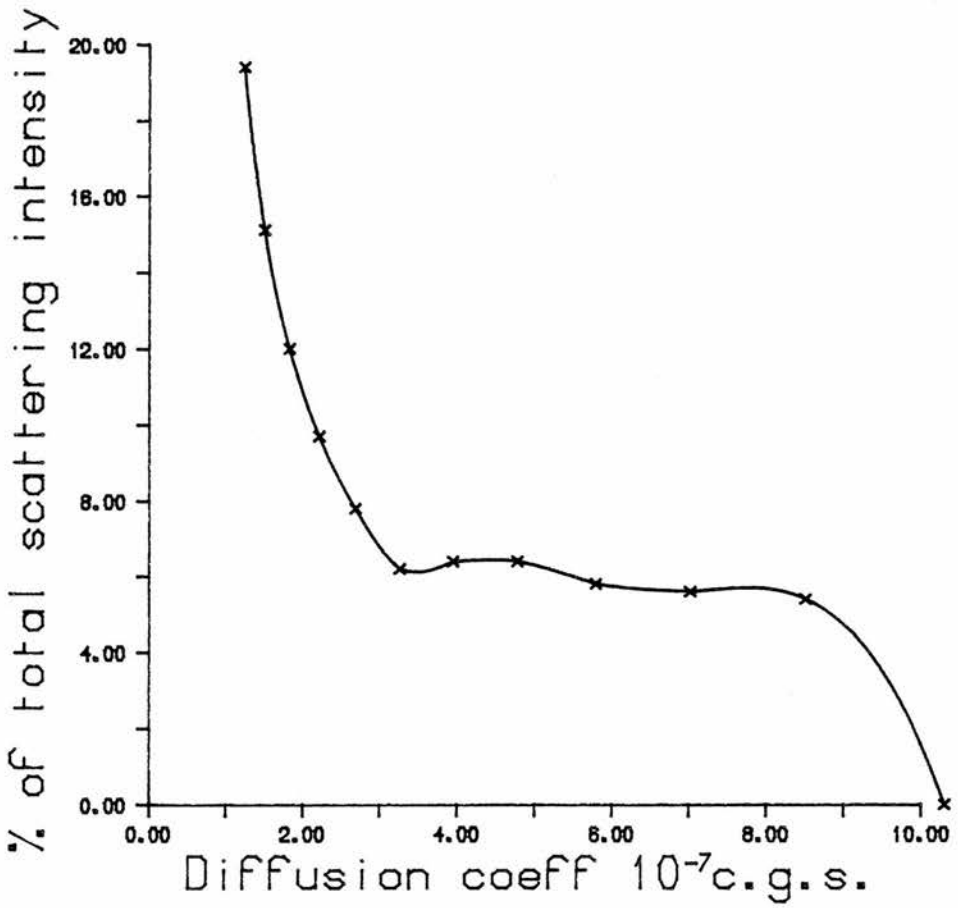

IV 7 2 Small angle neutron scattering results.

The reasons for being able to limit the problems created by aggregation in neutron small angle scattering studies were discussed chapter II section 2.

Fig. IV 11 below shows the Guinier representation of small angle neutron scattering profile from the 44KD gelatin binding domain of fibronectin.

Fig. IV 11:

Guinier plot of scattering intensity for 44k collagen binding domain.

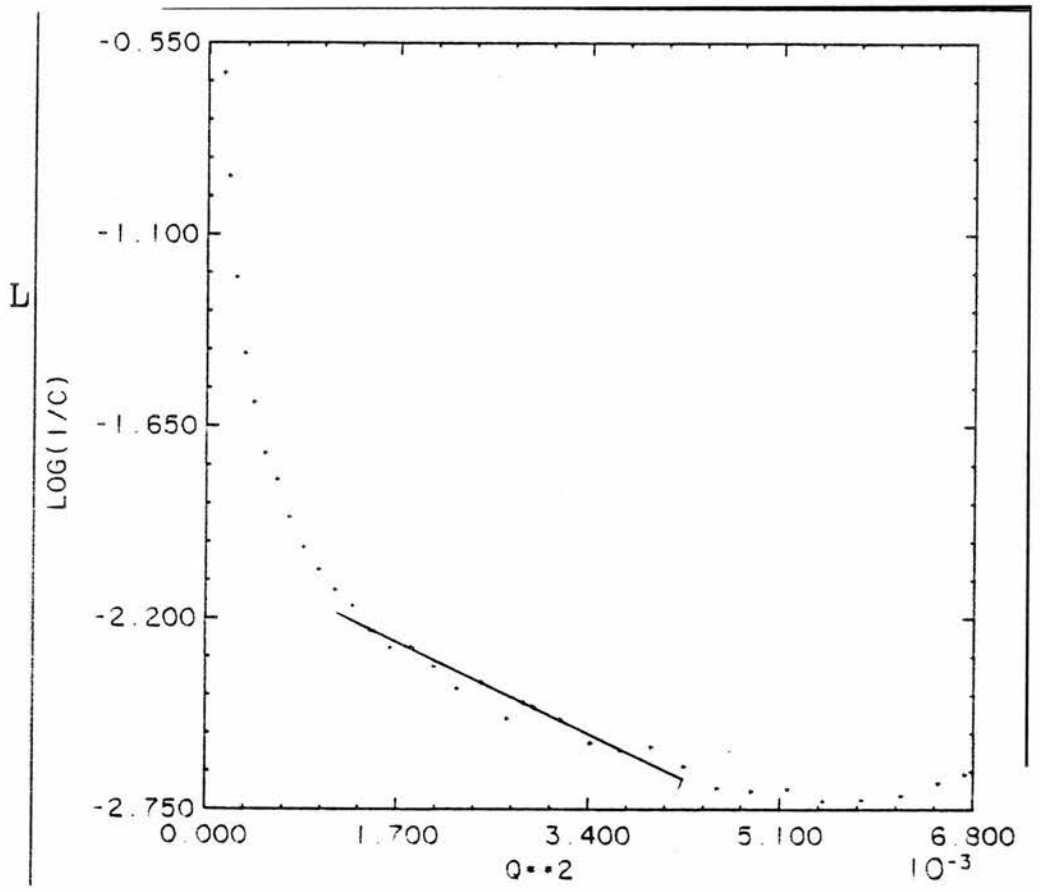

The radius of gyration with a Guinier range of 0.7 to 1.47 for the product Rg.Q was approximately 2 nm. Aggregation is still present but the approximation shown on the fig ure IV 11 above seems realistic because the molecular weight determined by calculations from the extrapolated intensity at zero angle as determined in chapter II, is approximately 49 k D. This is compatible with the value determined by S.D.S.P.A.G.E for this domain of 44k D.

IV 7 3 Hydrodynamic interpretation.

Because of the presence of aggregation in the solution , the determination of the radius of gyration of the 44 k d gelatin binding domain is not very accurate. The measured Rg is approximately 2 nm. The radius R , of a spherical protein of 44 k D Mr ,with 30 % hydration approximately2.6 nm . The corresponding Rg is $(3/5)^{-1/2}$ R that is : 2 nm . It is reasonable therefore to conclude that this domain is roughly spherical.

IV 8 GENERAL REMARKS ABOUT A MODEL CONSTRUCTION.

IV 8 1 Introduction.

A realistic model of fibronectin in solution must try to integrate not only results from this work but also results from the literature . It must be pointed out that some authors do not follow this rule and seem to ignore all results which do not fit with their models (i.e.: From the interaction between the N terminal part of the two chains Wolff et al. 1988 describe fibronectin as spherical ignoring all previous hydrodynamic work . Roco et al. 1983,1987 build string like models, made of very small size bead type subunits, ignoring the limited enzyme digestion and denaturation results clearly indicating the presence of large ordered domains).

Because of the multidomain multifunctional structure of fibronectin the models can be defined for convenience at three different levels:

A) The hydrodynamic model. In this model the shape of the molecule is restricted to an ellipsoid of revolution. The dimensions of the ellipsoid are estimated by calculations from the measure of hydrodynamic parameters. This model does not describe the shape of the molecule with high accuracy. Because ellipsoids of revolution are amongst the few structures whose hydrodynamic properties can be described by exact formulae (Perrin 1934), the model accuracy is theroretically limited only by the accuracy of the measure of hydrodynamic parameters and does not requires any other data.

B) The next degree of resolution are models that can define not only the general shape of the molecule but also the relative position of the two chains. At this level, no attempts can be made to define the size and precise position of the various

domains. Those models will integrate hydrodynamic determinations of previous section as well as results from fluorescence or even enzymatic limited digestion studies performed on the complete fibronectin molecule. Often no perturbation (i.e. labelling), is required. This allows study of the molecule in the state closest to native . Thus the low resolution models bring a limited amount of information but are not subject to errors induced by fragmentation (i.e. a possible rearrangement of the domains after fragmentation).

C) In the case of a multi domain molecule such as fibronectin, a higher resolution model can also be proposed because spectroscopic evidence shows that fibronectin domains retain their conformation even after isolation from the native molecule:

α) The circular dichroism spectrum of the intact fibronectin molecule can be derived from the combination of the spectra of the various domains (i.e Odermatt et al. 1982) .

β) Works by Ingham et al 1984 and Franchesi et al 1985 show that thermal denaturation properties,(as well as ,again, circular dichroism spectra), are not affected by a change in pH or by ligand addition. As the diffusion coefficient is affected by a pH change (Williams 1982) it is possible to conclude that fibronectin is made of independent domains. A possible three domain structure (Wallace et al. 1981) has been proposed from thermographic studies.

γ) By expression in E.Coli of fragments of fibronectin of various sizes (Obara et al. 1987),it has been shown that a 70 kD fragment containing the cell attachment peptide RGDS has the same cell attachement efficiency as the complete fibronectin molecule. This also is an indication that this molecule is made of independent domains,(providing the cell attachement assay technique does not result in a destruction of the tertiary structure of the fibronectin molecule).

Those facts , showing with a reasonable confidence that the structure of the domains is not altered by their isolation from the intact molecule , allow the proposal of models derived from informations on the intact molecule as well as from the purified domains.

IV 8 2 The problem of modelling non rigid structures by hydrodynamic techniques.

A number of recent advances in hydrodynamic studies are due to De La Torre and his co workers (see De La Torre et al 1977 a,b,c; De La Torre et al 1978 ,Bernal et al 1980,1981,). Those authors used spheres of various volumes and arrangements for the

modelling of large macromolecules in solutions. All those studies refer to models where the spheres are disposed in rigid associations. In a more recent work (De La Torre et al. 1985), the case of two spheres connected by a flexible link has been studied. From this work it can be concluded that the modelling , from hydrodynamic data, of a molecule made of many subunits connected by flexible connections is not yet possible .

Some electron microscopic studies (Engel et al.1981, Odermatt et al. 1982 , Erickson et al. 1981) , seem to support the flexible model but as pointed out before those pictures are definitely not compatible with the hydrodynamic behaviour of the fibronectin molecule.

Fortunately there is little evidence that the fibronectin structure in solution is non rigid. Some electron-spin-resonance data (Lai et al. 1984 & 1983 ,claim non rigidity but those results are not satisfactory because of possible non rigid label-protein association as discussed in chapter VI below. More serious is the data from fluorescence polarization of Wiliams et al (1982) showing some flexibility of the N terminus end of fibronectin labeled with fluorescein. The label is attached near to the N-terminal part of the protein (position n° 3). Once again it is difficult to assume that the motion of the label is due to large flexible domain of the protein rather than to motions restricted to the molecule's N-terminal section. As discussed above in section 5 of this chapter ,the existence of structurally independent domains is not at all compatible with a compact structure . The work of Homandberg , (1986) , even showed that non covalent interactions occur between the various domains of fibronectin .

In conclusion although one cannot be fully positive about the existence of the fibronectin molecule in solution as a rigid structure , this hypothesis can be made with a reasonable degree of confidence .

IV 9 An hydrodynamic ellipsoid model for the fibronectin molecule in solution.

IV 9 1 Introduction.

The basic idea of this model is to determine the type and the semi-axis a & b of an ellipsoid of revolution having the same hydrodynamic properties as the molecule . Two types of ellipsoids can be defined : prolate or oblate , see Fig. IV 12 . They are respectively called "ellipsoide allongé" or "ellipsoide aplati" in the work of Perrin (1934) , which is the reference for all the hydrodynamic work with ellipsoid models because it presents the relations between a and b and the diffusion coefficients .

Fig. IV 12 :

Ellipsoids of revolution .

Prolate ellipsoid : a > b .

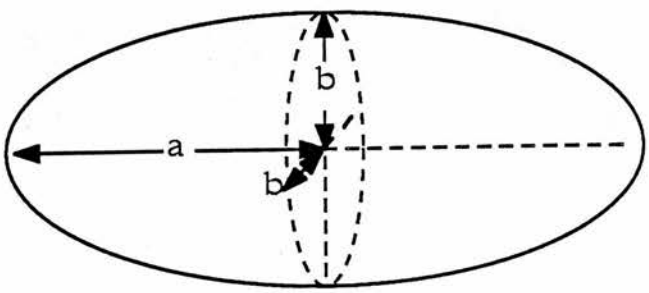

Oblate ellipsoid : a < b .

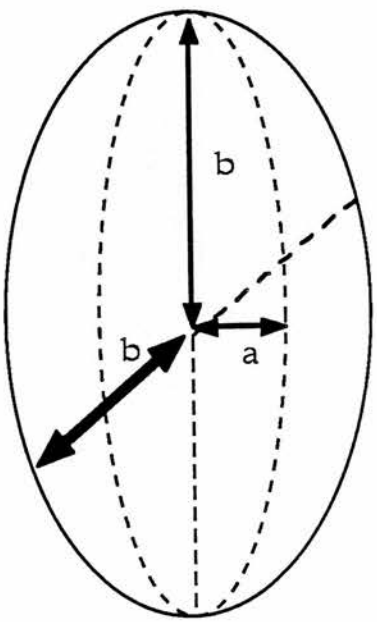

The extension of the ellipsoid : p , is defined as p = a / b .

Various techniques allow the estimation of a and b :

A) The classical way is based on the fact that the following hydrodynamic parameters are a function of a and b:

The radius of gyration : Rg .

The translational diffusion coefficient Dt

The rotational diffusion coefficient θ .

a and b can be deduced from the comparison between the experimental measurement of one of those parameters and its estimation calculated from the volume of a spherical protein with the same degree of hydratation . Obviously the results will be much influenced by the degree of hydration which is arbitrarily chosen.The viscosity of the solvent must be known accurately and that is generally not true. Furthermore the measure of θ or Dt is based on a generally complex interpretation of the measured experimental parameters which also can be a source of errors .

B) An alternative method is to measure the neutron or X-ray scattering intensity profile of a solution of the molecule over a large range of scattering angle Q . The fitting between the experimental curve and theoretical curves obtained with ellipsoids with various sizes and shapes (i.e. different a & b) is then examined. This allows a choice of the model corresponding to the best fit between the experimentally determined curve and these obtained theoretically from a hydrodynamic model. This technique was applied to fibronectin by Sjoberg et al. 1987 . The major problems associated with it are :

α) That , as pointed out by Guinier (1955), two very different objects can have very similar scattering curves.

β) The optical parameters of the X ray or Neutron scattering camera , for technical reasons (i.e. finite size of the beam , plane detector), are far from being perfect and can lead to serious distortions in the scattering profile curve. (This can be shown by the differences between the radius of gyration of the fibronectin molecule in published data and in the results from this work . Those optical defects requires processing the data through desmearing and deconvolution steps to try to minimise the effects of those problems.

C) It is also theoretically possible to calculate the ellipsoid dimensions : a and b , if at least two of Dt, Rg or θ are known . This last method of determination is not frequently used by experimentors. From the measure of the rotational diffusion coefficient θ, and the translational diffusion coefficient Dt respectively by electric birefringence and photon correlation experiments (See for example Bernengo et al.

1981) a and b were determined in various molecules. The problem in those determinations are:

α) That the rotational diffusion coefficient, θ, is often obtained from electric birefringence experiments .Although θ is a very sensitive function of the a and b, the theory relating θ to the decay of the birefringence is not always satisfactory . This can cause serious errors in the calculation of θ from electric birefringence experiments as discussed in paragraph II 8 . Fortunately if θ is not easy to determine . Decay rates for various ellipsoids models have been related to the theoretical decays of a spherical molecule of the same molecular weight . (See Tao 1969 and paragraph II 5 6).

β) That for certain extensions p can vary substancially without creating much change in the relations between the hydrodynamic parameters.

Technique B ,despite the recording of a full scattering curve (Fig IV 8) could , unfortunately , not been applied here .

IV 9 2 Determination of the type of ellipsoid by interpretation of the results from the electric birefringence measurements .

The theoretical background for the electric birefringence measurements and analysis was described in chapter II , paragraph 5 .6 above . The interpretation of the results was developed by Tao in 1969 from the decay of fluorescence polarization but expanded later to birefringence by Wengener et al.(1979). We shall see how the type of decay of the birefringence (multi or single exponential), as well as the relaxation times can yield information on the molecular structure. The principle is to compare the observed birefringence relaxation time , τ_{Fn} , to the relaxation time , τ_d, of a spherical protein of the same molecular weight .

The ratio of the relaxation times τ_n for various ellipsoid shapes to the relaxation time τ_d, of a sphere of same mass has been calculated (Tao 1969) and represented in Fig IV 13 & 14 below. From the curves of Fig IV 13 & 14 , it can be immediately deduced , for any value of the relaxation time of an equivalent sphere, that the prolate ellipsoid model of fibronectin has multi-eponential birefringence decay curve and that for an oblate ellipsoid a single-exponential decay is a very good

approximation .As pointed out above in IV 2 , fibronectin in 150 mM ionic strength buffer shows a birefringence decay that can be described by a single exponential decay of field induced birefrinegence. The first conclusion of this measurement is that , if fibronectin is a structure with an extension p, of less than 0.2 or more than 5 approximately ,the ellipsoid model for fibronectin should be an oblate type.

The fact that the signal , obtained at high field , can be described by a single exponential decay is also a proof that no molecular flexibilty can be detected by this technique .

IV 9 3 Determination of the dimensions of the ellipsoid by the use of the birefringence relaxation time and the radius of gyration .

As the molecular weight of fibronectin is known , it is possible to calculate the extension of the ellipsoid model if some hypothesis is made on the degree of hydratation of the molecule . This is shown below:

It is possible to calculate the theoretical relaxation time , τ_d of a spherical protein of molecular weight Mr with a percentage of hydratation δ (g water/ g dry protein) , from equations IV 1 to 5 below . For a sphere the birefringence relaxation time τ_d is related to the rotational diffusion coefficient θ , by:

$$\tau_d = 1/6 \quad \theta^{-1} \text{ (IV 1).}$$

For a sphere of radius r , with η as the solvent viscosity , θ is given by :

$$\theta = k T (8 \Pi \eta \ r^3)^{-1} \text{ (IV 2).}$$

The relation between the radius ,r , of a protein and its molecular weight Mr ,partial specific volume vo and degree of hydration δ , is :

$$r^3 = 3/4 \pi \, Mr (vo + \delta) / N \text{ (IV 3).}$$

By combining IV 1 , IV 2 and IV 3 :

$$\tau_{d\,(n\,sec)} = 10^9 \eta (N \, k T)^{-1} Mr (vo + \delta) \text{ (IV 4).}$$

With : η = 0.009 c.g.s. and k T = 41.1 10^{-15} c.g.s. at 25 ° C

$$\tau_{d\,(n\,sec)} = 364 \ 10^{-6} Mr (vo + \delta) \text{ (IV 5).}$$

The theoretical relaxation time , τ_d , of a spherical protein of Mr equals to 500 k D , as fibronectin and the ratio of the observed relaxation time to the calculated one are represented below in Table IV 4 for various degrees of hydration .

Table IV 4 : Determination of the ratio of the observed relaxation times , τ_{obs} to the theoretical ones , τ_d .

τ_d (μ sec)	δ (% g H_2O/g dry protein.)	τ_{obs} / τ_d
0.131	0	6.1
0.140	5	5.7
0.169	10	5.4
0.167	20	4.8
0.186	30	4.3
0.204	40	3.9
0.222	50	3.6

From the curve of Fig IV 14 the corespondence can be found between τ_{obs} / τ_d and p the ellipsoid extension. If we add some information like the measured Rg , the dimensions can then be estimated. This allows calculation of the model volume . The ratio of this calculated volume to the dry volume should correspond to the degree of hydratation chosen as hypothesis. This is shown in table IV 5 below .

Table IV 5 : Calculation of the volume of an ellipsoid model and its degree of hydratation from the measure of Rg and τ_{Fn}.

τ_{Fn} / τ_d		p	Rg	δ	a	b	vol_{obs}
δ of model (%).							
6.1	13.5	7.3	0	0.85	11.5	470	< 0
5.7	13	7.3	5	0.88	11.5	490	<0
5.4	11.5	7.3	10	1	11.5	554	< 0
4.8	10.5	7.3	20	1.1	11.5	610	< 0
4.3	9.5	7.3	30	1.21	11.5	670	5
3.9	8.5	7.3	40	1.35	11.5	750	20
3.6	7.5	7.3	50	1.53	11.2	850	35
4.8	10.5	8.9	20	1.34	14	1100	75

Fig IV 13 :

Ratio of the relaxation times of a prolate ellipsoid to a sphere of the same mass as a function of p^{-1}. (From Tao 1969).

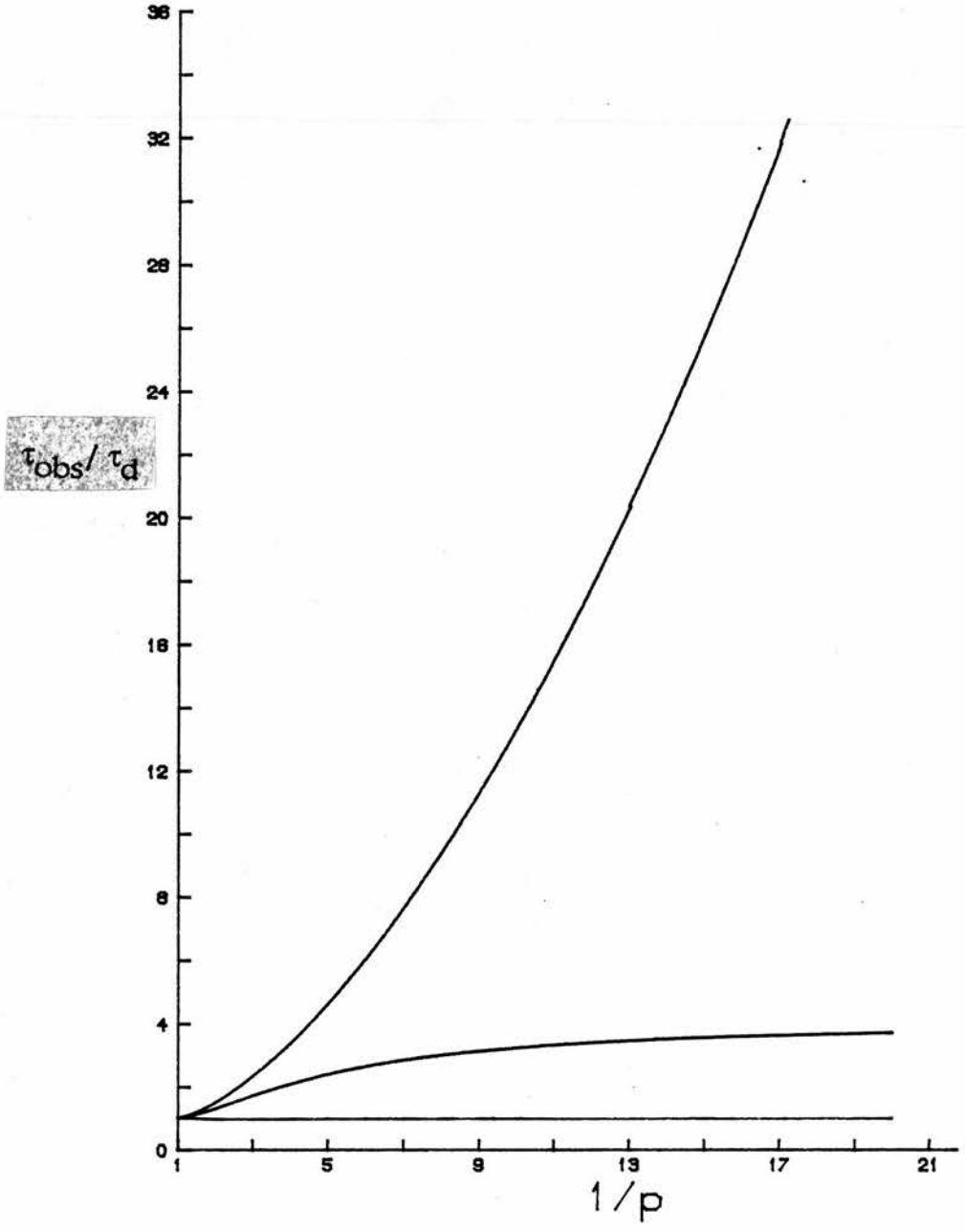

Fig IV 14:

Ratio of the relaxation times of an oblate ellipsoid to a sphere of same mass as a function of p (From Tao 1969).

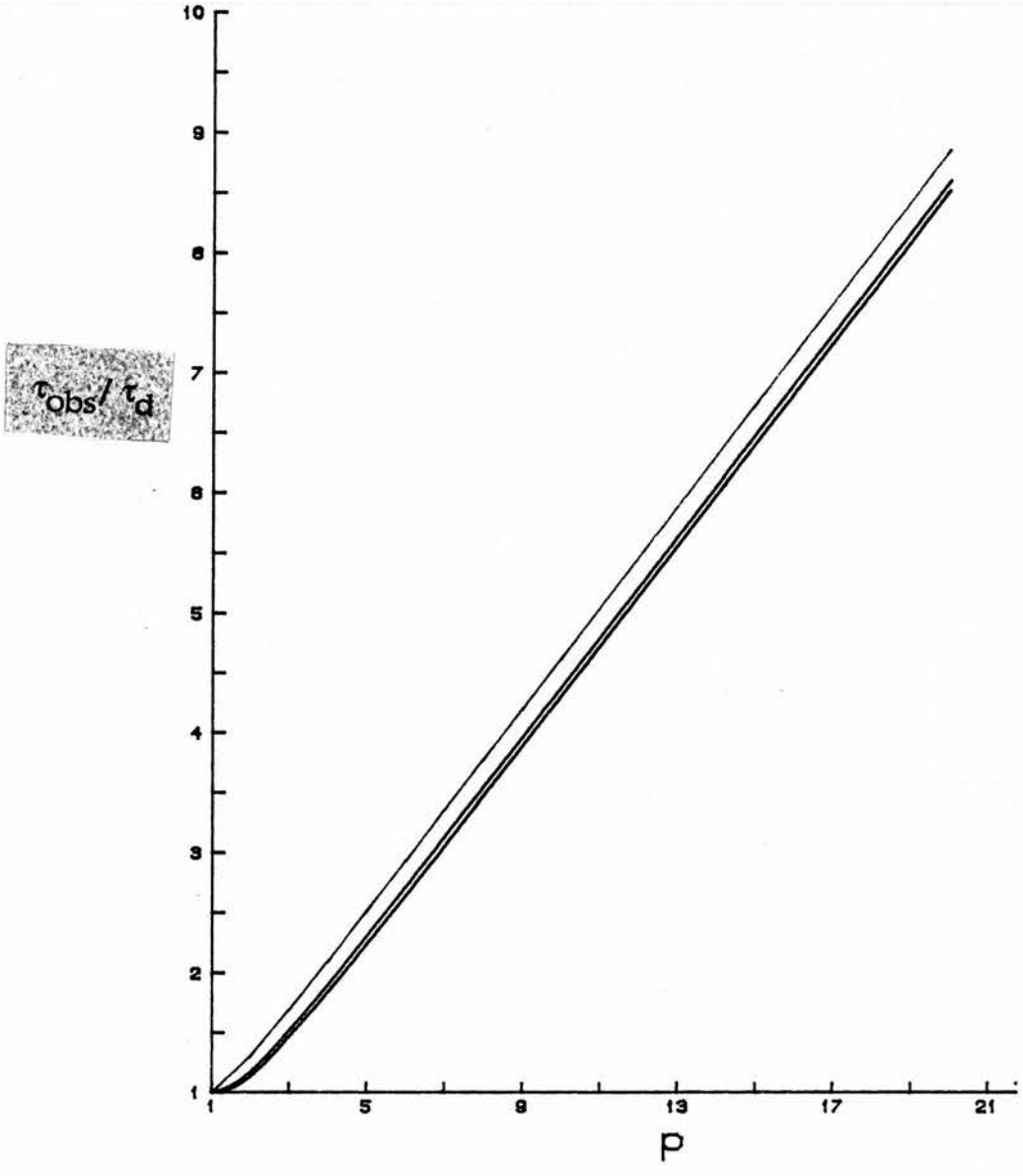

The degree of hydratation , δ chosen as a hypothesis to calculate the ellipsoid extension , p , is compared to the degree calculated from the ratio of the volume of the model to the dry volume of the protein . The model dimensions are obtained by the combination of the estimated extension and measured radius of gyration . The comparison between those degrees of hydratation shows that it is clear that the method of calculation is not applicable to those meassurements .

The conclusion of this section is , that although the birefringence data fit well with a prolate ellipsoid with an extension of about ten , it seems difficult to find an ellipsoid with an extension precisely fitting with the birefringence data and any observed radius of gyration (either from this work or as published values of Sjoberg et al. 1987) . This problem will be discussed in IV 9 6 below

IV 9 4 Estimation of the dimensions of the ellipsoid by combination of the measured rotational diffusion coefficient θ and translational diffusion coefficient Dt

It is also possible to apply the analysis of Bernengo et al. 1981 which combines the rotational diffusion coefficient θ, measured by electric birefringence and the translational diffusion coefficient Dt to work out the dimensions of the ellipsoid . This method has been described by Daune et al 1961. The translational diffusion coefficient Dt is related to the dimensions of the equivalent ellipsoid by the relation :

$$Dt = (k\ T\ \ t(p)) / (6 \Pi\ \eta\ a\ p^{2/3}) \quad (IV\ 6\ ).$$

The rotational diffusion coefficient is related to the dimensions by the relation :

$$\theta = r(p)\ k\ T / (8\ \pi \eta\ a^3\ p^2) \quad (IV\ 7)$$

Where t (p) and r (p) are two functions of p.From those two relations it can be shown that :

$$(D^3 / \theta\ )(27\ \Pi\ \eta^2 / k^2T^2) = t^3(p)\ r^{-1}(p) \quad (IV\ 8)$$

Table IV 6 , below presents the calculations of $27\ \Pi\ \eta^2 / k^2T^2$ for various experimental and theoretical values of D_t^3 and θ .

Table IV 6

Dt ($\times 10^{-7}$ c.g.s.).	θ ($\times 10^{3}$ sec^{-1})	$(D^3 / \theta)(27 \Pi^2 \eta^2 / k^2T^2)$
2.25	208	0.7
2.35	208	0.8
2.9	208	1.5
2.35	111	1.5

The work from Bernengo shows that the value of $(D^3 / \theta)(27 \Pi \eta^2 / k^2T^2)$ should be , for oblate ellipsoids , in the range of 1 to 1.5 approximately . In the measurements presented over in Table IV 6 , for various values of D , $(D^3 / \theta)(27 \Pi \eta^2 / k^2T^2)$ is significantly less than 1 .

To achieve a value of 1.5 for this product (compatible with an oblate ellipsoid with p equals to 10) either the diffusion coefficient should be 25 % higher than the measured one or the relaxation time should be 88 % more than the observed one . It is unlikely that experimental errors are of this size . We conclude that this is instead due to the fact that a modelling of the shape of the molecule as an ellipsoid is not possible with this technique . This once again will be discussed below in IV 9 6 .

IV 9 5 Principle of the determination of the dimensions of an ellipsoid from the measure of its radius of gyration and diffusion coefficient.

As the hydrodynamic interpretation of the birefringence experiments is not easy , an estimation of the model parameters will now be attempted from the relations between the radius of gyration Rg and the translational diffusion coefficient Dt . The relations between a and b , and Dt, (Perrin 1934) are different for prolate and oblate ellipsoids . Those two types will be considered separately in paragraphs A and B below.

A) For a prolate ellipsoid (a > b) , if p is the ratio b/a, the radius of gyration (Rg) and the translational diffusion coefficient (Dt), can be both expressed as a function of a and b .

$$Rg = a [(1+ 2p^2)/5]^{-1/2} \quad (IV\ 9\ ).$$

$$Dt = (k\ T\ t(p)) / (6 \Pi\ \eta\ a\ p^{2/3}) \quad (IV\ 10\ ).$$

Where : k is Boltzmann's constant , T the temperature (Kelvins) , η: The solvent viscosity (Poises) , t (p) is a function depending on the type of ellipsoid : Prolate or

oblate . t (p) is expressed as follow for a prolate ellipsoid (a > b) :

$$t(p) = p^{2/3} (1- p^2)^{-1} \text{Ln} [\{1+ (1- p^2)^{1/2}\} p^{-1}] \quad (\text{IV } 11)$$

From equations IV 10 1 & 2 we get :

$$a = Rg [(1 + 2p^2)/5]^{+1/2} \quad (\text{IV } 12).$$

$$Dt . Rg \ 6 \Pi \ \eta (\kappa T)^{-1} = [(1 + 2p^2)/5]^{1/2} \ t'_1(p) \quad (\text{IV } 13).$$

Where $t'_1(p)$ is afunction of p which is fully developed in equation IV 14 below:

$$t'_1(p) = (1- p^2)^{-1} \text{Ln} [\{1+ (1- p^2)^{1/2}\} p^{-1}] \quad (\text{IV } 14)$$

So from the calculation of $Dt . Rg \ 6 \Pi \ \eta (\kappa T)^{-1}$ a value for the function of p : $[(2 + p^2)/5]^{-1/2} \ t'_1(p)$, is found and p can be determined. This relation is plotted in fig IV 16 . Once p is known , a is calculated from IV 12 and b is by definition the product of p times a .From the examination of Fig IV15 it is obvious that for a prolate ellipsoid , the determination is accurate only if p is less than say 0.2 , (i.e. if a is at least five times bigger than b).

B) Oblate

From paragraph A over :

$$a = Rg [(1 + 2p^2)/5]^{+1/2} \quad (\text{IV } 12).$$

$$Dt . Rg \ 6 \Pi \ \eta (\kappa T)^{-1} = [(1 + 2p^2)/5]^{1/2} \ t(p) \quad (\text{IV } 13).$$

Where : k is Boltzmann's constant.

T is the temperature (0 Kelvin) .

η is the solvent viscosity. (Poises)

t (p) is a function depending on the type of ellipsoid : Prolate or oblate . t (p) is expressed as follow for an oblate ellipsoid (b > a) :

$$t(p) = p^{2/3} (p^2 - 1)^{-1} \text{ Arc Tg} [(p^2 - 1)^{1/2}] \quad (\text{IV } 15)$$

From equations IV 12 & 13 we get :

$$Dt . Rg \ 6 \Pi \ \eta (\kappa T)^{-1} = [(1 + 2p^2)/5]^{1/2} \ t'_2(p) \ (\text{IV } 16).$$

where $t'_2(p)$ is developed in equation IV 17 below.

$$t'_2(p) = (p^2 - 1)^{-1} \text{ Arc Tg} [(p^2 - 1)^{1/2}] \ (\text{IV } 17).$$

So from the calculation of $Dt . Rg \ 6 \Pi \ \eta (\kappa T)^{-1}$ a value for the function of p:

$[(2+p^2)/5]^{-1/2}\ t'_2(p)$, is found and p can be determined. This relation is plotted in fig IV 17. Once p is known : a is calculated from eq. IV 12 and b is by definition the product of p by a .From the examination of Fig IV 16 , it is obvious that for a prolate ellipsoid , the determination is accurate only if p is less than say 2 .

The two major problems with this determination from Rg and Dt only , are that the accuracy of the determination is poor for oblate elipsiods and , as pointed out in paragraph IV 9 1 , the determination of the radius of gyration by the Guinier approximation is a source of errors . This determination is dependent on the range of Q chosen for the approximation , thus Rg cannot be measured with an extremely high accuracy . From results from IV 4 it is shown that the determination of Dt is more consistent but subject to errors in the determination of the viscosity , so it can be seen that most of the error in the experimental parameters is due to the determination of Rg.

This can be applied to the fibronectin molecule. The determination of the radius of gyration , Rg , depends on the range of Q chosen for the Guinier approximation and it is difficult to fix an exact value for the radius of gyration. Results from IV 4 were in a range from 7 to 7.5 nm with a possible average of 7.3 nm. The diffusion coefficient , Dt , shown little variation and can be estimated at 2.25 to 2.35 10^{-7} cgs.

Table IV 7 below shows the value for $Dt\ .\ Rg\ 6\,\Pi\,\eta\,(k\,T)^{-1}$ corresponding to Rg and Dt . (η = 0.009 c.g.s , T = 25 0 C , k T = 41.1 10^{-15} c.g.s.).

Table IV 7.

Rg (nm)	Dt (10^{-7} c.g.s)	$Dt\ .\ Rg\ 6\,\Pi\,\eta\,(k\,T)^{-1}$ (c.g.s)
7	2.25	0.650
7.3	2.25	0.678
7.5	2.25	0.696
7	2.35	0.679
7.3	2.35	0.708
7.5	2.35	0.727

$Dt\ .\ Rg\ 6\,\Pi\,\eta\,(k\,T)^{-1}$ can vary ,depending on the estimations of Dt and Rg between 0.650 and 0.725 c.g.s. From examination of Fig IV 15 and IV 16 , it can again be concluded that the ellipsoid model for fibronectin must be an oblate ellipsoid if the deviation from spherical shape is marked . Unfortunately the resolution is not high enough in the measurement of Rg and Dt to allow any precise values for p to be deduced from this data. It is then clear that the determination of the parameters of an oblate ellipsoid for fibronectin cannot be determined from the measure of Rg and Dt alone .

Fig IV 15 :

Representation of : $Dt \cdot Rg\ 6\Pi\ \eta\ (\kappa T)^{-1} = [(1+2p^2)/5]^{1/2} t(p)$,

for a prolate ellipsoid.

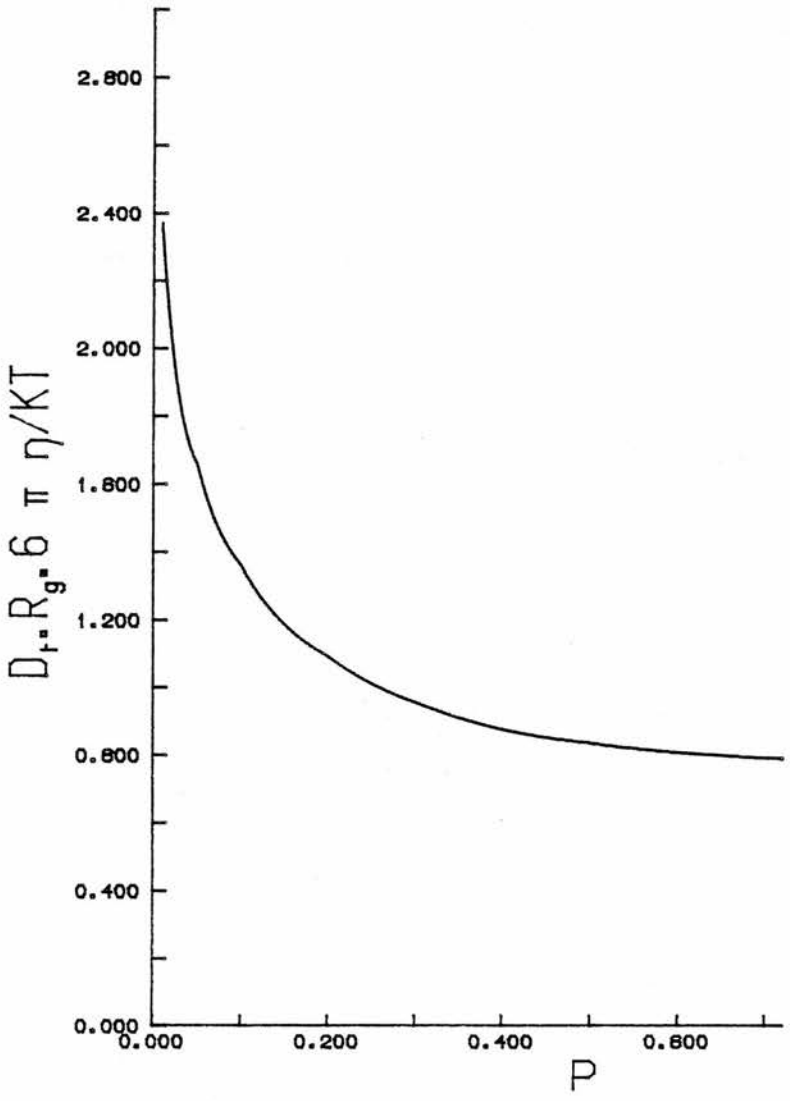

Fig IV 16 :

Representation of : $Dt \cdot Rg\ 6\Pi\ \eta\ (\kappa T)^{-1} = [(1+2p^2)/5]^{-1/2}\ p^{-2/3}\ t(p)$

, for a oblate ellipsoid.

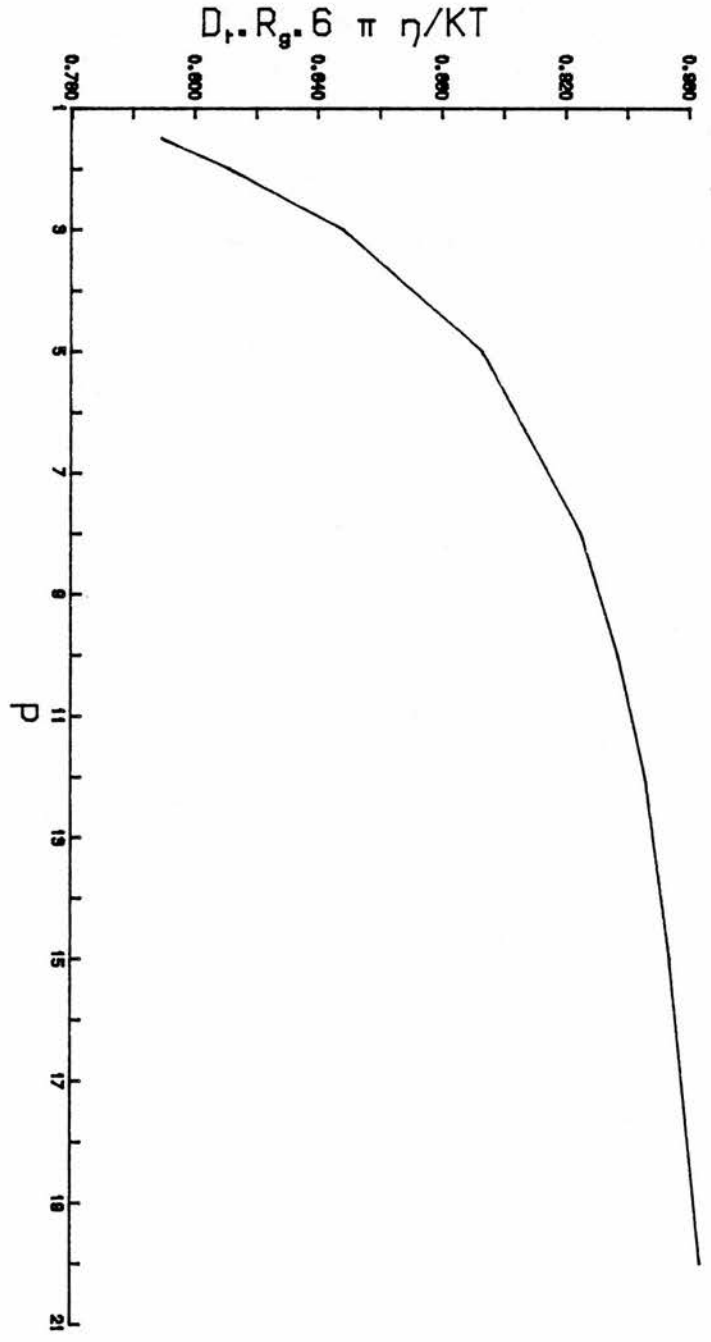

IV 9 7 Final remarks about the ellipsoid model.

Hydrodynamic parameters obtained from different techniques (using the same buffer at the same temperature) have been compared in sections IV 9 3 ,to 5 above . This shows that it is impossible to find an ellipsoid that shows exactly a radius of gyration of 7.3 nm , a translational diffusion coefficient of 2.2 10^{-7} c.g.s. , a rotational diffusion coefficient of 208 10^{3} $s^{-1}$and would still have a proper molecular weight and a reasonable volume and hydratation degree. The work from Sjoberg et al. (1987) is not exempt from those flaws . The degree of hydratation is extremely high (60 %) , the fitting with the measured diffusion coefficient is not very good ,especially considering the fact they use a high value for the viscosity of 10^{-2} c.g.s.

Several experimental factors might cause this problem . They have been described in sections corresponding to each technique . The main concerns are summarized below:

A)For Dt and θ : there is no precise knowledge of the viscosity. Both are obtained after a complex interpretation of the raw signal .

B) For Rg the validity of Guinier approximation depends on the shape of the particle . The choice of the Q range for the Guinier approximation interferes with the result (see table IV 3 over) .

The most likely explanation is that a rigid homogeneous ellipsoid does not represent a good approximation of the shape of the fibronectin molecule . The problem created by the possible flexibility has already been described in section IV 9 3 . But one of the conclusions of the electric birefringene study described in section IV 9 2 , was that no internal flexibility could be detected at physiological ionic strength .

Furthermore the observed diffusion coefficient is too low to match the other parameters . If internal flexibilty was perturbating the photon correlation signal this would show the molecule diffusion coefficient as too fast .We can then assume that the fact that the observed data do not match the ellipsoid model is not due to perturbations created by molecular flexibility.

The most likely hypothesis is that an ellipsoid cannot model the fibronectin shape satisfactorily . However with an entirely different analysis and also the help of different techniques a conclusion similar to that of Sjoberg et al can be drawn , that is that the fibronectin molecule can be represented as a flat structure approximately enclosed in an oblate 10 nm diameter and approximately 1/10 extension .

IV 10 Possible models of plasma fibronectin .

IV 10 1 The problem of electron micrograph studies.

An alternative technique to the investigations in solution is to try to "see" the shape of the molecule by electron microscopy. We shall see now why this does not work with fibronectin .

First , the electron micrographs obtained by various teams , reviewed in I 7 1 , show little agreement between themselves . Some teams show patch type images while others show images that look like a more or less bent hair pin . Those are the only electron micrograph pictures showing fibronectin as an ordered structure (Engel et al. 1981,Odermatt et al. 1982 ,Erickson et al. 1981). They are absolutely incompatible with any hydrodynamic data in physiological conditions. The very extended structure they show does not fit at all with measured diffusion coefficient or radius of gyration. Other studies show only very low resolution images (Kotelianski et al 1981,Tooney et al. 1983) which are often irregular and cannot be of any help in modelling the structure.

Classic electron microscopy techniques do not seem appropriate to the study of the three-dimensional properties of fragile soluble macromolecules such as fibronectin. The treatment of the sample might create artefacts in steps such as adsorption on a grid , staining and dehydratation where the molecule is submitted to conditions which can cause denaturation . Thus the pictures obtained might be far from representing the structure in solution. Considering the large differences between hydodynamic data and electron micrographs we can assume that the preparation of fibronectin for electron microscopy results in a deformation of the three-dimensional structure of fibronectin.

The only way to overcome those denaturation problems would be the use of the frozen hydrated technique. The frozen hydrated electron microscopy technique study specimens extremely quickly frozen in amorphous ice, therefore the samples remain in a native ,wet state(for a review of this technique see Stewart et al. 1986). The samples are not undergoing any treatment likely to denature them, like staining and adsobpsion on a grid, but are simply frozen in vitreous ice. Providing the contrast between ice and the sample is large enougth to allow the visualisation of the sample, this clearly is the electron microscopy technique which can most reliably be applied to fragile biological structures. It must be pointed out that the contrast between protein molecules and water is poor and that it is not clear whether or not it is possible to use this technique with relatively small structures like fibronectin. A possible application that will be tested with the new electron microscope facilities in Edinburgh University biochemistry dpt. , will be the determination of the distances between the binding sites on the fibronectin

molecule. By labelling ligands with heavy metals their position in a frozen hydrated sample can be easily determined , the distance between two labels could then be assumed as the distance between the binding sites.

As a conclusion to this electron microscopy problem , in the absence of any data obtained with the frozen hydrated technique and considering the remarks above , the results from electron microscopy will not be considered too seriously for the construction of models of plasma fibronectin in solution.

IV 10 2 Possible basic models for fibronectin .

Attempts to define the overall dimensions of the molecule have been presented in paragraph IV 9 . The conclusions were similar as those from Sjoberg et al 1987 . The fibronectin molecule can be represented as a flat structure approximatly equivalent to an oblate ellipsoid of revolution with a main radius of 10 nm and approximately 10 times axial ratio. This is a very interesting property because this nearly limits the structure to a plane . Once the general shape is defined the next point is to try to find out how the chains are constituted and how they interact together .

The evidence showing that fibronectin is made of protease resistant domains connected by non organised structures has been presented in IV 8 2 above .We can define the molecule as being composed of two chains made of structured domains connected by more unstructured sections. At this stage it is not possible to define the chains more precisely . This will be done in section IV 10 3 below.

The next point to consider is how the two chains are connected together. The existence of fibronectin as a double disulphide bonded dimer has been known for some time (Engvall 1978) , but several more recent works investigated those connections

A) In 1986 it has been shown by Skorskengaard et al. et al that the C terminal ends of the two chains should be linked by double antiparallel disulphide bonds 20 and 16 residues before the C end.

B) The region of the double disulphide bridge must be compact and not easily accesible to the solvent because reduction of those particular bonds is very slow (Williams et al. 1983).

C) Results from Robinson et al (1984) show that strong non covalent interactions exist between the two chains. This also suggests that an increase in the molecule overall diameter at low ionic strength can take place without requiring a separation of the two chains.

D) A fluorescence transfer study from Wolff et al. (1988)demonstrated that the N terminal ends of both chains were close to each-other.

Two basic models with parallel and anti-parallel chains can be proposed as in Fig IV 17 & 18 below .

Fig IV 17 ;
Model A : Parallel chain configuration.

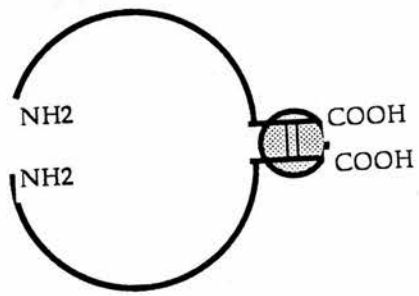

Fig IV 18 :
Model B : Anti-parallel chain configuration.

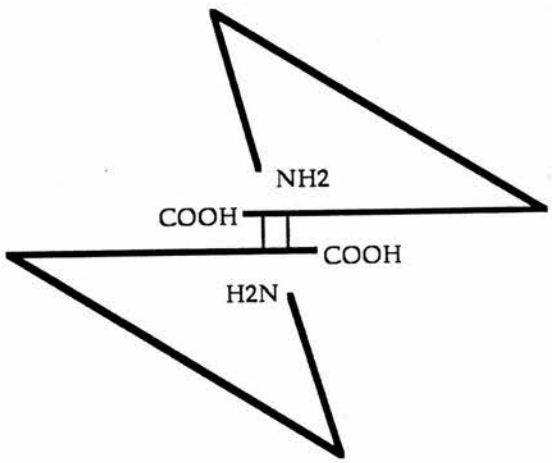

IV 10 3 A higher resolution model.

Electric birefringence data described in this thesis shows that the molecule has a very low electric dipole for its size. The conclusion was that the absence of a noticeable birefringence at low concentrations should be the consequence of a symmetry within the molecule , as suggested by the anti-parallel disulphide bonding as described in above. This would mean that the antiparallel model model B is more likely than model A .

We can also try to integrate in this model the hydrodynamic parameters obtained with the purified domains. The conclusion of section IV 7 was that the gelatin binding domain was spherical . The determination of the diffusion coefficient of the 150 kD central domain was presented in section IV 6 above and shows a Dt of 3.1 10^{-7} c.g.s. As discussed this means that this domain is fairly extended. A possible structure is presented in Fig IV 19 below.

Fig IV 19 :

Proposed model for the tertiary structure of plasma fibronectin in solution.

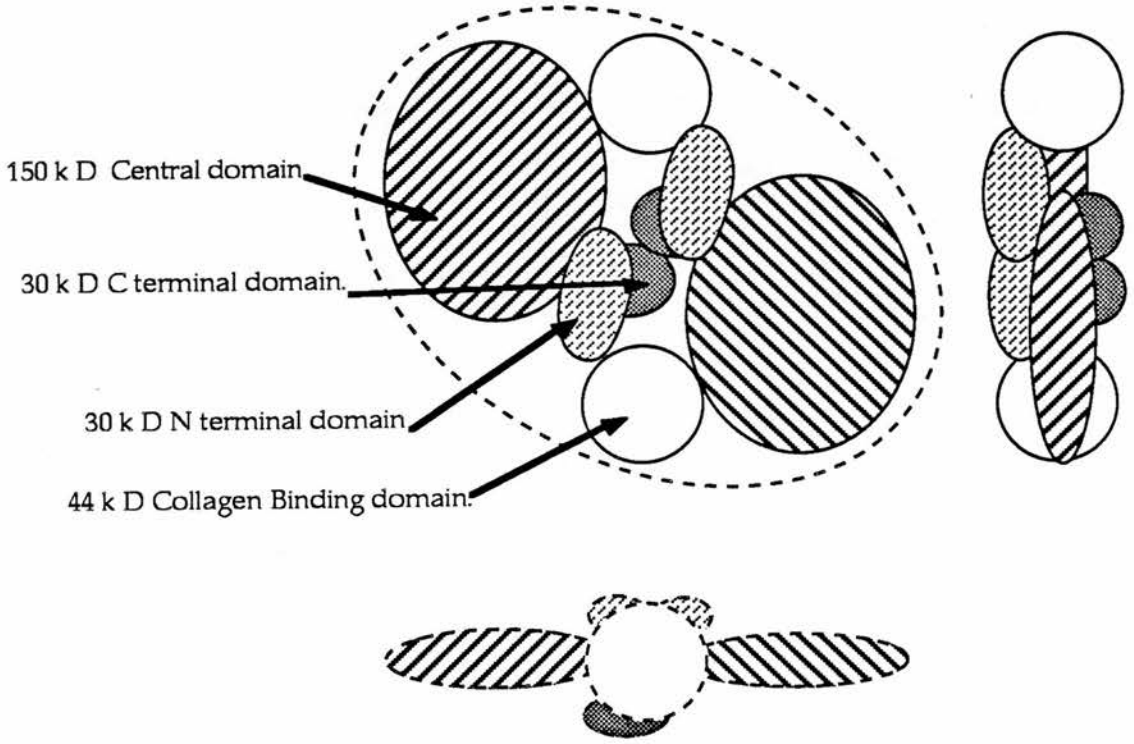

It is then possible to check that the following important features are properties of this model:

A) The flat structure as shown by the hydrodynamic is maintained :

α) The presence of a large proportion of the mass of the molecule in a central position

could explain why the radius of gyration is small when compared to the hydrodynamic data.

β) The shape is not a revolution ellipsoid in accordance with the results from the analysis presented in section IV 9 above .

γ) This flat structure allows free access from both sides for the various ligands,

δ) Accessibilty of N terminal end to allow cross-linking by factor VIIIa ,(Williams 1982), is also possible .

B) The work from Wolff et al. (1988) showed that the N-terminal ends of the two chains had to be close to each other ,but the structure of the molecule is also relatively compact .

C) Strong interchain interactions may exist as the surface of contact is extensive (Robinson et al.1984).

D) The results from Homandberg et al (1986) which defined how the domains interact are in a very good agreement with this model: The 29 Kd N terminal domain interacts with the C terminal 40 K d strong heparin binding domain, the collagen binding domain does not bind to any other except weakly to itself (this self aggregation was checked by the scattering experiments from this work presented in section V 6).

E) The symmetry of the model could also explain the electric birefringence data .

F) Despite a compact structure including the interchain bonds ,the region close to the C end must be accessible as easy proteolysis occurs with plasmin (Petersen et al. 1982) .This can easily be explained despite the relativly large molecular weight of plasmin by enzyme attack at the flat sides.

CHAPTER V

A STUDY OF THE PLASMA FIBRONECTIN FROM CANCER PATIENTS

V 1 BACKGROUND:

Fibronectin involvment in cancer and metastaticprocesses has been studied along three lines , all related to early events of metastasis . Three points emerge.

A) Synthesis of specific fibronectins by changes of the primary structure (Wagner et al. 1981, Seikiguchi et al. 1985, Matsuura et al. 1985 , Castellani et al. 1986, Borsi et al. 1987) and sugar side chains composition (Wagner et al. 1981, Nichols et al. 1986, Castellani et al. 1986).

B) Modification at the cellular receptor level by changes of receptor distribution (Chen et al. 1986, Virtanen et al. 1987),and fibronectin deposition rates in the matrix (Sherbet et al. 1982, Virtanen et al. 1987).

C) Degradation of fibronectin by tumour cells (Wen -Tien et al . 1984 ,Barlatti et al. 1986, Chen et al. 1987,Tryggvason et al. 1987 , Zucker et al. 1987). Specific enzymes might have been described (Stevens et al. 1985).

Surprisingly the position of fibronectins in the next stage ,anchoring of the cell migrating in the blood stream has been much less studied . De Petro et al. 1983 showed that transformation enhancement activity in plasma of tumour patients was linked with fibronectin . In this chapter it will be shown that the hydrodynamic properties of plasma fibronectin from patients with metastatic breast cancer are different from those of plasma fibronectin from healthy people.

V 2 FIBRONECTIN PREPARATION.

The preparation steps are very important in helping to define what causes the changes in hydrodynamic properties described below in V 3 , therefore those steps will be descibed below .

20 ml blood samples were collected , in the ward, from patients with clinically confirmed metastatic breast cancer . The samples were treated immediately with 20 % sodium citrate ,25 mM EDTA , 1 volume per 4 volumes blood and transferred on ice to the Biochemistry Department to be centrifuged at 3500 rpm for 5 minutes with a bench centrifuge . The cell pellet was discarded, plasma samples were either frozen at - 20 C or immediately processed by centrifugation 10,000 g for 1 h followed by chromatography on

$2cm^2$ x 1 cm gelatin sepharose column as described in III 1. Elution of the sample was carried out with 4M urea 50 mM tris pH 7.4 .

In order to test the possible influence of the elution buffer on aggregation properties one sample was eluted by: 1 M Arginine 50 mM tris pH 7.4 . Extensive dialysis in 50 mM tris , 100 mM NaCl , pH 7.4 (dialysis buffer)was performed to remove any traces of urea .

To rule out any possible artefactual contamination , two samples were rechromatographed on heparin sepharose column rinsed by dialysis buffer eluted by 1 M NaCl 50 mM Tris 1mM EDTA pH 7.4 and redialysed in dialysis buffer .

PMSF 0.05 mM and EDTA 5 mM were added to all buffers used for purification . All specimens were tested by 5 or 6 % discontinuous PAGE gels .

To test the influence of filtration , (required for light scattering), on the aggregation property , one sample was centrifuged in order to pellet any material with a sedimentation constant over 23 S . When filtering the samples care was taken to avoid any disturbance leading to aggregation .

Those preparations steps are summarised in Fig V 1 below .

V 3 RESULTS FROM LIGHT SCATTERING

Normal plasma fibronectin was studied in section IV 2 above . The results from cancer patients samples are presented below :

V 3 1 Samples purified by gelatin affinity only (4 Samples) :

D population 1(c.g.s.)	D population 2 (c.g.s.)	Polydispersity %
$0.29 \pm 0.07\ 10^{-7}$	$0.97 \pm 0.4\ 10^{-7}$	55

Molecular Weight aprox 4000 KD.Fig V 1 shows the scattering intensity as a function of diffusion coefficient for one sample.Fig V 2 shows a Zimm plot for one of those samples.

V 3 2 Samples repurified on heparin sepharose (2 Samples):

D population 1(c.g.s.)	D population 2 (c.g.s.)	Polydispersity %
$1.12 \pm 0.2\ 10^{-7}$	$2.8 \pm 0.3\ 10^{-7}$	38

Fig V 1.

Preparation of fibronectin samples .

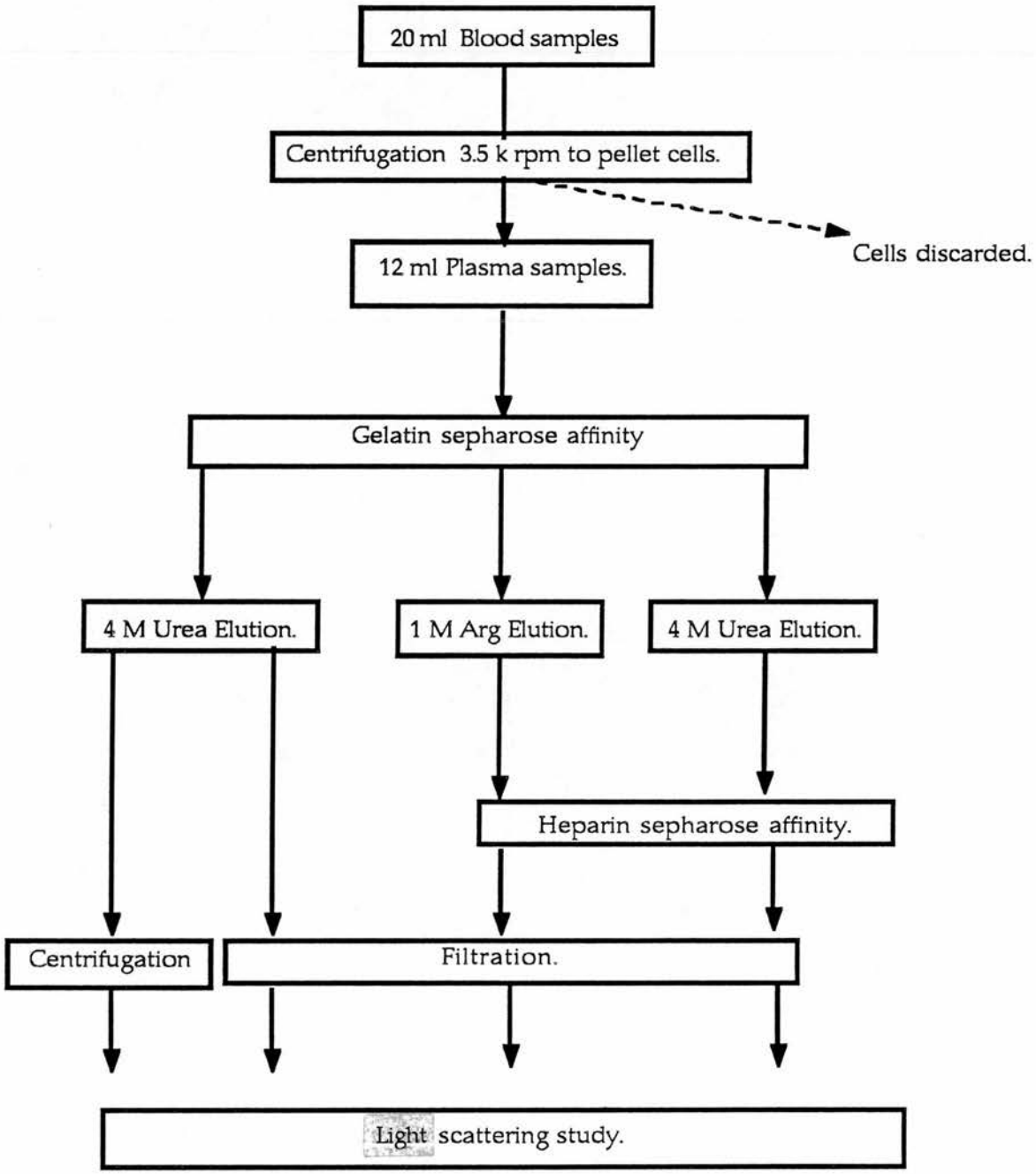

Fig V 2:

Scattering intensity as a function of diffusion coefficient , sample purified by gelatin affinity only .

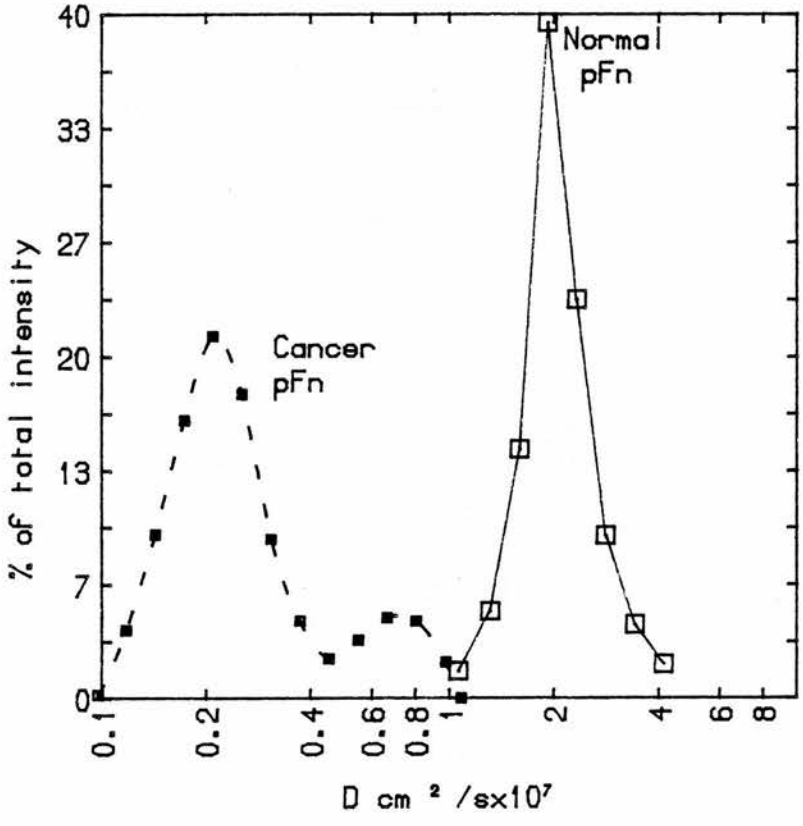

Fig V 3 :

Zimm plot of a sample purified by gelatin affinity only.

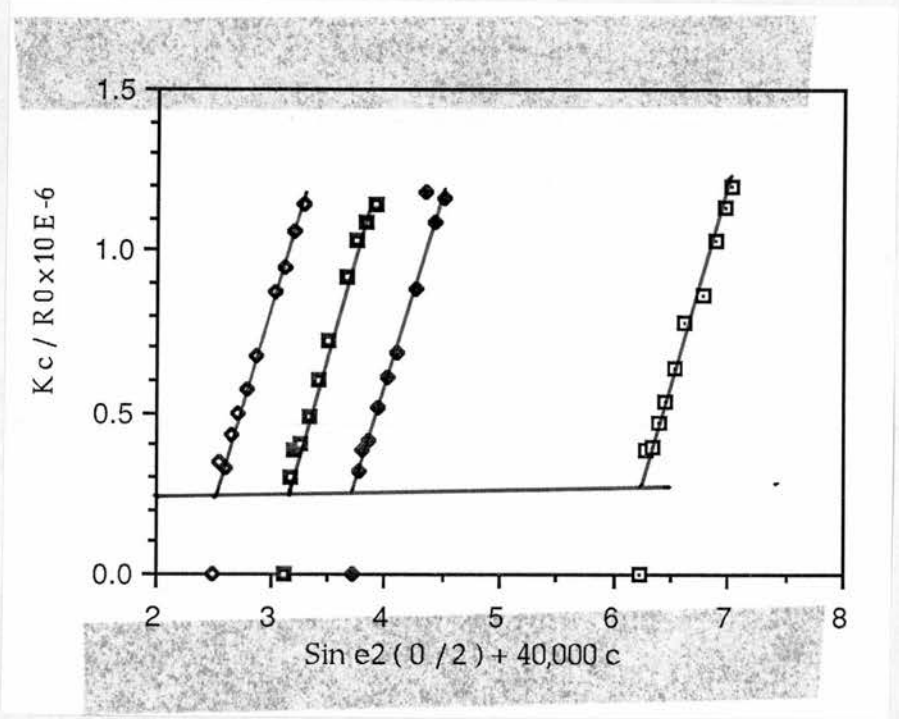

V 4 THERMOLYSIN LIMITED DIGESTION.

In an attempt to explain the differences in aggregation properties between normal plasma fibronectin and cancer patient plasma fibronectin limited thermolysin digestion was performed as described in III 2.

It has been shown (see I 3 1,2,3 & I 4 2,3) that fibronectin produced by normal or transformed cells in culture showed many differences from fibronectin from plasma . It is also well known that cellular fibronectin is much less soluble than plasma fibronectin . To test the possibility of the presence in plasma of cancer patients of significant amounts of cellular fibronectin ,limited thermolysin digestion of cancer patients plasma fibronectin was carried out under the conditions described in III .

PAGE gels and their scans are presented in Fig V 4 ,5 & 6 . They show no differences between the control and the cancer patients plasma fibronectin samples . The material just over 30 K, present in all cell type fibronectins as described by Seikiguchi et al. (1985), is absent.

This shows that fibronectin present in the plasma of metastatic cancer is similar to normal plasma fibronectin . The observed differences in aggregation properties cannot be explained by the presence in the plasma of metastatic patients of a large amount of cellular or tumour type fibronectin .

Fig V 4 :
P.A.G.E

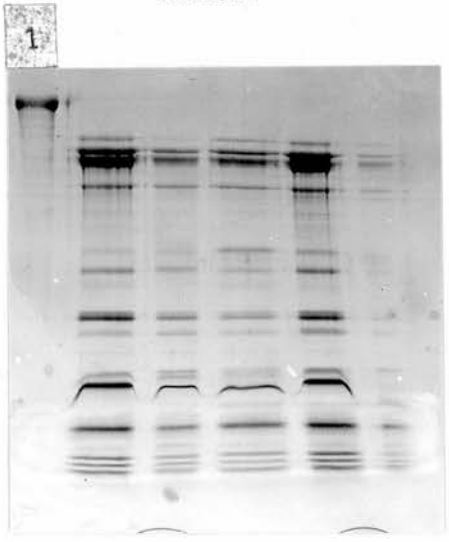

Lane 1: Undigested normal plasma fibronectin .

Lane 2:Thermolysin digest of normal plasma fibronectin.

Lanes 3 to 6 : Thermolysin disgest of cancer patient plasma fibronectin .

Fig V 5
Scan of P.A.G.E (5 15 %)
Thermolysin fragments of normal plasma Fn.

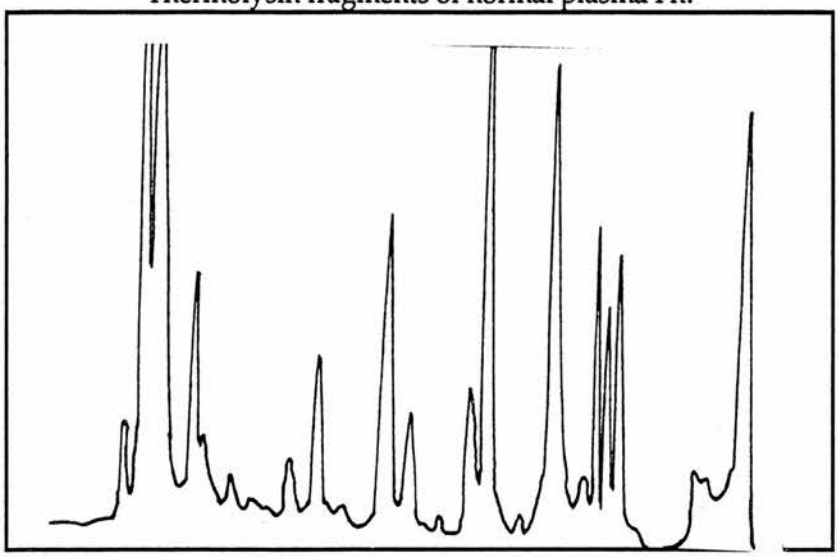

Fig V 6
Scan of P.A.G.E. (5 15 %)
Thermolysin fragments of cancer patient plasma Fn.

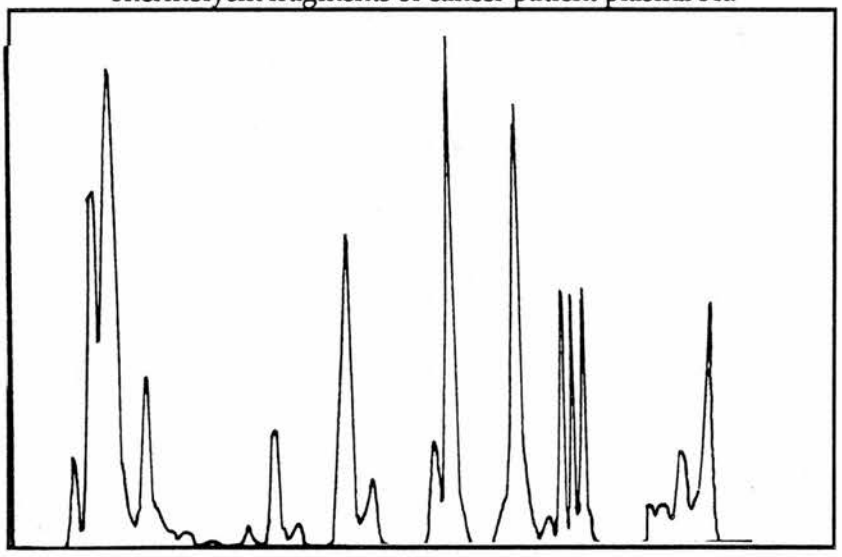

96 kD 69 kD 44kD 30 kD 20 kD 14 kD

V 5 CONCANAVALIN-A AFFINITY CHROMATOGRAPHY.

To test the possibility of a change in distribution of the carbohydrate side-chains in fibronectin from cancer patients plasma, affinity chromatography with immobilised concanavalin-a(con-A) was performed as follow:

1.5 ml con-A sepharose beads , equilibrated in : Tris 50 mM, NaCl 25 mM , 2 mM Co^{2+}, 2 mM Mn^{2+} were added to the thermolysin digested samples in the same buffer .

After incubation with gentle stirring for 2 h ,samples were decanted ,the supernatant was collected , the beads were resuspended in 1 .5 ml equilibration buffer incubated with stirring for 30 minutes . This step was repeated three times .

Elution was realised by adding 100 microl of 1 M methyl-mannoside 40 mM EDTA and spinning the beads at high centrifugal field to compress them as much as possible . The supernatant was analysed by gradient page presented , with scans in Fig V 7 & 8 .

Fig V 7
Scan of P.A.G.E. (5 15 %) Concanavalin-A binding thermolysin fragments of normal plasma Fn.

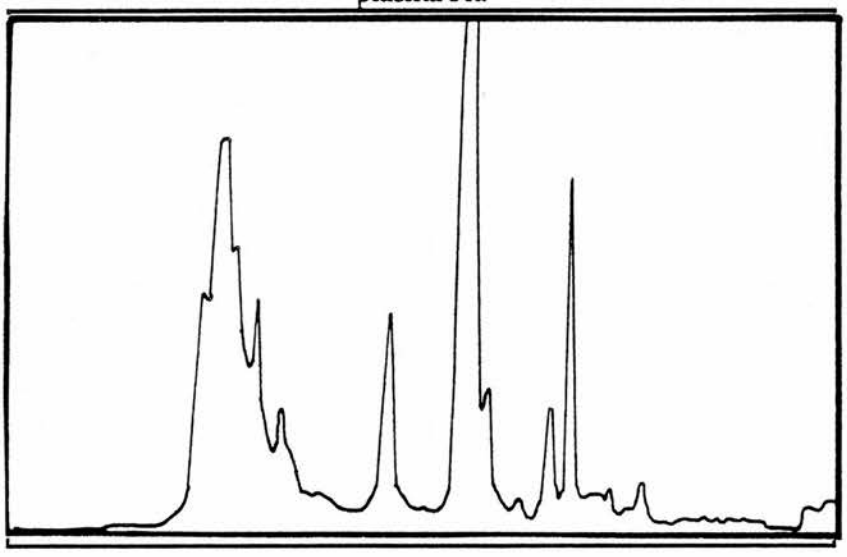

96 kD 69 kD 44kD 30 kD 20 kD 14 kD

Fig V 8 :
Scan of P.A.G.E.(5 15 %) :Concanavalin-A binding thermolysin fragments of a cancer-patient plasma fibronectin specimen .

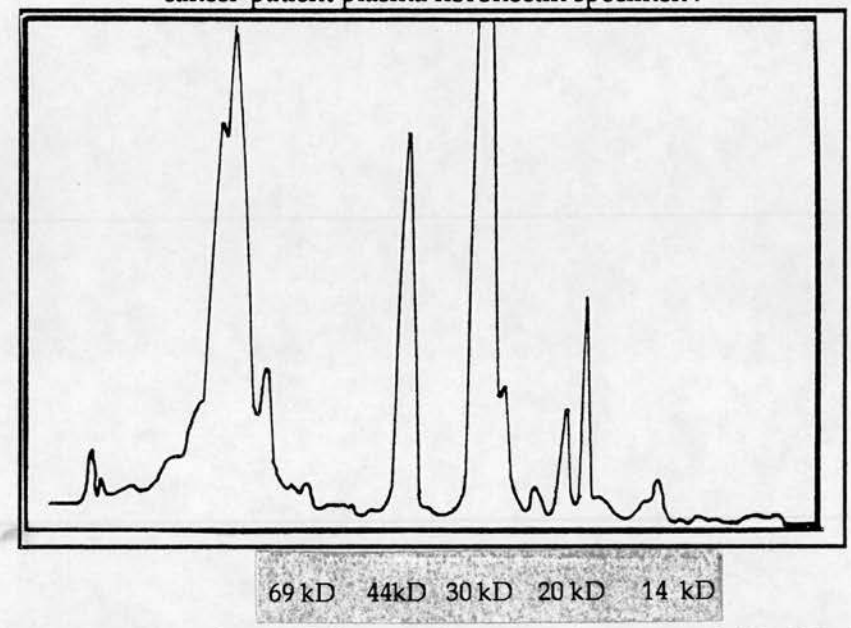

There is no significant difference between the scans of S.D.S.P.A.G.E. of concanavalin-A binding thermolysin generated fragments of plasma fibrononectin from healthy individuals amd metastatic patients . This is a proof that no large change in the distribution of the concanavalin-A binding carbohydrate chains can be detected. The observed difference in aggregation properties then cannot be related to a large scale modification in the distribution of those chains .

V 6 DISCUSSION AND INTERPRETATION OF THE RESULTS:

The results from this work reveals the presence of high molecular weight material associated with fibronectin purified from clinically confirmed metastatic patients' plasma .

V 6 1 Are those aggregates genuine fibronectin.

The first problem is to quantify the amount of high molecular weight material in the preparation and identify it with fibronectin .

A) Intensity of light scattering is proportional to the square of the mass of the scattering particles and thus to sixth power of their size , so clearly to allow detection of the higher diffusion coefficient values (i.e. smaller sizes particles .) the large Mw

material must represent a small number fraction of the samples . It must be noted that filtration might have removed some larger material .

B) The presence of a large amount of contaminants different from fibronectin would be detected on the PAGE control gels . Assuming contaminants were present but not detected, the preparation procedure (as shown on fig V 9), was designed to remove them : either they could be eluted by 4 M urea only and therefore would not show up on material eluted from gelatin column by 1 M Lysine , or they would be eluted by

high ionic strength and therefore be eluted before fibronectin during the 1 M NaCl wash of the gelatin column . The aggregates were still present on material rechromatographed on heparin sepharose ; furthermore binding to gelatin and heparin at physiological salt concentrations is a property of fibronectin only . Thus the combination of the various preparation procedures rules out the presence of a significant amount of contaminant in the samples .

C) We must explain why the high diffusion coefficient population (i.e. the low molecular weight population of the cancer patients fibronectin), has a translational diffusion coefficient (D) value different from the one of normal plasma-Fibronectin. This is not surprising since the diffusion coefficient of the high diffusion coefficient population has to be extrapolated from data showing polydispersity and therefore the precision is not high enough to allow a fine distinction to be made .

V 6 2 Nature of the large aggregates.

The origin of the low D population (i.e. high molecular weight large aggregates), has to be discussed . As shown above , identification with fibronectin seems clear but it is more difficult to say to which form of fibronectin they belong to and whether they can exist in vivo .

As shown in V 4 & 5 attempts to relate this aggregation property to a primary structure modification or con-A binding sugars changes in distribution have not been successful . As the aggregates represent a minor component in the samples it is impossible to rule out the possibility that a modification of carbohydrate side-chains of a small amount of fibronectin molecules or the presence of very little oncofoetal fibronectin could be missed by the lack of sensitivity of the tests performed . But the presence in the blood stream of fibronectin synthesised only by tumour tissues seems unlikely because tumour

cells have been shown to degrade fibronectin in tissues (see I 13 3 above), and it would be difficult for fibronectin produced in tissues to diffuse considering its binding properties. Furthermore the amount produced would be very low compared to existing plasma fibronectin . So the most logical conclusion is that those aggregates are genuine plasma Fibronectin modified in an unknown manner within the blood stream .

The findings from this work are in accordance with the changes in biological properties of cancer patients plasma fibronectin shown by other studies (i.e. DePetro et al. 1983) . Perhaps it could represent a form used by the metastatic cells to anchor at the surface of a blood capillary in their target organ .

V 6 4 The problem of copurifying contaminant:

Aggregation can also be due to the presence of a very small amount of co-purifing contaminant binding to fibronectin in a non stoechiometric ratio and therefore promoting aggregation . The chances for this hypothesis to be correct are very slim considering the fibronectin purification technique but cannot be completely ruled out .

V 6 5 Possibility of the presence of the aggregates in vivo .

The presence of those large aggregates in vivo cannot be stated with certainty . They clearly existed at concentrations similar to the in vivo situation so they do not result from aggregation induced by an artificially too high concentration . On the other hand considerable size reduction after Heparin affinity suggests that they cannot easily dissociate after formation , thus considering the exclusion limit of the gelatin affinity column they would be excluded from the gelatin column being directly eluted in the first preparation step .

So the more likely hypothesis is that they form during the preparation where the use of urea or 1 M Lysine buffer leads to unfolding of the protein . An alternative possibility is that binding to gelatin during preparation triggers a conformational change leading to aggregation in the particular case of this cancer patient plasma fibronectin .

CHAPTER VI

EFFECTS OF HEPARIN BINDING ON THE CONFORMATION OF FIBRONECTIN.

VI 1 INTRODUCTION.

In this chapter ,data from light scattering and neutron small angle scattering will show that heparin binding to fibronectin induces no macromolecular conformational change in the molecule but triggers some aggregation . The possibility that polymerisation could occur under those conditions will be examined .

The codistribution of fibronectin and heparan sulphate type proteoglycans in extracellular matrix (Hedman et al. 1982, Hayman et al. 1982), and basal lamina (Laurie et al 1982) , is well known . Heparan sulphates have also been shown to align with stress fibres of the cytoskeleton and may represent a part of the linkage system between extracellular matrix and cytoskeleton (Woods et al. 1984 & Singer et al 1987). The classical technique to investigate the presence and distribution of molecules in the matrix is immunofluorescence microscopy which obviously detects only fibrillar insoluble fibronectin. Heparan sulphate proteoglycans are found on the cell surface and may possibly link cytoskeleton and matrix components (Woods et al 1984) . They can also possibly act as collagen receptors (Koda et al 1985).

Many studies with fibronectin have been carried out with Heparin as a subsitute for heparan-sulphates which are much less easily available (and more expensive). Furthermore the difference between those two types of carbohydrates is only due to the degree of sulphation and is not always perfectly defined .This was also what was chosen in this study because there was no carbohydrate biochemist available and it was impossible to run in a time consuming heparan-sulphate purification without help and advice. Heparin interactions with fibronectin have been described in I 3 1 above .

The influence of the binding of heparin-like carbohydrates on the three-dimensional structure of fibronectin has to date only been studied by circular dichroism and electron spin resonance . Osterlund et al. (1985) studied the circular dichroism spectra of fibronectin in the presence of cellular heparan sulphate and found a change in the spectra upon heparan addition . This confirmed the results obtained by Welsh et al(1983) ,using the same technique with heparin . An electron spin resonance study by Ankel et al. (1986), also reported a conformational change due to heparin binding .

VI 2 SAMPLES AND TECHNIQUES.

Heparin was purchased from Sigma. Plasma fibronectin was purified as described in chapter III. Photon correlation was described in II 1, molecular weight measurements by light scattering in II 2 and neutron scattering in II 3 above.

VI 3 RESULTS FROM PHOTON CORRELATION SPECTROSCOPY.

VI 3 1 Experimental conditions.

The conditions were as follow:

A) The fundamental sample time was calculated directly by the system in order to place particles with a Stokes diameter of 20 nm in the centre of a hundred fold size scale as described in II 1 9 above.

B) No correction was made for buffer viscosity which was assumed to be the same as that of pure water.

C) Each recorded measurement was the accumulation of several runs. The software calculated the mean value of photomultiplier counts integration for each run and rejected any run with a significant difference in integration.

D) The "Far point " estimation of the mean scattering intensity from the correlation function was compared to the integration of the photomultiplier counts (see II 1 6 above). This permitted the determination of the influence of very large aggregates or dust out of the measuring range on the diffusion coefficient measurement.

E) The "In range " index was then defined by the ratio of the far point to the total integration of photomultiplier counts. This was performed for each run and was typically over 99 % for crude fibronectin specimens. This showed that there was no significant contribution due to out of range scattering material in the samples. These good conditions for the measurement were also confirmed by the fact that the value of the diffusion coefficient of crude fibronectin was not dependent upon the angle of measurement as expected for a molecule that is small compared to the wavelength of the incident light.

F) The scattering from heparin was found to be negligible at the concentrations used in those experiments.

G) It is important to notice that as heparin preparations tends to be heterogenous in molecular weight it is preferable to give heparin concentrations in mass per volume rather than in molar concentrations.

H) The relatively low angle of 40 degrees was chosen to measure the diffusion

coefficient in order to ensure that the contribution of large molecular weight material (i.e. with a size non negligible compared to the incident wavelength),would be detected even if this high molecular weight material was present at low concentrations . As the scattering intensity of those large particles is strongly dependent on the scattering angle, their contribution to the scattering fluctuations used to determine D is more obvious at low angles, even if they represent only a minor part of the sample .

VI 3 2 Results and interpretation .

Table VI 1 :

Results from photon correlation spectrocopy measurements.

Buffer : Tris 50 mM , NaCl 100 mM , pH 7.35, angle 40 ,temperature 25 0C .

Sample	Heparin conc mg/ml	$CaCl_2$ mM	D cm^2/sec x 10-7
Bovine plasma fibronectin (400mg/ml)	0	0	2.33 +– 0.014
Same	60	0	1.69 +- 0.3
Same	60	20	1.93 +- 0.14

The diffusion coefficient decreased significantly upon the addition of heparin . This corresponding to a 38% increase of Stokes radius for heparin concentration of 60 mg/ml . These results could be explained either by a conformational change (i.e. a large expansion of the molecule), or by the association of fibronectin-heparin complexes to form large aggregates .

The large increase, upon the addition of heparin , of the standard deviation (from less than 1 % to 17 %), should be noted . This indicates that a simple change in conformation does not fully explain this data , but rather indicates that an aggregation phenomenon, less easily reproducible, might have occurred.

The addition of calcium did not fully abolish the effects of heparin and the specimens still demonstrated a Stokes radius increase of 19 % . This could be explained only by the formation of aggregates insensitive to calcium or by an irreversible change in the conformation of fibronectin after heparin binding . It was not possible to increase the calcium concentration in order to try to dissociate those aggregates . Since the structure of fibronectin is dependent on the ionic strength, the addition of a high amount of calcium would result in an unfolding of the fibronectin molecule and therefore would interfere with the heparin induced modification of the diffusion coefficient .

After filtration of a calcium treated sample through a 100 nm filter there was only a minor decrease of the diffusion coefficient compared to samples before heparin treatment

:2.26 10^{-7} cgs compared to 2.33 10^{-7} cgs . The filter pore size of 100nm is bigger than 5 times the fibronectin molecule stokes radius approximately , corresponding to a diffusion coefficient under around 0.4 10^{-7} cgs . Furthermore addition of calcium up to 20 mM in the absence of heparin results in a nearly similar change with a diffusion coefficient of 2.28 10^{-7} c.g.s . Those last two facts strongly back the hypothesis that the observed change in D is a consequence of aggregation and not of a change in the conformation of the fibronectin molecule .

Fig VI 1 : Relation between heparin addition and D .

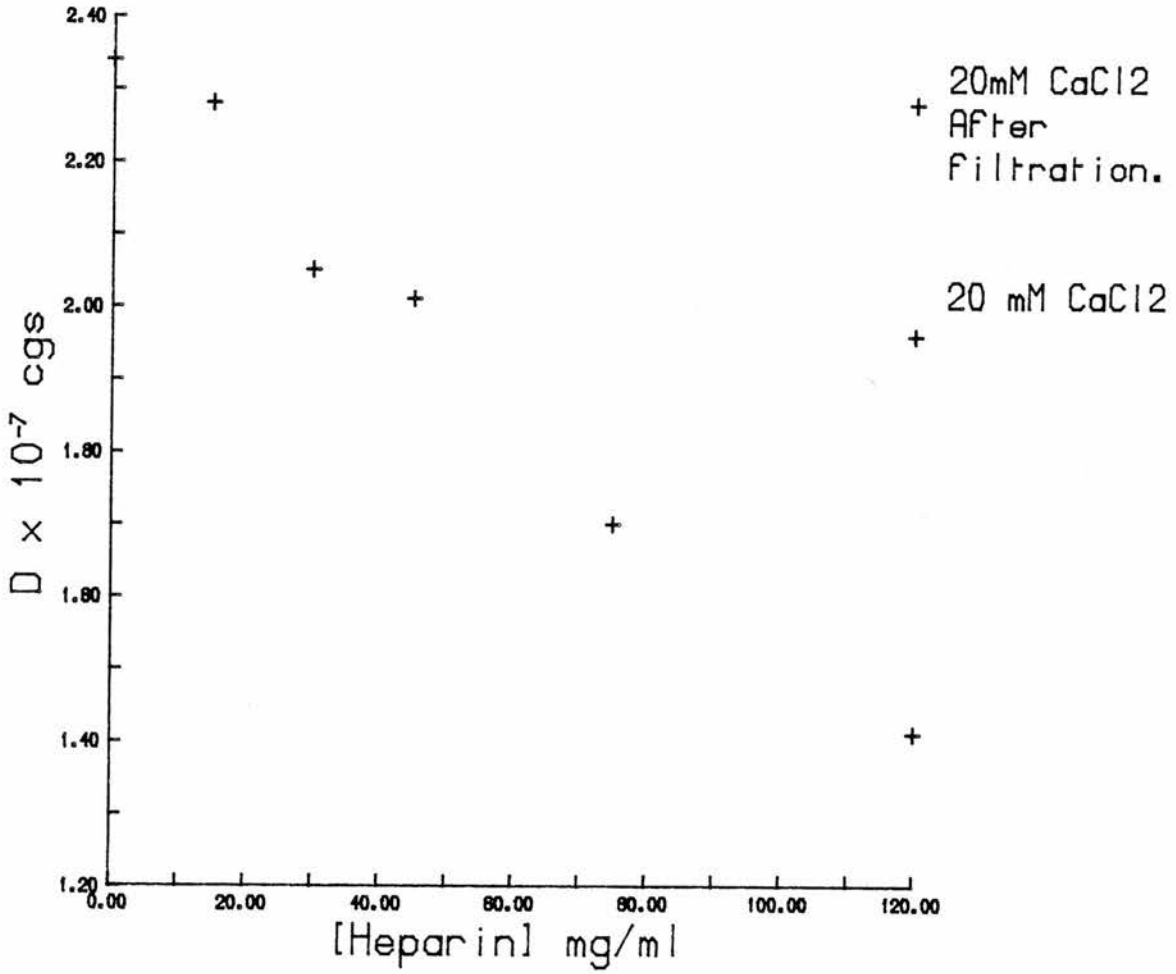

A steady decrease is observed in the diffusion coefficient measured at 40 angular degrees upon heparin addition (see Fig. VI 1). Once again if a conformational change was responsible one would expect a saturation which is not detected.

VI 4 RESULTS FROM MEASUREMENTS OF THE ANGULAR DEPENDENCE OF LIGHT SCATTERING.

VI 4 1 Introduction and experimental parameters.

The angular dependence of the scattering from the fibronectin solutions were plotted by classical representation of Kc/R_θ as a function of $Sin^2 (\theta / 2)$. θ is the scattering angle and K is an optical constant equal to: $2 \Pi^2 n^2 (dn/dc)^2 / N \lambda^4$,where dn /dc represents the refractive index increment with concentration , n the refractive index of the solvent , λ is the wavelength of the incident light , c is the concentration of the molecule studied , R_θ is the excess scattering intensity of the solution relative to toluene. The molecular weight has been shown to be the reciprocal of the normalized intercept of the extrapolations at concentration and angle equals to zero (see II 2 above).

Practical considerations , namely the very low fibronectin concentration and the fact that only comparative profiles upon heparin addition were required , dictated that only one fibronectin concentration was measured.

This method of representing the data demonstrated any polydispersity due to the presence of particles with very different Rg and molecular weight (Zimm 1948). The presence of a majority of small Rg particles ,presenting a scattering profile with little angular dependence , with a minority of large Rg particles ,which gives a scattering profile showing a large increase of intensity at low angles, will show up on this representation as a curvature of the lines of the angle dependent data. To minimise experimental errors due to the source or to detection the various precautions described in II 2 3&4 were followed.

The following parameters were used :

A) Rayleigh ratio for toluene $18.3\ 10^{-6}$ c.g.s.

B) Laser wavelength was 514.5nm .

C) Fibronectin extinction coefficient: 12.8 for a 1 % solution.

D) It was not possible to measure the value of the index increment dn/dc at our working wavelength. We used an approximate value of 0.19. Since our purpose was only to compare the molecular weight of fibronectin in the presence and the absence of heparin this did not represent a problem.

VI 4 2 Datafrom angular dependance of light scattering .

Fig 2 Shows a representation of Kc/R_θ as a function of $Sin^2 \theta$ before and after heparin addition.

Fig VI 2:

Intensity of ligtht scattering by a fibronectin solution with various heparin additions.

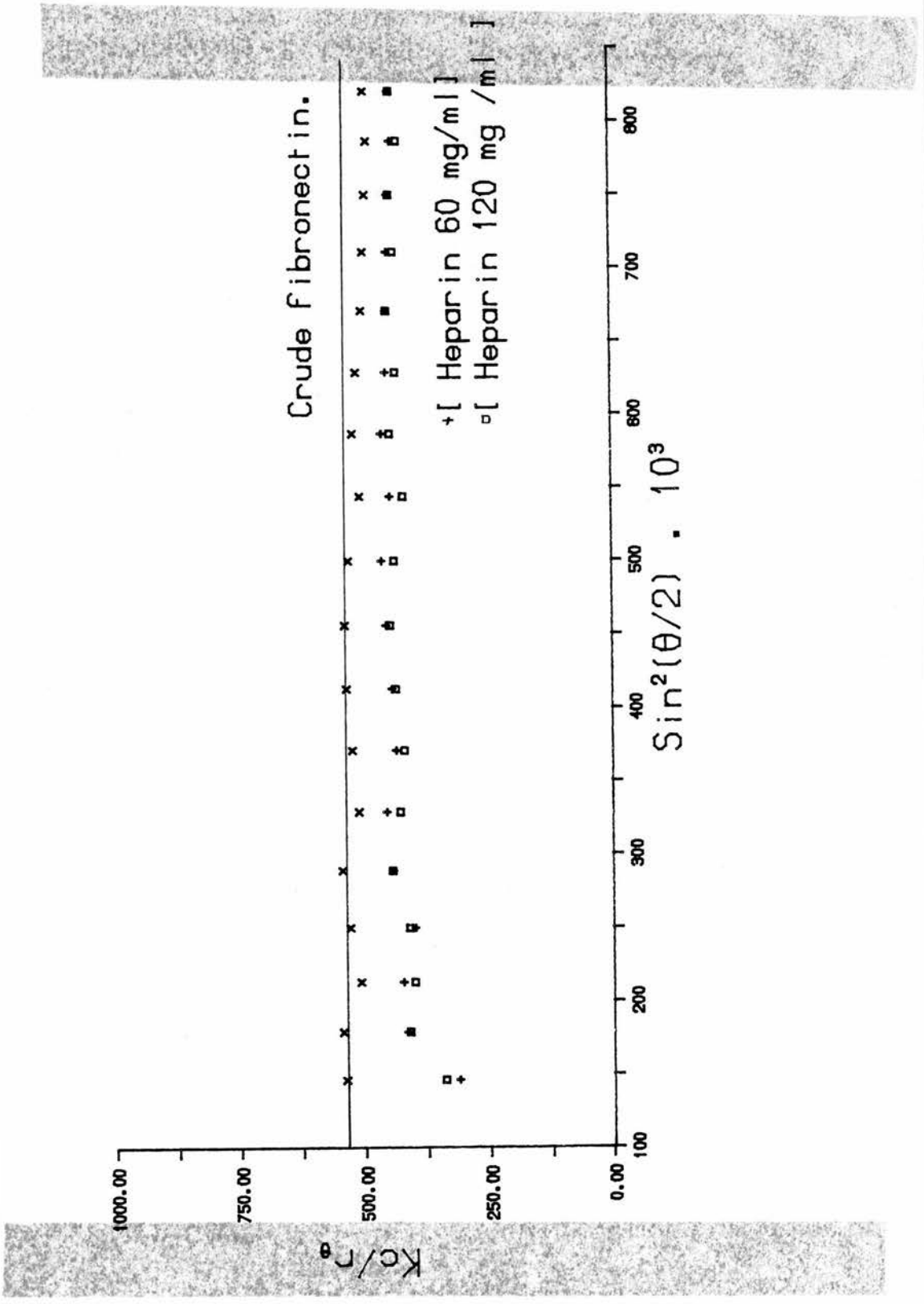

VI 4 3 Interpretation.

The representation of normalized intensity Kc/R_θ as a function of angle demonstrates a clear decrease in Kc/Rθ upon heparin addition. This demonstrates that the molecular weight is increasing. A slight curvature at low angles upon heparin addition is also observed . This has been shown by Zimm (1948), to be a consequence of polydispersity and reflects the presence of:

A) Heparin-fibronectin complexes made of only one fibronectin molecule with a small Rg and relatively low molecular weight .

B) Complexes made by the association of many fibronectin and heparin molecules with a large Rg and very high molecular weight.

The decrease of Kc/R_θ after heparin addition is proof that an increase in average molecular weight occurs. Thus the decrease of the diffusion coefficient is due to aggregation and not only to a change of conformation of the fibronectin molecule.

VI 5 RESULTS FROM NEUTRON SMALL ANGLE SCATTERING.

VI 5 1 Data.

The camera for neutron scattering experiments, "D 11 " , data collection and analysis have been described in II 3 above . The distance from sample to detector was 10 m ,10Å wavelength neutrons being used , Q .Rg ranges for Guinier approximations were from 0.69 to 1.47. The Guinier representations are shown in Fig. VI 3 & 4 below.

Fig VI 3

Guinier plot of small angle neutron scattering.

Sample: Crude Fibronectin.

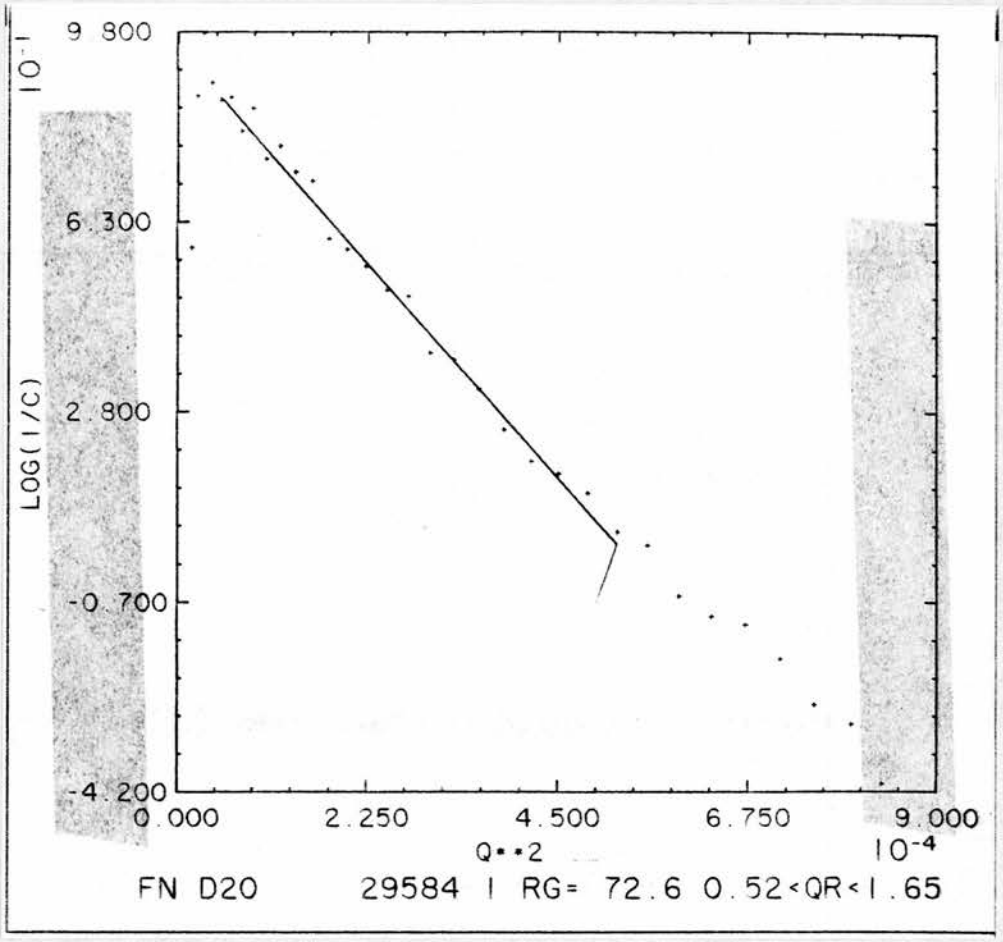

Fig VI 4

Guinier plot of small angle neutron scattering.

Sample: Fibronectin with heparin 60 μ g /ml .Filtered through 100 nm pore diameter filter.

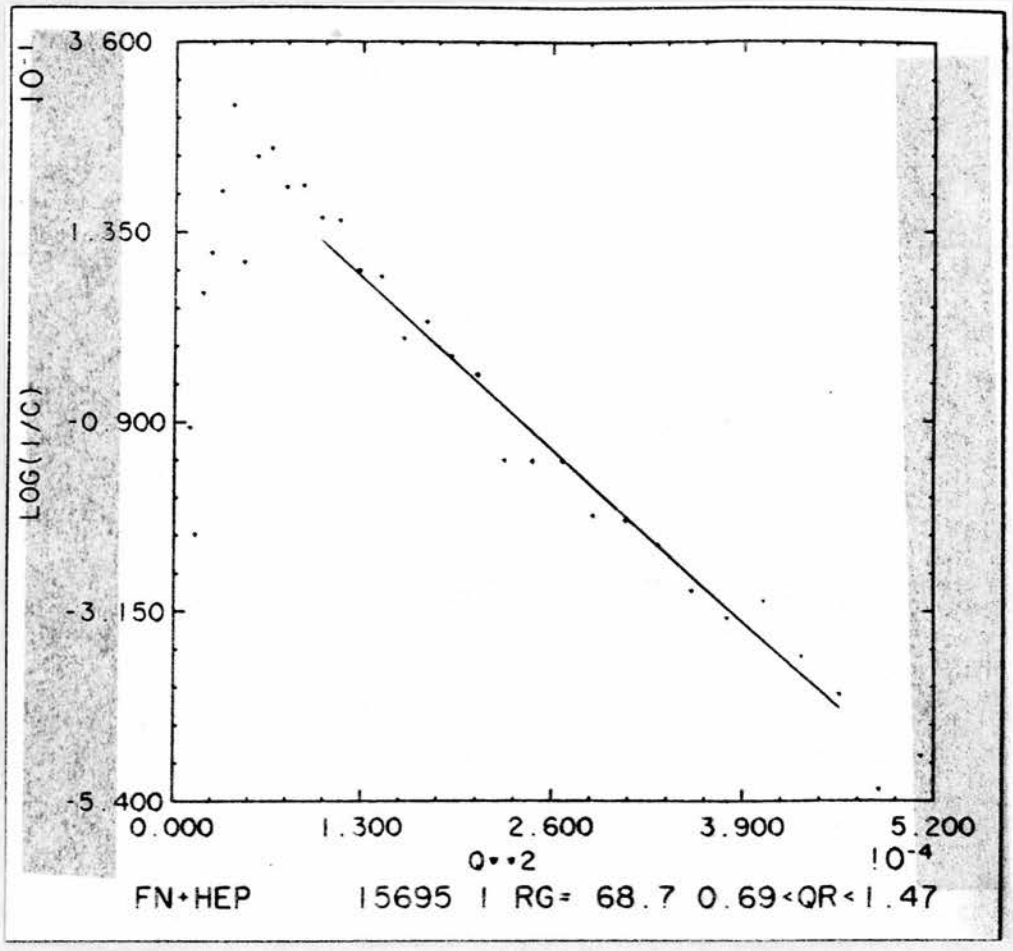

VI 5 2 Interpretation of the small angle neutron scattering data.

Tab. VI 2 :Radius of gyration determined by small angle neutron scattering.

Buffer: D_2O Tris 50 mM NaCl 100 mM pH 7.4

Sample	Rg
Plasma fibronectin	7.3 nm
Same + heparin filtered through 100nm pore diameter filter, [heparin] = 100mg/ml	6.9 nm

The determination of the radius of gyration of filtered fibronectin-Heparin complexes by neutron small angle scattering data rules out the possibility of any large change in conformation as shown by the lack of a significant change in the radius of gyration.

VI 6 EVIDENCE REPORTED IN THE LITERATURE OF CONFORMATIONAL CHANGES IN FIBRONECTIN AFTER ADDITION OF HEPARIN TYPE CARBOHYDRATES .

In contradiction with the results presented above three papers present evidence for a change in conformation of fibronectin upon heparin addition. Two of them (Welsh et al. 1983, Osterlund et al.1985), are circular dichroism studies the remaining one (Ankel et al. 1986), is mainly based on electron spin resonance technique.

VI 6 1 Electron spin resonance study .

Despite the fact that their own sedimentation studies showed no change in sedimentation coefficient ,Ankel et al. (1986) reported a change in fibronectin conformation in the presence of heparin at a 50 to 1 heparin / fibronectin molar ratio. This was based on electron spin resonance (ESR) data. This result from ESR seems vulnerable because of the following points:

A) At 4 0 C fibronectin-heparin complexes are insoluble and form visible precipitates . This would result ,if the spin-label-protein association was rigid , in a dramatic change in mobility of the label . This is not observed in this work.

B) No mention is made of the temperature control system used . Temperature shifts of as little as half a degree between or during runs could account for some of the observed differences.

C) A microwave power of 30 mW was used although 5-10 mW seems the maximal power

permissible (Jost et al. 1979) , and a high amplitude modulation was employed . Both of these may result in spectrum distortion.

D) No proper spectrum analysis was made (ie defining peak positions and peak to peak differences in height and position.) .The high noise also created a uncertainty in the determination of the position of the high field extremum in the spectra resulting in considerable uncertainty in the measured splitting values.

E) The estimation of the weakly immobilized label with the use of a 120kD fragments is probably wrong because the area under the two low field peaks in Fig 3a of reference 18 seems in a 1 to 1 ratio rather than 20 to 1 as suggestedin this work.

F) There is no evidence that relating the protein motion to the label motion is appropriate in this case because of the lack of evidence of rigid spin-label-protein association. As stated in paragraph A above , there is even evidence that the two motions are not related.

G) Apparently no attempts were made to avoid the polydispersity problem such as filtration or centrifugation of the specimens before the measurements.

H) Those experiments were performed on a machine possessing only low sensitivity and a single scan mode not suited to the detection of small variations.

Therefore we may conclude that because the association is not rigid , no deductions on the fibronectin overall conformation are possible and that observed differences are the result of either a very local change in conformation resulting in a greater label freedom or a change in the polarity of the environment .

VI 6 2 Circular dichroism studies.

Two circular dichroism studies (Welsh et al. 1983, Osterlund et al.1985) ,show a clear change in fibronectin CD spectrum induced by heparan-fibronectin (Osterlund et al.1985) or heparin-fibronectin (Welsh et al. 1983), complex formation. They both concluded that the secondary structure of fibronectin was changed upon heparan or heparin binding. As this spectrum alteration occurs at very low heparan fibronectin molar ratios of 1 to 100 heparan/fibronectin (Osterlund et al.1985), requiring the association of multiple fibronectin molecules on one heparan chain , the authors suggested that this change in secondary structure might be due to polymerisation or formation of large complexes with heparan .

It must be noted that:

A) For both works:

α) No clear estimation of the polydispersity is possible by this technique .

β) Aggregation is known to perturb CD spectrum (see Mc Calley et al. 1972).

γ) The effects of heparin type sugar additions on the spectra differs between the two publications.

B) In the work by Welsh et al. (1983):

α) There is no convincing proof that the measured signal was due to specific changes in Tyrosine or proline residues, hairpin bends , β-turns or γ-turns.

β) It cannot be said that fibronectin contains little or no β-sheet or α-helix.

γ) Changes observed at high pH may be due to the sensitivity of S-S bonds in those conditions.

C) In the work of Osterlund et al. (1985) : As pointed out by the authors the changes were possible even with a very low heparan/fibronectin molar ratio. We believe, as noted by these authors , that the observed variations in the spectra are due to polymerisation or aggregation rather to a change in secondary structure. Those results would then confirm the findings from this work.

VI 7 CONCLUSION : CONSEQUENCES FOR FIBRONECTIN IN VIVO.

The study of Heparin-fibronectin complexes presented in this chapter show :

A) By neutron scattering of fibronectin-Heparin complexes after filtration ,that no large change in conformation of the fibronectin molecule occurs after heparin binding.

B) By light scattering that the molecular weight of unfiltered complexes increased upon heparin addition coupled to a decrease in diffusion coefficient.

Despite those two points the two CD studies mentioned over in VI 6 6 show alteration of fibronectin spectra upon heparin-type carbohydrates even after a small heparan addition. As fibronectin is known to be composed of independent domains and that the heparin binding sites represents only a fraction of the molecule we believe that those alterations are a consequence of aggregation.

We cannot completely rule out a possible minor change in conformation undetected by our experimental techniques. Nevertheless if this minor change was restricted to the heparin binding domain , C.D. studies would probably be unable to detect it as well . A large change in conformation certainly does not occur after heparin-fibronectin complex formation.

Addition of calcium inhibits the complex formation (Richter et al. 1985) . Calcium addition does not entirely reverse the changes in diffusion coefficient with

unfiltered material and filtration was required to reverse entirely those changes . We therefore believe that some of the aggregates are calcium insensitive. This could be due either to it being impossible for calcium ions to diffuse in very dense aggregates or to the formation of covalent fibronectin polymers by inter molecular disulphide bridge formation.

We might therefore suggest that some in vitro polymerisation of fibronectin could be triggered by heparin-like carbohydrate interaction with fibronectin . Formation of non covalent complexes of multiple fibronectin molecules on one carbohydrate chain might create the conditions required for some polymerisation of fibronectin.

Heparan sulphate proteoglycans (for review see Hook et al. 1984), are present in the extracellular matrix as:

A) Integral membrane components (Kjellen et al. 1980) with their protein section imbedded in the membrane . It is believed that they can possibly create a link between matrix and cytoskeleton .

B) Membane associated structures (Hedman et al. 1982) . Those structures are bound through their carbohydrate or protein section to a receptor embedded in the membrane .

Fibronectin has been shown to be associated with heparan sulphate in vivo (Laurie et al. 1983), and in the matrix deposed by cultured cells (Hedman et al. 1982). Heparan-fibronectin aggregate formation is impossible in vitro because heparan sulphate is immobilized as a membrane associated structure .

Association of fibronectin with heparan on the cell surface also differs from the fibronectin association with fibronectin-receptor in the sense that more than one fibronectin molecule can be attached to on one carbohydrate chain. This would create clusters of fibronectin at the surface of the cells. This is impossible with fibronectin directly linked to fibronectin-receptor where only one fibronectin molecule can be present at a time on the receptor. Creating heparan-multi fibronectin complexes with fibronectin molecules close to eachother could be an important step in matrix formation. It must be noted that the heparan-fibronectin interaction is much stronger in vivo than in vitro (Hedman et al .1982 b).

We have shown that the fibronectin conformation is not affected upon heparan-fibronectin complex formation but that polymerisation of fibronectin is possible . This suggests that a factor might help to trigger the transition of heparan-fibronectin into a stronger association. This factor ,obviously missing in vitro, could perhaps be responsible for fibronectin polymerisation with inclusion of heparan-fibronectin complexes in the polymers. This would explain the stronger heparan-fibronectin association observed with heparan-fibronectin created in vivo.

Transformed cells, unable to create a proper extracellular matrix, synthesize undersulphated heparan sulphate (Pejler et al. 1987), unable to bind immobilized fibronectin, but show a normal fibronectin synthesis but poor fibronectin retention (Wen tien et al. 1982)J.This is no surprise as fibronectin is strongly dependent on sulphation for heparin type carbohydrate binding (Ogamo et al. 1985) . We suggest that the creation of multi fibronectin complexes on the cell surface heparan sulphate and their processing by an unknown mechanism into a much stronger association is a critical step for proper matrix deposition and assembly .

GENERAL CONCLUSION

In this thesis various physicochemical techniques have been applied to the study of the fibronectin molecule in solution .

From the work presented in chapter IV it can be concluded that , although each of those techniques can yield accurate results their interpretation is not easy because the amount of information given by each method is limited . However the simultaneous application of several complementary techniques has proved valuable. The comparison between the measurements of the radius of gyration , the translational and rotational diffusion coefficients has been carried out . The use of all three of those parameters was of particular interest . This showed that the approximation of the shape of the fibronectin molecule to an ellipsoid of revolution is not possible . This confirms that this approximation process , performed in most physicochemical studies , should ideally not be.... applied unless it has been shown that at least three parameters depending on the shape fit the same ellipsoid .

In this specific study of the fibronectin molecule many biochemical studies were described in the literature . This published information, as well as the measurements on isolated fragments , allowed refinement of the the model .

Crystallographic techniques have not been succesfully applied to fibronectin yet. At present it seems that the classical methods of crystallisation cannot , at present , allow production of crystals from fibronectin .

The physicochemical techniques in solution can also be used for comparative studies . Chapters V and VI shows that studies in solution can produce interesting comparative results in pathological or physiological situations .

In chapter V , the case of the study of the diffusion coefficient of plasma fibronectin from metastatic cancer patients , shows that light scattering could rapidly detect fine changes that are difficult to establish with other techniques .

Chapter VI described how the investigation of the properties of the three-dimensional structure of the fibronectin molecule in the presence of heparin in vitro can be related to the understanding of the formation of the extracellular matrix .

REFERENCES.

Akiyama SK , YamadaKM.
1985 **J Biol Chem** 260(19) 10402-5 .

Alexander SS , Colonna G , Yamada KM , Pastan I , Edelhoch H .
1978 **J.Biol.Chem.** 253 5820-5824 .

Ali IU , Hunter T.
1981 **J.Biol.Chem.** 256 7671-7667.

Aplin JD , Hughes CD , Jaffe CL , sharon N.
1981 **Exp.Cell.Res.** 134 488-494.

Ankel EG , Homandberg G , Tooney NM , Lai CS.
1986 **Arch Biochem Biophys** 244 50-6 .

Argraves WS , Pytela R , Suzuki S , Millan JL , Pierschbacher MD , Ruoslahiti E .
1986 **J.Biol.Chem.** 261 12922-12924 .

Aumailley M , Timpl R .
1986 **J.Cell.Biol.** 103(4) 1569-1575.

Baker M .
1985 **Biochem.Biophys.Res.Comm.** 130 1010-1014.

Balian G , Click E , Crouch E , Davidson M , Bornstein P .
1978 **J.Biol.Chem.** 254 1429-1432 .

Benoit H.
1951 a **Ann. Phys.** 6 561-609.

Benoit H.
1951 b **J.Chim. Phys.** 49 517-522.

Bentley kl , Klebe RJ , Hurst RE , Horowitz PM .
1985 **J Biol Chem** 260 7250-6.

Bernal GJM , DeLa Torre J.G .
1980 **Biopolymers** 19 751-766.

Bernal GJM , DeLa Torre J.G .
1981 **Biopolymers** 20 129-139 .

Berne B , Peccora B
1974 "Dynamic light scattering" Academic Press.

Bernengo JC , Bezot P, Bezot C , Roux B , Marion C.
1981 **Ber. Bunsen-Ges. pys. Chem.** 85 657,661.

Beyth RJ , Culp LA .
1984 **Exp Cell Res** 155(2) 537-48 .

Borsi L , Carnemolla B , Castellani P , Rosellini C , Vecchio C , Allemanni G , Chang SE , Taylor-Papadimitriou C , Pande H , Zardi L.
1987 **J.Cell.Biol.** 104 595-600 .

BronnerFraser M .
1986 **Dev Biol** 117 528-36 .

Brown PJ , Juliano RL .
1987 **Exp Cell Res** 171(2) 376-88.

Castellani P , Siri A , Rosellini C , Infusini E , Borsi L , Zardi L .
1986 **J.Cell.Biol.** 103 1671-1677.

Chen WT , Wang J , Hasegawa T , Yamada SS , Yamada KM .
1986 **J.Cell.Biol** 103 1649-1470.

Chen JM , Chen WT .
1987 **Cell** 48 193-203 .

Chernousov MA , Metsis ML , Koteliansky VE.
1985 **FEBS Lett.** 183 365-369.

Cuatrecasas P , Wilchek M , Anfinsen CB .
1968 **Proc.Nat.Acad.Sci.USA** 61 636-643 .

Cummins .
1973 **Phys.Rev.Lett.** 12, 150-155 .

Daune M ,Freund L ,Spech G.
1961 **J. Chim. Phys.** 59 485-491.

Debye P.
1944 **J.Applied.Phys.** 15 338.

Debye P.
1947 **J.Phys.and Colloid. Chem.** 51 18.

Dedhar S , Ruoslahiti E , Pierschbacher MD.
1987 **J.Cell.Biol.** 104 585-593.

De-Petro G , Barlatti S , Vartio T , Vaheri A.
1983 **Int.J.Cancer.** 31 157-162 .

DeLa Torre J.G. , Bloomfield V.A.
1977 a **Biolpolymers** 16 1747-1763 .

DeLa Torre J.G. , Bloomfield V.A.
1977 b **Biolpolymers** 16 1765-1778

DeLa Torre J.G. , Bloomfield V.A.
1977 c **Biolpolymers** 16 1779-1793.

DeLa Torre J.G. , Bloomfield V.A.
1978 **Biolpolymers** 17 1605-1627.

Dessau W , Adelmann B , Timpl R , Martin G .
1977 **Biochem.J.** 169 55-59.

Di-Renzo MF , Tarone G , Comoglio PM , Marchisio PC .
1985 **Eur J Cancer Clin Oncol** 21 85-96 .

Donaldson D , Mahan J , Hasty D , MCcarthy JB , Furcht LT.
1985 **J.Cell.Biol.** 101 73-78 .

Doty P , Edsall JP .
1950 **Adv.Protein.Chem.** 6 50-55 .

Duband JL , Rocher S , Chen WT , Yamada KM .
1985 **J.Cell.Biol.** 102 160-178

Duksin D , Bornstein P .
1976 **Proc.Natl.Acad.Sci. USA.** 74 3433-3437 .

Edelman GM .
1983 **Science** 219 450-457.

Einstein A .
1910 **Ann.Phys** (Leipzig) 33 1275 .

Engel J , Odermatt E , Engel A , Madri A , Furthmayr H , Rodhe H , Timpl R .
1981 **J .Mol.Biol.** 150 97-120.

Engel J , Richter H , Hormann H , Schultness T , Houseley Z .
1985 **Biol.Chem. HOPPE SEYLER** 366 985-991.

Engvall E , Ruoslahiti E , Miller EJ .
1978 **J EXP.MED.** 147 1584-1595.

Engvall E , Bell IR , Ruoslahiti E .
1981 **Coll.Rel.Res.** 1 505-516.

Erickson H , Carrel N , McDonaught I .
1981 **J.Cell.Biol.** 91 673-678 .

Fagan JB , Yamada KM , DE Crombrugge B , Pastan I .
1979 **Nucleic.Acid Res.** 10 5925.

Fahrney DE , Gold AM .
1963 **J.Amer.Chem.Soc.** 85 997.

Fellin FM , Barsigian C , Rich E , Martinez J.
1988 **J.Biol.Chem.** 263 1791-1799.

Forastieri H , Ingham KC .
1983 **Arch.Biochem.Biophys.** 227 358-366 .

Forastieri H , Ingham KC .
1985 **J.Biol.Chem.** 260 10546-10550 .

Francheschi De Carreira F , Castellino F.
1985 **Arch.Biochem.Biophys.** 243 284-291 .

Fredericq E, Houssier C.
1973 in "Electric dichroism and electric birefringence."
Monographs on Physical Biochemistry , Harrington W and Peacocke A.R. ed .
Clarendon press Oxford.

Garciapardo A , Pearlstein E , Frangione B .
1983 **J.Biol.Chem.** 258 12670-12674.

Garciapardo A , Pearlstein E , Frangione B.
1985 **J.Biol.Chem.** 260 10320-10325.

Giancotti PG , Comoglio PM , Tarone G .
1985 **Exp.Cell.Res.** 163 47-62 (86).

Glan TT , Hadhazy C , Mikecz K , Sipos A .
1985 **Histochemistry** 82(2) 149-58.

Grassi P, Massoulie J,Timpl R .
1983 **Eur.J.Biochem.** 133 31-38.

Griffin CA , Calaycay I , Shively JE , Smith RL.
1986 **Thromb.Res** 43 469-477.

Guinier A , Fournet G .
1955 in "Small Angle Scattering Of X-Rays", **John Willey** New York .

Hayman E , Oldberg A , Martin G , Ruoslahiti E .
1982 **J.Cell.Biol.** 94 28-35 .

Hedman K , Johansson S , Vartio T , Kjellen L , Vaheri A , Hook M .
1982a **CELL** 28 663-671 .

Hedman K , Johansson S , Vartio T , Kjellen L , Vaheri A , Hook M .
1982 b **J.Cell.Biol** 94 28-35 .

Homandberg GA , Erickson JW .
1986 **Biochemistry** 25 6917-6925 .

Homandberg GA .
1987 a **Thromb.Res.** 48 321-328

Homandberg GA .
1987 b **Thromb.Res.** 48 329-335

Hook M , Kjellen L , Johansson S , Robinson A.M.
1984 **Ann.Rev. Biochem.** 53 847- .

Hormann H , Jelinic V , Richter H .
1983 **Hoppe Seylers Z Physiol Chem** 364 1011-8.

Hormann H , Richter H , Jelinic V .
1985 **Thromb Res** 39(2) 183-94 .

Hormann H , Richter H .
1986 **Biopolymers** 25 947-958.

Hormann H , Richter H , Jelinic V .
1987 **Thromb Res** 46(1) 39-50 .

Horwitz A , Duggan K , Buck C , Beckerle MC , Burrige K .
1986 **Nature** 320 531-533 .

Humpfries MJ , Akiyama SK , Olden K , Yamada KM .
1986 **J.Cell.Biol** 103 (6) 2637-2647.

Humphries MJ , Ayad SR .
1983 **Nature** 305 811-3.

Ibel K .
1976 **J.Appl.Cryst.** 9 296-309 .

Ingham KC , Shelsea A , Broekelmann T , McDonald J .
1984 **J.Biol.Chem.** 259(19) 11901-11907 .

Ingham KC ,Landwehr R, Engel J.
1985 **Eur.J.Biochem.** 148 219-224.

Ingotz RA , Massague J.
1986 **J.Biol.Chem.** 261 4337-4345.

Isemura M , Kan M , Yamaguchi Y , Munakata H , Aikawa J , Yamane I , Yosizawa Z.
1984 **Biochim.Biophys.Acta** 799 276-281.

Jacrot B.
1976 **Rep.Prog.Phys.** 39 911-953 .

Jacrot B , Zaccai G.
1981 **Biopolymers** 20 2413-2426.

Jilek F , Hormann H .
1979 **HoppeSeyler** 360 597-603 (79) .

Johansson S.
1985 **J Biol Chem** 260(3) 1557-61 .

Jones GE , Arumugham RG , Tanzer L.
1986 **J.Cell.Biol.** 103(5) 1663-1670.

Jost P , Griffith OH .
1979 in " Spin Labelling Theory and applications " **Academic Press** .

Kawamura K , Tanaka M , Kamitama F ,Higashino K , Kismioto S.
1983 **Clin.Chem.Acta.** 131 101-108 .

Kawasaki Y , Horie H , Takenaka T .
1986 **Brain Res** 397(1) 185-8 .

Kerr J.
1875 **Phil.Mag.** 9 157-163.

Kerr J.
1880 **Phil. Mag** . 50 337-346 .

Keskioja J , Lahito M , Vartio T .
1986 **BBA** 882 367-376.

Kjellen l , Oldberg A , Hook M .
1980 **J.Biol.Chem** 255 10407-10413 .

Kleinman HK , MCgoodwin EB , Martin G.
1978 **J.Biol.Chem.** 253 (16) 5642-5646.

Koda JE , Rapraeger A , Bernfield M .
1985 **J.Biol.Chem.** 260(13) 8157-8162.

Kornblihtt A , Pedersen K , Baralle F .
1983 **PNAS** 80 3218-3222.

Kohrnblitt AR , Vibepedersen K , Baralle FE.
1984 **EMBO. J** 3 221-226 .

Kornblihtt A , Umezawa K , Pedersen K , Baralle F.
1985 **EMBO. J** 4(7) 1755-1759 .

Koteliansky V , Glukhova M , Bejan M , Smirnof V , Filimonof V , Zalite O .
1981 **Eur.Jour.Biochem.** 119 619-624 .

Kradin RL , Zhu Y , Hales CA , Bianco C , Colvin RB .
1986 **Am J Pathol** 125(2) 349-57.

Kurkinen M , Taylor A , Garrels JA , Hogan BLM .
1984 **J.Biol.Chem.** 259 5915-5922 .

Laemmli UK .
1970 **Nature** 227 680-689.

Lai CS , Tooney NM .
1983 **Arch.Biochem.Biophys.** 228 465-473 .

Lai CS , Tooney NM , Ankel EG .
1984 **Biochemistry** 23 6393-6397.

Laurie-GW, Leblond-CP, Martin-GR .
1982 **J Cell Biol** 95(1) 340-4 .

Laurie GW , Leblond CP , Martin GR .
1983 **Am J Anat** 167(1) 71-82.

Lawler J , Hynes RO.
1986 J.Cell.Biol. 103(5) 1635-1648.

Liu M.C. , Suiko M .
1987 **Arch.Biochem.Biophys.** 255 162-167.

Ledger P , Tanzer M .
1981 **J.Biol.Chem.** 257 3890.

Matsuura H , Hakomori SI .
1985 **PNAS** 82 6517-6525.

McCarthy JB , Hagen ST , Furcht LT .
1985 **J.Cell.Biol.** 102 179-188 .

Mc Caley RC , shimshick EJ , Mc Conell HM.
1972 **Chem.Phys.Lett.** 13 115-119.

McDonaugh R , Petersen T , Th?gersen H , Skorstengaard K , All . .
1981 **FEBS Lett.** 127 174-178 .

McDonald JA , Quade BJ , Broekelmann TJ , La-Chance R , Forsman K , Hasegawa E
1987 **J.Biol.Chem.** 262(7) 2957 .

McKeowlongo P , Mosher DF .
1985 **J.Cell.Biol.** 100(2) 364-374.

McKeownLongoPJ , Mosher DF.
1983 **J Cell Biol** 97(2) 466-72 .

Mellado P , DeLa Torre J.G .
1982 **Biopolymers** 21 1857-1871.

Molnar J , Hoekstra S , Ku CS , VanAlten P .
1987 **J Cell Physiol** 131(3) 374-83.

MorissonP. Edsall JT ,Miller SG.
1948 **J.am.Chem. Soc** 70 3103-17.

Mosher DF , Schad P , Vann J .
1979 **J.Biol.Chem.** 255 1181-1190.

Mosher DF .
1984 **Mol Cell Biochem** 58(1-2) 63-8 .

Mosher DF , MCkeowlongo P .
1984 **J.Biol.Chem.** 259(19) 2210-2215 .

Mosher DF , McKeownLongo PJ .
1985 **Biopolymers** 1985 24(1) 199-210 .

Mosseson M , Chen AB , Huseby RM .
1975 **Biochim.Biophys.Acta** 386 509-524 .

Mosseson M , Ankel EG , Evans D , Kane C , Amrani D , Homandberg G .
1985 **Arch.Biochem.Biophys.** 238 652-663 .

Murthy Kd.D , Diwan A.R. , Simmons S.R. , Albrecht R.M. , Cooper S.L.
1987 **Scanning. Micros.** 1 765-773.

Nagata K , Humphries M , Olden K , Yamada KM .
1985 **J.Cell.Biol.** 101 386 394 .

Nichols EJ , Fenderson BA , Carter WG , Hakomori SI .
1986 **J.Biol.Chem.** 261 11295-1130 .

Obara M , Kang MS , Rocherdufour S , Kornblitt A , Thieri JP , Yamada KM .
1987 **FEBS Lett.** 213 (2)261-264 .

Odermatt E , Engel J , Richter H , Hormann H .
1982 **J .Mol.Biol.** 159 109-123 .

Ogamo A , Nagai A , Nagasawa K.
1985 **Biochim Biophys Acta** 841(1) 30-41 .

Olden K , Pratt RM , Yamada KM .
1979 **Proc.Nat.Acad.Sci. USA.** 76 3343-3347 .

Oppenheimermarks N , Grinell F.
1984 **Exp.Cell.Res.** 152 467-475.

Osterlund E , Eronen I , Osterlund K , Vuento M .
1985 **Biochemistry** 24(11) 2661-2667..

Ouaissi MA , Afchain D , Capron A , Grimaud JA.
1984 **Nature** 308 380-2 .

Ouaissi MA , Capron A .
1985 **Ann Inst Pasteur Immunol** 136C(2) 169-85.

Owens RJ , Baralle F .
1986 **EMBO.J.** 5 2825-2830.

Parent JB , Yeo TK , Yeo KT , Olden K .
1986 **Mol.Cell.Biochem.** 72 21-23 .

Patthy L , Trexler M , Vali Z , Banyai L , Varadi A .
1983 **FEBS Lett.** 171 131-136 .

Patthy L .
1985 **CELL** 41(3) 657-663.

Paul JI , Schwartzbauer JE , Tamkun JW , Hynes RO.
1986 **J.Biol.Chem.** 261 12258-12265 .

Pavlov M , Feodorov B.
1986 **Biofisika** (USSR) 31 964-970.

Pecora B .
1964 **J.Chem.Phys.** 40 1604-1608 .

Perkins SJ .
1988 **New Comprehensive Biochemistry** 11b 146-265 .

Perrin F .
1934 **J.Phys.Radium** 5 497-511.

Petersen T , Th?gersen H , Skorstengaard K , Pedersen K , Sahl P , Jensen L.
1983 **PNAS** 80 137-141.

Porath J , Flodin P .
1959 **Nature** 183 1657-1659.

Presciotta Peters D , Mosher DF.
1987 **J.Cell.Biol.** 104(1) 121-130 .

Pusey PN , Koppel DE , Sceaffer DW , Camerini Ottero RD , Koenig SH.
1974 **Biochemistry** 13 652-960.

Pytela R , Pierschbacher MD , Ruoslahti E .
1985 a **Proc Natl Acad Sci USA** 82(17) 5766-70.

Pytela R , Pierschbacher MD , Ruoslahti E .
1985 b **Cell** 40(1) 191-8 .

Richter H , Wendt C , Hormann H .
1985 **Biol Chem Hoppe Seyler** 1985 366(5) . 509-14 .

Robinson R , Hermans J .
1984 **Biochem.Biophys.Res.Comm.** 124 718-725.

Rocco M , Carson M , Hantgan R , MCdonagh J , Hermans J .
1983 **J.Biol.Chem.** 258 14545-14549 .

Rocco M , Infusini E , Daga MG , Gogioso L , Cuniberi C .
1987 **EMBO.J.** 6 2343-2349.

Ruoslahiti E , Hayman EG , Pierschbacher MD , Engvall E .
1982 **Meth.In Enzym.** 82 803-831.

Ruoslahiti E , Pierschbacher MD .
1984 **Nature** 309 30-33.

Ruoslahiti E , Suzuki S , Hayman EG , Ill CR , Pierschbacher MD .
1987 **Meth.In.Enzymol.** 144 430-7.

Salonen EM., Vartio T, Hedman k ,Vaheri A .
1984 **J.Biol.Chem.** 259 1496-1514.

Salonen EM., Sakelsa O , Vartio T, Vaheri A ,Nielsen L , Zeuthen J .
1985 **J.Biol.Chem.** 260 12302-12307 .

Schwartzbauer J , Tamkun J , Lemischka I , Hynes RO .
1983 **CELL** 35 421-431 .

Seidah NG , Manjunath P , Rochemont J , .
1987 **Biochem.J.** 243 195-203 .

Seikiguchi K , Siri A , Zardi L , Hakomori SI .
1985 **J.Biol.Chem.** 260 (8) 5105-5114.

Singer-II, Scott-S, Kawka-DW, Hassel JR
1987 **Exp Cell Res** 173(2) 558-71.

SiriA , B alza E , Carnemolla B , Castellani P , Borsi L , Zardi L .
1986 **Eur J Biochem** 154(3) 533-8 .

Sjoberg B , Pap S , Osterlund E , Osterlund K , Vuento M .
1987 **Arch.Biochem.Biophys.** 255 347-.

Skorstengaard K , Jensen L , Petersen T , Magnusson S .
1986 **Eur.Jour.Biochem.** 154 15-29 .

Skorstengaard K , Th?gersen H , Petersen T .
1983 **Eur.Jour.Biochem.** 140 235-243.

Skorstengaard K , Thogersen HC , Vibe-pedersen K , Petersen TE , Magnusson S .
1982 **Eur.J.Biochem.** 128 605-623 .

Smith H , Riggs J , Mosesson M .
1978 **Cancer res.** 39 4138-4144 .

Smolushowski M.
1908 **Ann.Phys** 25 205-.

Stathakis N , Mosesson M .
1977 **J.Clin.Inv.** 60 855 865.

Stathakis N , Mosesson M ,Chen AB , Galanakis DK.
1978 **Blood** 51 1211,1222 .

Stenman S , Vaheri A .
1978 **J Exp.Med.** 148 1054-1064

Stenman S , Wartiovaara J , Vaheri A.
1977 **J.Cell.Biol.** 74 453-467

Stenman SUM , Salonen C, Osterlund K , Kussela P
1983 **J.Mol.Immunol.** 20 149-153.

Sternberg J , Kimber S.J .
1986 **J Embryo.Epx.Morph.** 91 267-282 .

Steven FS , Griffih MM , Alhamad R.
1985 **Eur.Jour.Biochem.** 149 35-40 .

Stewart M, Vigiers G.
1986 **Nature** 319 631-635.

Stuhrmann HB , Miller A .
1978 **J.Appl.Cryst.** 11 325-345.

Taksaki S , Yamashita K , Suzuki K , Iwanaga S , Kobata A .
1979 **J.Biol.Chem** 254 8548-8553.

Tao T.
1969 **Biopolymers** 8 , 609-632.

Teng A , Rifkin C .
1979 **J.Cell.Biol.** 80 784-790.

Tikani L , Kumar S , Takio K , Ericsson LH , Wade RD , Ashida K , Walsh KA .
1986 **Biochemistry** 25 3171-3184.

Tooney NM , Mosesson M , Amrani D , Hainfiel J , Wall J .
1983 **J.Cell.Biol.** 97 1686-1692.

Tryggvason K , Hoyhta M , Salo T.
1987 **BBA** 907 191-217 .

Urushihara H , Yamada KM .
1985 **J.Cell.Physiol.** 126 . 323-332 .

Vartio T .
1986 **J.Biol.Chem.** 261 9433-9437.

Vartio T , Seppa H , Vaheri A .
1980 **J.Biol.Chem.** 256 471-477.

Veil-Douhala V , Planchenault T.
1986 **PNAS** 83 5377-5381 .

Venyaminof SY , Metsis ML , Chernoussof MA , Koteliansky V .
1983 **Eur.Jour.Biochem.** 135 485-489.

Vesterberg O , Hansen L , Sjosten A .
1976 **BBA** 491 160-166 .

Virtanen I , Lehto P , Vartio T.
1987 **Int.J.Cancer** 39(3) 361 .

Vuento M , Vaheri A .
1979 **Biochem.J.** 183 331-337 .

Vuento M , Steneman UH , Salonen E , Osterlund K , Kussela P.
1983 **Mol. Immunol.** 20 149-153.

Wagner DD , Ivatt R , Destree AT , Hynes RO .
1981 **J.Biol.Chem.** 256 11708-11715 .

Weber K , Osborn M.
1969 **J.Biol.Chem.** 244 4406-4412 .

Wegener WA , Dowben RM , Koestler VJ.
1979 **J.Chem.Phys.** 70 622-632.

Welsh E.J. Franglou E.R. ,Moriss E.R. , Rees D.A.
1983 **Biopolymers.** 22 821-831.

Wen Tien C , Olden K , Bernard B , Fong CHU .
1984 **J.Cell.Biol.** 98 1546-1555.

Williams EC , Janmey PA , Ferry J , Mosher DF.
1982 **J.Biol.Chem.** 257 14973-14978.

Williams EC , Janmey PA , Johnson RB , Mosher D F.
1983 **J.Biol.Chem.** 258(9) 5911-5914.

Wolff K , Lai CS .
1988 **Biochemistry** 27 3483-3487.

Woods A , Hook M , Kjellen L , Smith CG , Rees DA.
1984 **J.Cell.Biol** 95 1743-1753 .

Woods-A, Hook-M, Kjellen-L, Smith-CG, Rees-DA.
1984 **J Cell Biol** 99(5) 1743-53 .

Wrann M .
1978 **Biochem.Biophys.Res.Commun.** 84 269-274 .

Wright SD , MeyerBC .
1985 **J Exp Med** 162 762-7.

Yamada KM .
1978 **J.Cell.Biol.** 78 520-541.

Yamada KM .
1982 **Immunochem.Extracellular Matrix** 1 111-123 .

Yamaguchi Y , Isemura M , Yosizawa Z , Kan M , Sato A.
1986 **Int.J.Biochem.** 18 437-443 .

Zardi L , Siri A , Carnemolla B , Santi L .
1979 **CELL** 18 649-657 .

Zardi L , Carnemolla B , Siri A , Petersen T , Paolella G , Sebastio G , Baralle FE .
1987 **EMBO** 6 2337-2342 .

Zhu B , Fisher S , Pande H , Calaycay J , Shively J , Laine R .
1984 **J.Biol.Chem.** 259 3962-3970 .

Zhu BC , Laine RA
1987 **Arch.Biochem.Biophys.** 252 1-6

Zimm
1948 **J.Chem.Phys.** 16 1099-.

Zucker S , Wieman JM , Lysik RM , Wikie D , Ramamurthy NS , Golub LM , Lane B
1987 **Cancer Res.** 47(6) 1608.

APPENDIX 1

F.E.B.S. Lett. Vol 238 p 5 to 8 (1988).

L.Vuillard , A. Miller and P.J.H. Sizer.

"Plasma fibronectin prepared from patients with metastatic breast cancer shows in vitro aggregation property"

Volume 238, number 1, 5–8 FEB 06316 September 1988

Plasma fibronectin prepared from patients with metastatic breast cancer shows in vitro aggregation property

Laurent Vuillard, Andrew Miller and Philip J.H. Sizer

Department of Biochemistry, University of Edinburgh Medical School, Hugh Robson Building, George Square, Edinburgh EH8 9XD, Scotland

Received 14 July 1988

Plasma fibronectin purified from the plasma of metastatic breast cancer patients has been studied by light scattering. It clearly shows abnormal self-aggregation properties; the possible significance of these findings to the in vivo situation is discussed.

Fibronectin; Cancer; Light scattering; (Plasma, Man)

1. INTRODUCTION

Fibronectins are a class of extracellular glycoproteins (520 kDa) (review [1]). Their primary structure can vary and depends on the alternative splicing of a unique gene which can generate at least ten different variants [2]. The molecules are composed of the concatenation of three types of homologous sequences [3] forming two similar, but not identical, chains linked near the carboxy-terminus end by two interchain disulphide bonds. One of the most striking features of the fibronectin molecules is that they are made of a succession of protease-resistant domains which can bind specifically to one or more of heparin, fibrin, factor VIIa, C1q, cell surface, DNA, gelatin collagen [1].

In solution, plasma fibronectin as studied by light scattering techniques does not show any significant self-aggregation properties [4], but fibronectins are present in the extracellular matrix in an insoluble, fibrillar, form [5].

Correspondence address: L. Vuillard, Department of Biochemistry, University of Edinburgh Medical School, Hugh Robson Building, George Square, Edinburgh EH8 9XD, Scotland

Receptors to fibronectin on the cell surface have been described [6] and a transmembranous continuity between cytoskeleton and fibronectins through the receptor has been demonstrated [7]. The association of fibronectin with the matrix assembly receptor has also been reported [8]. The position of fibronectin in the cell attachment process is therefore very important and it is probable that fibronectins are likely to be the extracellular matrix protein in closest contact with cells.

The involvement of fibronectin in cancer and metastatic processes has been investigated along three separate lines all related to early events of metastasis leading to the detachment of cells and their penetration into the blood stream:

(i) Synthesis of specific fibronectins by alterations of the primary structure [9] and carbohydrate side chains composition [10].

(ii) Modification at the cellular receptor level [11] and deposition rates of fibronectin in the matrix [12].

(iii) Degradation of fibronectin by tumour cells [13]. Specific enzymes have been described [14].

Surprisingly the role of fibronectins in the next stage, that is anchoring of the cell migrating in the blood stream, has been much less studied. De Petro et al. [15] have shown that transformation enhancement activity in the plasma of tumour pa-

Published by Elsevier Science Publishers B.V. (Biomedical Division)
00145793/88/$3.50

tients was linked with fibronectin. We report here evidence, from a light scattering study, that plasma fibronectin from breast metastatic cancer patients possesses significantly different hydrodynamic properties from normal plasma fibronectin.

2. MATERIALS AND METHODS

All affinity chromatography media were from Pharmacia (Sweden), and all other chemicals (analytical grade) were from BDH (England).

2.1. *Protein purification*

Blood samples were treated with 20% sodium citrate, 25 mM EDTA (1 vol. per 4 vols blood) and centrifuged at 200 × *g* for 5 min in a bench centrifuge. The supernatant was removed and was either frozen at −20°C or processed immediately as follows.

To remove any precipitates the plasma was centrifuged at 10000 × *g* for 1 h and then chromatographed on a 2 cm^2 × 1 cm gelatin-Sepharose column as described [16]. The sample was eluted with 4 M urea, 50 mM Tris-HCl (pH 7.4) but in order to test its possible influence on aggregation, 1 M arginine, 50 mM Tris-HCl (pH 7.4) was also used for one sample with no detectable difference. Exhaustive dialysis in 50 mM Tris-HCl, 100 mM NaCl, pH 7.4 (dialysis buffer), was then performed to remove any urea traces.

To eliminate any possible artefactual contamination two samples were rechromatographed on a heparin-Sepharose column rinsed by dialysis buffer and then eluted by 1 M NaCl, 50 mM Tris-HCl, 1 mM EDTA (pH 7.4) and redialysed in dialysis buffer.

PMSF (0.05 mM) was present in all buffers and EDTA (5 mM) was added to all buffers used for purification. All specimens were examined by 5 or 6% discontinuous PAGE gels according to Laemmli [17].

2.2. *Photon correlation spectroscopy*

All work presented here was performed on a type 4700c Malvern system (Malvern Instruments, England). The argon-ion laser (Innova 4, USA) was used at 514.5 nm with a power of approx. 150 mW.

For measurements on the fibronectin molecule the experimental time was set between 5 and 15 s with no noticeable difference between results. Each measurement involved the accumulation of a number of runs; the software calculated the mean value of total counts for each run and rejected any run with a significant difference in integrated counts.

To remove any possible dust or contaminant from the 1 cm diameter quartz cells (ALV Lasers, FRG), they and their teflon caps were stored in pure sulphuric acid. Prior to use they were washed 20 times with double-distilled water to remove any traces of acid and three times further with filtered sample buffer to ensure that the buffer composition of the sample would not be altered by some remaining water. All buffers and all but one sample were filtered through 200 nm pore size Nucleopore filters (USA). These are well known for their highly constant pore size as well as low retention of the sample because of their design as flat surfaces as opposed to ordinary filters which have mesh-like surfaces.

To test the influence of filtration one sample was centrifuged and showed no difference in properties from filtered samples. When filtering the samples care was taken to avoid any disturbance leading to aggregation. We avoided the use of metal needles which leads to metal contamination thereby triggering fibronectin polymerisation, as well as creating high-speed flows possibly leading to aggregation.

The first-order correlation function was calculated from the measured second-order and related to the diffusion coefficient *D* and polydispersity index (review [18]). No correction was made for buffer viscosity which was assumed to be the same as pure water. The analysis by the software has a specific feature to estimate the diffusion coefficient distribution for polydisperse solutions. The software retains in the memory the shape of correlation functions for a large number of diffusion coefficients. It then calculates a multiexponential curve and fits it with the observed one. It is important to note that no assumption about the distribution of particles is made.

2.3. *Molecular mass determination by light scattering*

When the concentrations were high enough to produce permissible signal-to-noise ratio, molecular mass estimations were made using the classical method of Zimm [19].

3. RESULTS

Fig.1 shows the diffusion coefficient/scattering intensity profile for normal plasma fibronectin (open squares) and for one sample of gelatin affinity-purified fibronectin from metastatic cancer patient plasma (black squares).

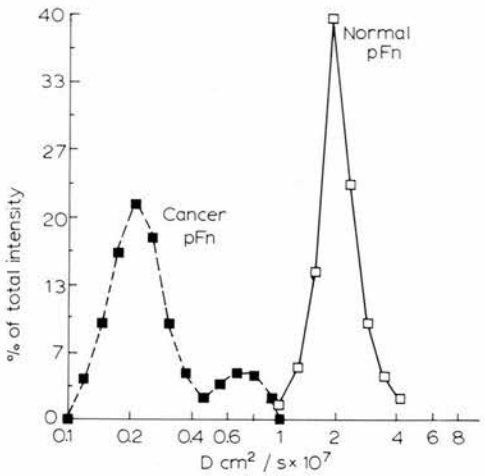

Fig.1. Diffusion coefficient/scattering intensity profile of (□—□) normal plasma fibronectin and (■---■) one sample of gelatin-affinity purified fibronectin from plasma of metastatic cancer patient.

Table 1

Sample	Polydispersity (%)	Molecular mass (kDa)
(1) Samples purified by gelatin affinity only (4 samples):		
D population 1 (cm^2/s) $0.29 \pm 0.07 \times 10^{-7}$	D population 2 (cm^2/s) $0.97 \pm 0.4 \times 10^{-7}$	55	4000
(2) Samples repurified on heparin-Sepharose (2 samples):			
D population 1 (cm^2/s) $1.12 \pm 0.2 \times 10^{-7}$	D population 2 (cm^2/s) $2.80 \pm 0.3 \times 10^{-7}$	38	
(3) Normal plasma fibronectin: Monodisperse distribution $D = 2.2 \times 10^{-7}$ (cm^2/s)		10	500

4. DISCUSSION

The most immediate result of our study is that plasma fibronectin prepared from metastatic cancer patients, when studied by dynamic light scattering, presents a polydisperse distribution, with two populations with markedly different diffusion coefficients. This contrasts with fibronectin purified from healthy individuals which presents a monodisperse distribution as shown in fig.1 as well as in the literature [4].

The analysis of the measured diffusion coefficients shows that: (1) Fibronectin from metastatic cancer patients which was purified solely on gelatin-Sepharose comprises two populations of material larger than normal plasma fibronectin. (2) Heparin-repurified samples comprise one population of larger objects and one population of slightly smaller objects.

(i) Proof that the material scattering light is fibronectin:

– The presence of protein contaminating the fibronectin preparation would be detected on the PAGE control gels.

– If contaminating material had been present, it would have been removed by the combination of various preparation procedures: for example, if the contaminants were eluted by 4 M urea only and they would not appear with material eluted from the gelatin column by 1 M arginine or repurified on the immobilised-heparin column, otherwise contaminants would have been eluted by high ionic strength, and therefore be eluted before fibronectin during the 1 M NaCl wash of the gelatin column.

– Furthermore, fibronectin alone binds to gelatin at high salt concentration and heparin at physiological salt concentration.

(ii) How much material is in an aggregated form?

The intensity of light scattering is proportional to the square of the mass of the scattering particles and thus to the sixth power of their size; so, clearly to allow detection of the higher diffusion coefficient values (i.e. those particles with smaller sizes) the high molecular mass material must represent a small number fraction of the total sample.

(iii) Why does the high diffusion coefficient population of fibronectin from cancer patients have a translational diffusion coefficient value (D) different from that of normal plasma fibronectin?

This is not too surprising, since the diffusion coefficients have to be calculated from a correlation function containing two decay rates, therefore the resolution is low. It is important to note that this is not a problem of noise but simply that the resolution is low when the distributions of two populations are close which means that the decays in the correlation function are not sufficiently dissimilar to estimate them precisely (the same problem occurs with Scatchard plots when two binding sites have similar dissociation constants). In addition, this loss in resolution is a direct consequence of the polydispersity and it lowers the quality of the diffusion coefficient measurements but the presence of aggregation is clearly established. This is confirmed by the very high values of the polydispersity index.

(iv) The important point established by our measurements is the presence of a low D population (i.e. large aggregates) in plasma fibronectin purified from metastatic cancer patients. As shown above in point (i), identification with fibronectin is clear but it is more difficult to determine whether such aggregates exist in vivo:

– They clearly exist at concentrations similar to the in vivo situation.

– The exclusion limit of the gelatin affinity column (Sepharose 4B) is smaller than that of the heparin affinity column (Sepharose CL6b). Despite this fact a considerable reduction in the size of the aggregates occurs after heparin affinity repurification. This would suggest that aggregates cannot easily dissociate after formation.
– Because of their size they would be excluded from the gelatin column, being directly eluted in the first preparation step. So, the more likely hypothesis is that they form during the preparation where the use of urea or 1 M arginine buffer leads to unfolding of the protein. The presence of these large aggregates in vivo cannot be stated with certainty.
– They are not the consequence of filtration because one sample that had been centrifuged still presented abnormal aggregation.

(v) We can only speculate on the origin of fibronectin presenting this abnormal aggregation property in vitro.

The presence in the blood stream of fibronectin synthesised by tumour tissues seems unlikely because tumour cells have been shown to degrade fibronectin in tissues [13] and fibronectin produced in tissues would have considerable difficulty migrating considering its binding properties. Furthermore, the amount produced would be very low compared to existing normal plasma fibronectin. Our conclusion is that the aggregates detected are genuine fibronectin with a different structure from that of normal plasma fibronectin. It could be present in plasma from confirmed metastatic cancer patients through modification in the blood of a small fraction of preexisting plasma fibronectin or could represent a form used by the metastatic cells to anchor at the surface of a blood capillary in their target organ.

REFERENCES

[1] McDonagh, J. (1985) Plasma Fibronectin: Structure and Function, Dekker, New York.
[2] Kohrnblitt, A.R., Umezawa, K., Pedersen, K. and Baralle, F. (1985) EMBO J. 4, 1755–1759.
[3] Petersen, T., Thogesen, H., Skorstengaard, K., Pedersen, K., Sahl, P., Sottrup-Jensen, A. and Magnusson, S. (1983) Proc. Natl. Acad. Sci. USA 80, 137–141.
[4] Williams, E.C., Jamney, P.A., Ferry, J.D. and Mosher, D.F. (1982) J. Biol. Chem. 257, 14937–14978.
[5] Hedman, K., Johansson, S. and Vartio, T. (1981) Cell 28, 663–671.
[6] Giancotti, P.G. and Comoglio, P.M. (1986) Exp. Cell Res. 163, 47–62.
[7] Horwitz, A., Duggan, K., Buck, C., Beckerle, M.C. and Burrige, K. (1986) Nature 320, 531–533.
[8] Prescottia-Peters, D. and Mosher, D.F. (1986) J. Cell Biol. 104, 121–130.
[9] Matsuura, H. and Hakomori, S.I. (1985) Proc. Natl. Acad. Sci. USA 82, 6571–6575.
[10] Nichols, E.J., Fenderton, B.A., Carter, W.G. and Hakomori, S.I. (1986) J. Biol. Chem. 261, 11295–11301.
[11] Juliano, R.L. (1987) Biochim. Biophys. Acta 907, 261–269.
[12] Altitalo, K. and Vaheri, A. (1981) Adv. Cancer Res. 37, 111–158.
[13] Barlatti, S., Adamoli, A. and DePetro, G. (1986) Matrix Biol. 11, 174–182.
[14] Wen-Tien, C., Olden, K., Bernard, B. and Fong, C. (1984) J. Cell Biol. 98, 1546–1555.
[15] DePetro, G., Barlatti, S., Vartio, T. and Vaheri, A. (1983) Int. J. Cancer 31, 157–162.
[16] Ruoslahiti, E., Hayman, E.G., Pierschbacher, M.D. and Engvall, E. (1982) Methods Enzymol. 82, 803–831.
[17] Laemmli, U.K. (1970) Nature 227, 680–687.
[18] Pusey, P.N., in: Photon Correlation and Light Beating Spectroscopy (Cummins and Pike, E. eds) Plenum, New York.
[19] Zimm, B.H. (1948) J. Chem. Phys. 16, 1093.

APPENDIX 2

Possible evidence for two heparin-binding classes of vitronectin in bovine plasma leading to a new preparation technique for vitronectin from bovine serum .

A2 1 ABSTRACT .

Vitronectin binding to heparin depends on the treatment which vitronectin undergoes during its preparation . In this section the possible existence the presence of vitronectin with high and low affinity to heparin in bovine serum and plasma is shown . This could also allow a faster non denaturing vitronectin preparation technique .

A2 2 A SHORT PRESENTATION OF VITRONECTIN .

Vitronectin is a protein identified in plasma (Hayman et al. 1983) , and tissues (Dahlback et al. 1986) . It exists in two forms of Mr 65 and 75 kD (Hayman et al. 1983 & Akama et al. 1986) . It has been shown that vitronectin is homologous with the S-protein of the complement system (Tomasini et al 1986) .

Vitronectin has been sequenced through its cDNA (Susuki et al. 1986) and the sequences responsible for various binding properties have been identified (Suzuki et al. 1984) .Vitronectin is involved in cell attachment processes (Hayman et al. 1985) . The binding of vitronectin to cells is mediated via a cellular receptor binding to the peptide RGD of vitronectin (Pytela et al. 1985) .The cellular vitronectin receptor has been sequenced and is found to be homologous to the fibronectin cellular receptor (Suzuki et al 1986) .

The functions of vitronectin in the complement system might be to act as a regulation of the killer complex (Muller-Eberhart 1985) possibly through a trypsin cleavage of Vitronectin (S-Protein.) (Bhakdi 1982) .

Vitronectin has been shown to bind to the thrombin-antithrombin III complex in serum (Ill et al. 1985) .

Vitronectin can bind to heparin but not in physiological conditions (Barnes et al 1983, Hayashi et al. 1985) . Heparin binding to vitronectin was also tested in a functional assay . Heparin binding to vitronectin inhibits the vitronectin neutralisation of activation of thrombin and factor Xa (Lane et al. 1987) .In this last work, the

dissociation constant of the vitronectin-heparin complex was found to be independent of the Mw of heparin and equal to 10^{-8} M . The affinity of vitronectin to heparin is increased when vitronectin is exposed to guanidine or reduced and carboxymethylated. Radiolabelled heparin exhibits a dissociation constant of 4 10 -8 M with vitronectin.

A 2 3 MATERIALS.

Glass beads (type 15032, 0.15 mm diameter), and analytical grade chemicals were from BDH (U.K.). Prior to use , glass beads were washed in pure sulphuric acid then exaustively in water then packed in a 20cm2 by 60 cm column . Heparin sepharose was from Pharmacia (Sweden). Bovine blood, which was made non clotting by addition of 1/9 vol/vol ACD, was collected in a plastic container, centrifuged for 10 minutes 10.000g to pellet blood cells. Plasma was then pumped and processed as described below.

A 2 4 PREPARATION OF THE SERUM SPECIMENS.

Vitronectin was prepared either from plasma or from serum. When serum was required it was obtained from plasma by adding calcium up to 40 mM and raising pH to aproximately 7. 8 . This material was incubated 2h at 37 C leading to formation of a solid gel . It was then centrifuged 15 min 10, 000 g and incubated at room temperature overnight still leading to formation of a fair amount of insoluble material . Centrifugation 15 min 10, 000g resulted in the separation of the insoluble clot and serum .

A2 5 AFFINITY CHROMATOGRAPHY ON GLASS BEADS .

All the preparation was carried out at 4 C . The column was equilibrated with 50 mM Tris , 200mM NaCl, 5 mM EDTA pH 7.9 at 25 C .

150 ml of serum or plasma were loaded at a flow of 100ml/h, washed with 1.5 l of equilibration buffer at a flow of 150 ml/h . To allow a sharp transition in pH upon next buffer the column was then rinsed with 100 ml of water . Elution was carried out by rinsing by 200 mM NaHCO3 buffer pH 9.7 at a flow of 100 ml/h . 15 ml fractions were collected .

A2 6 AFFINITY CHROMATOGRAPHY ON HEPARIN .

The peak fractions of the previous step (aprox. 200 ml), were dialysed twice against 100mM phosphate buffer pH 6 then once against 50 mM Phosphate , 100 mM NaCl . This resulted in the formation of a precipitate which was removed by centrifugation 5 min at 10, 000 g . The supernatant was loaded on a 2 cm^2 by 5 cm heparin affinity column equilibrated by the last dialysis buffer . It was then washed by 25 ml of the same buffer, 10 ml of 20 mM phosphate pH 6.1 buffer . A flow of 15 ml/h was kept for those first three steps . Elution was carried out by pumping 100 mM Tris pH 7.5 at a flow of 8ml/h . This was sometimes followed y 50 mM Tris 1 M NaCl pH 7.5 at the same flow .

A2 7 P.A.G.E

Polyacrylamide gel electrophoresis was carried out as described in chapter II section 4 .

A2 8 RESULTS FROM AFFINITY CHROMATOGRAPHY ON HEPARIN .

The fractions from the heparin affinity steps were analysed by P.A.G.E. in denaturing and non denaturing conditions.

Fig A 2 1 shows the elution profile of heparin affinity .

Fig A 2 2 shows a 8 % PAGE of the heparin affinity step .

It is obvious from both the elution profile and the gels that two classes of molecules can be released from the heparin column:

A) The first one is released by the change in pH . It appears as two bands with Mr of 65 and 75 kD .

B) The other class needs an increase in the ionic strength to allow elution from the column . An important part of this fraction was represented by material with the same characteristics on P.A.G.E as the proteins eluting only with a pH shift .

Fig A 2 I :

Vitronectin preparation : elution profile of heparin affinity chromatography step .

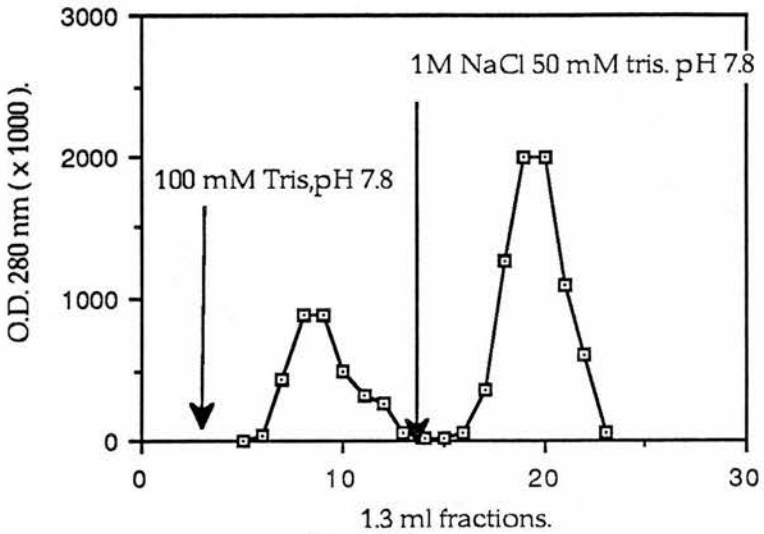

Fig A 2 2 :

S . D . S . P . A . G . E . of fractions from the heparin affinity chromatography step .

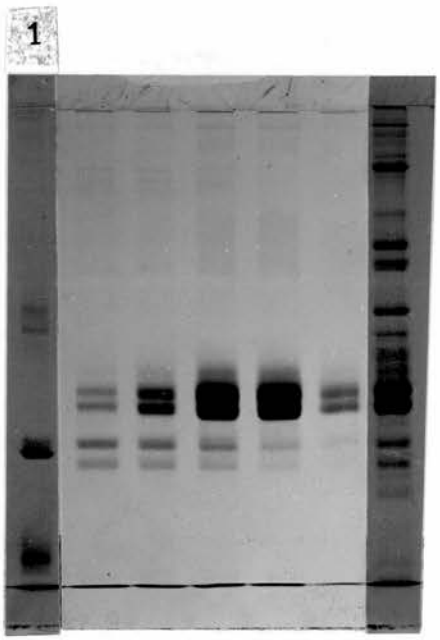

Lane 1 : MW markers : 96, input material mg .

Lane 2 to 6 : Fractions eluted by 100mM Tris pH 7.5

lane 7 : Fraction eluted by 1mM NaCl .

A 2 9 IS THIS MATERIAL VITRONECTIN ?

At the moment the identification of this material with vitronmectin is not absolute in the absence of specific antibodies . Nevertheless the following facts strongly suggests identity of the pH sensitive heparin binding material with vitronectin:

A) Same Glass binding properties .

B) Binding to heparin at low pH .

C) Elution from the heparin column by a by shift from pH 6.1 to 7.8

D) Same appearance on gelsas vitronectin : two bands at 65 and 75 k D .

As the pH insensitive heparin binding material has an apearance identical to that of the pH sensitive material and is also prepared by glass affinity ., it is likely that this material is vitronectin. . Absolute identification is dependent on the antibody availability which seems difficult at the moment .

A2 10 CONCLUSION

Those results are interesting because they show that Vitronectin can show two populations which differ in their affinity to heparin. :

A) One can remain bound to heparin at a pH superior to 7 at near physiological ionic strength and requires an increase of ionc trength to be realeased .

B) The other is released from an immobilised heparin column by simply raising the pH from 6.1 to 7.5 .

Those properties can give lead to a technique that could allow the preparation of purified vitronectin from bovine serum in two steps . This is performed under mild conditions as opposed to the classical methods that requires either :

A) exposure to 8 M urea which damages the molecule . (Ruoslahiti et al. 1987) .

B) Or a purification in four steps which is very time consuming . (Barnes et al. 1983).

REFERENCES OF APPENDIX 2

Akama T, Yamada KM, Seno N, Matsumoto I, Kono I, Kashiwagi H, Funaki T, Hayashi M.
1986 **J Biochem (Tokyo)** 100(5) 1343 51.

Barnes DW , Silnutzer J.
1983 **J.Biol.Chem** 258 12548-12552.

Bhakdi S, Tranum Jensen J
1982 **J Cell Biol** 94(3) 755 9.

Dahlback K, Lofberg H, Dahlback B .
1986 **Acta Derm Venereol (Stockh)** 66(6) 461 7 .

Hayashi M, Akama T, Kono I, Kashiwagi H .
1985 **J Biochem (Tokyo)** 98(4) 1135 8

Hayman EG, Pierschbacher MD, Ohgren Y, Ruoslahti E .
1983 **Proc Natl Acad Sci USA** 80(13) 4003 7.

Hayman EG, Pierschbacher MD, Ruoslahti E .
1985 **J Cell Biol** 100(6) 1948 54 .

Lane DA, Flynn AM, Pejler G, Lindahl U, Choay J, Preissner K .
1987 **J Biol Chem** 262(34) 16343 8.

Muller Eberhard HJ .
1985 **J Invest Dermatol** 85(1 Suppl) 47s 52s .

Pytela R, Pierschbacher MD, Ruoslahti E .
1985 **Proc Natl Acad Sci USA** 82(17) 5766 70.

Ruoslahti E, Suzuki S, Hayman EG, Ill CR, Pierschbacher MD .

1987 **Methods Enzymol** 144 430 7.

Suzuki S, Pierschbacher MD, Hayman EG, Nguyen K, Ohgren Y, Ruoslahti E .
1984 **J Biol Chem** 259(24) 15307 14 .

Suzuki S, Oldberg A, Hayman EG, Pierschbacher MD, Ruoslahti E .
1985 **EMBO J** 4(10) 2519 24 .

Suzuki S, Argraves WS, Pytela R, Arai H, Krusius T, Pierschbacher MD, Ruoslahti E .
1986 **Proc Natl Acad Sci USA** 83(22) 8614 8.

Tomasini BR, Mosher DF.
1986 **Blood** 68(3) 737 42.